A Dissertation Presented

By

Dinh Le Mary Chau

Submitted to the Faculty of the

University of Massachusetts Graduate School of Biomedical Sciences, Worcester

in partial fulfillment of the requirements for the degree of

DOCTOR OF PHILOSOPHY

August 6, 2007

Biomedical Sciences

COPYRIGHT

Portions of this thesis appeared in:

Chau MD, Tuft R, Fogarty K, Bao ZZ. (2006) Notch signaling plays a key role in cardiac cell differentiation. *Mech Dev*. Aug;123(8):626-40.

Chau MD**,** Bao ZZ**.** (2007) The Role of Notch1 in cardiac cell migration. *In preparation*

THE ROLE OF NOTCH1 IN CARDIAC CELL DIFFERENTIATION AND MIGRATION

A Dissertation Presented

By

Dinh Le Mary Chau

Approved as to style and content by:

_____

Charles Sagerstrom, Ph.D., Chair of Committee

_____

Jaime Rivera, Ph.D., Member of Committee

_____

Alonzo Ross, Ph.D., Member of Committee

_____

Fumihiko Urano, M.D., Ph.D., Member of Committee

_____

Frank Naya, Ph.D., Member of Committee

_____

Zheng-Zheng Bao, Ph.D., Dissertation Mentor

_____

Anthony Carruthers, Ph.D.,

Dean of the Graduate School of Biomedical Sciences

Interdisciplinary Graduate Program

August 6, 2007

ACKNOWLEDGEMENTS

"It takes a village to raise a child." – African proverb

No doubt that it has taken a village of people to guide, support, encourage, inspire and aid me throughout my time at graduate school. I owe each and every one of them my deepest gratitude. I would like to thank my mentor, Dr. Zheng-Zheng Bao, for giving me the opportunity to learn, and develop my skills as a scientist. Her willingness to help and her guidance has been invaluable.

I would like to extend my gratitude to my advisory committee for all of their invaluable guidance throughout my work. I would like to thank Dr. Charles Sagerstrom for serving as my committee chair, and consistently keeping me on track. I would also like to thank Drs. Alonzo Ross and Fumihiko Urano for their advice and support. I would like to thank Dr. Jaime Rivera for agreeing to serve on my committee late in the game. I would like to thank Dr. Frank Naya for serving as my external committee member, and for taking the time to read through my thesis.

I would like to thank members of the Bao lab, Daorong Guo, Jun Jiang, and Adrianne Kolpak, for their friendship, encouragement, and assistance. They have always provided me with moral support, advice, and a helping hand whenever I have struggled, or needed help. On a personal note, I would like to express my gratefulness to Adrianne Kolpak for always encouraging me, listening to my incessant ramblings and complaints, and supporting me through all my "meltdowns". She has been a supportive lab-mate, dear friend, and neighbor.

I would like to extend my deepest gratitude to all my friends for their love, support, encouragement and inspiration throughout my years at school. They have laughed and cried with me, and have cheered me on since the beginning. They have been instrumental to my success. I am lucky to have such amazing friends.

I would like to thank my parents for their love and encouragement throughout my life. I appreciate how much they try to listen to me discuss my work, despite not understanding a single word I say. I would also like to thank them for teaching me about determination, and the importance of hard work and persistence.

I would like to thank my in-laws, Thomas and Ruth Cronin, Joseph and Michele Cronin, Daniel Cronin, and Josephine Kasmedo, for loving and encouraging me, and for accepting me into their family from the moment I met them. I could never have asked for a better family in-law.

I would like to thank my sister, Anita Chau, and brother-in-law, Justin Garofano, for their love and support. In particular, I would like to thank my sister for the many, many years of love, encouragement and friendship she has given me. Mere words cannot express how much she means to me, and how much her love, and encouragement has carried me through. I could never have picked a better, more loving, caring, generous, and supportive sister.

Last, and certainly, not least, I would like to express my deepest gratitude to my husband, Thomas Cronin. There are not enough words to express my love, joy, and gratitude for having him in my life. He has been my biggest fan and cheerleader since my first day at graduate school, and has been a source of unwavering, unconditional strength, love, and inspiration for me. "I carry your heart with me (I carry it in my heart); I am never without it (anywhere I go you go, my dear; and whatever is done by only me is your doing, my darling)" – E.E. Cummings

ABSTRACT

The cardiac conduction system is responsible for maintaining and orchestrating the rhythmic contractions of the heart. Results from lineage tracing studies indicate that precursor cells in the ventricles give rise to both cardiac muscle and conduction cells. Using chick embryonic hearts, we have found that Notch signaling plays an important role in the differentiation of cardiac muscle and conduction cell lineages in the ventricles. Notch1 expression coincides with a conduction marker at early stages of conduction system development. Mis-expression of constitutively active Notch1 (NIC) in early heart tubes exhibited multiple effects on cardiac cell differentiation. Cells expressing NIC had a significant decrease in the expression of cardiac muscle markers, but an increase in the expression of conduction cell markers. Loss-of-function studies further support that Notch1 signaling is important for the differentiation of these cardiac cell types. Functional electrophysiology studies show that the expression of constitutively active Notch1 resulted in abnormalities in ventricular conduction pathway patterns.

During cardiogenesis, groups of myocardial cells become separated from each other, and migrate to form the trabeculae. These finger-like projections found within the ventricular chamber coalesce to generate the muscular portions of the interventricular septum, the thickened myocardium, and future sites of the conduction system. We have found that Notch signaling regulates the migration of cardiac cells during cardiogenesis. Over-expression of constitutively

active Notch causes cells to localize more centrally within the heart, while loss-of-Notch function results in cells distributed within the periphery of the heart. Staining of heart sections shows that Notch signaling regulates the expression of N-cadherin, the predominant adhesion molecule in cardiomyocytes. We find that the effects of Notch on cell migration are two-fold: delamination and cell motility. Time-lapse studies demonstrate that Notch signaling increases cell motility, but does not affect speed or directionality of migration. Furthermore, we find that the effects of Notch on cell migration is independent of its effects on differentiation.

TABLE OF CONTENTS

LIST OF FIGURES

CHAPTER I: Introduction

1.1 Congenital and acquired heart diseases

Intricate signaling, transcriptional, and translational networks regulate key cellular decisions that drive the assembly of stem and progenitor cells into functional organs. Insights into these processes will provide us with the opportunity to develop new therapies for human diseases.

A molecular network of cellular decisions controlling cardiac cell fate, myocyte differentiation and cardiac cell migration is required for the proper formation of the heart, the first organ to form and function during embryogenesis. The complexity of these gene regulatory cascades explains the vulnerability of the heart to perturbations before birth and into old age.

Congenital and acquired heart diseases represent the principle noninfectious cause of morbidity and mortality worldwide. Congenital cardiac malformations, the most common of birth defects, occur in 1% of the population worldwide [1]. Another 1-2% harbor more subtle cardiac abnormalities that become apparent with age. In the United States, heart disease is the number one killer of both men and women [2]. Another 5 million survive with insufficient cardiac function. Deciphering the key regulatory networks that govern proper cardiogenesis may lead to development of new therapies.

1.2 Cardiac development

The primary heart field and early cardiac transcription factors

The heart is the first organ to form and function during embryogenesis (Figure 1.1). In the chick embryo, at Hamburger and Hamilton (HH) stage 3, (embryonic day 7 (E7) in the mouse), the cells that are destined to form the heart arise in the anterior third of the primitive streak, excluding Hensen's node. Between HH stages 3 and 4 in the chick, these cells migrate bilaterally to form the left and right heart fields, also referred to as the primary heart field [3]. The basic helix-loop-helix (bHLH) transcription factors, Mesp1 and Mesp2, are required for the migration of these precardiac mesoderm cells. Mesp1 and Mesp2 double-deficient mouse embryos exhibit defects in the development of the cardiac and anterior-cephalic mesoderm [4]. Additionally, lineage analysis has demonstrated that the majority of the cells in the myocardium, and endocardium are derived from Mesp1 expressing mesoderm [5, 6].

Cardiomyocytes are produced in response to factors, including members of the bone morphogenetic protein (BMP) family, sonic hedgehog, fibroblast growth factor (FGF) 8, and Crescent, which are secreted from the endoderm [7]. These cardiogenic signals activate the expression of one of the earliest markers of heart precursor cells, Nkx2.5 [8]. In *Drosophila*, the Nkx2.5 homologue, tinman, is required for heart

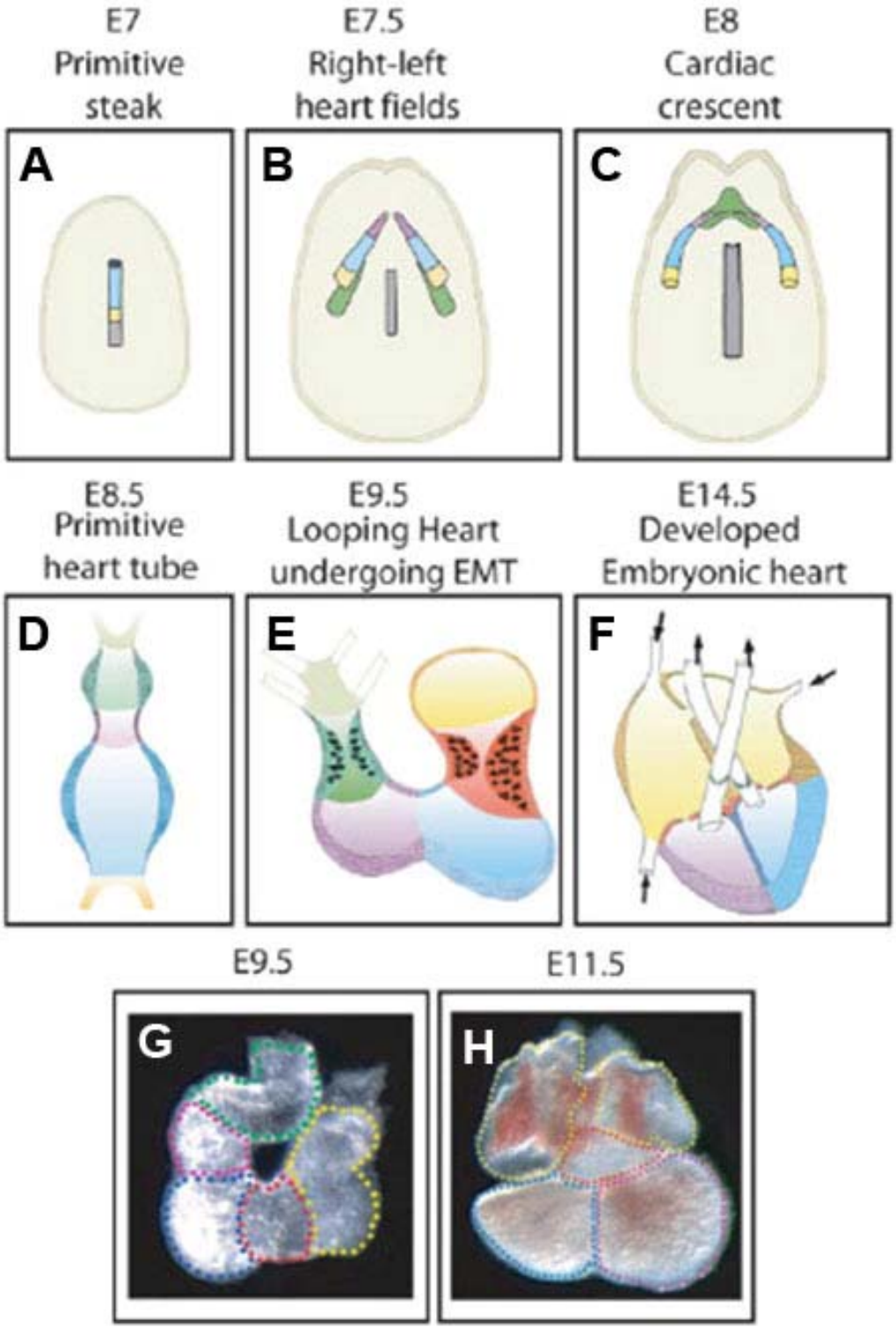
E7
Primitive
steak
E7.5
Right-left
heart fields
E8
Cardiac
crescent
A
B
C
E8.5
Primitive
heart tube
E9.5
Looping Heart
undergoing EMT
E14.5
Developed
Embryonic heart
D
E
F
E9.5
E11.5
G
H

[9]

Figure 1.1: Overview of heart development in the mouse. A: In the mouse, at embryonic day 7 (E7), Heart precursors arise from the anterior third of the primitive streak (blue and yellow), but not from the node (dark grey). B: As development proceeds, at around E7.5, the precursors migrate bilaterally forming the left and right primary heart fields. C: By E8, the primary (blue and yellow) and secondary (green) heart fields undergo anterior-medial migration and fusion to form the cardiac crescent. D: At E8.5, the linear heart tube is generated by fusion of the cardiac crescent at the embryonic midline. The primary heart field gives rise to the left ventricle (blue), right ventricles (purple), and atria (yellow), while the secondary heart field contribute to the outflow tract (green). E: Between E9.5-E10, the heart tube loops to the right to form a C-shaped structure. EMT is initiated in the AV canal (red) and outflow tract (green), and generates the cardiac valves and septa. F: Schematic drawing of the developed embryonic heart. G, H: Mouse embryonic hearts at E9.5 and E11.5.

formation, and activates the transcription of Mef2, which is necessary for myocyte differentiation [10]. Likewise, in *Xenopus*, mutations in Nkx2.5 block heart formation [11]. In mouse, however, Nkx2.5 is dispensable for recruitment of cells to the cardiac lineage and heart development arrests at the beginning of cardiac looping [12].

Nkx2.5 cooperates with the GATA family of zinc-finger transcription factors to activate cardiac gene expression [13]. The *Drosophila* GATA gene, *Pannier*, identifies cardiac cells because forced expression of Pannier results in additional cardiac cells [14]. In vertebrates, three GATA genes, GATA4-6, are expressed in the heart [15]. GATA4 deficient mouse and GATA5 zebrafish null embryos exhibit cardiac bifida (bilateral heart tubes), and fewer cardiac myocytes [16, 17]. GATA6 null mice die prior to heart induction around E5.5-E7.5 due to defects in the extraembryonic endoderm [18, 19]. Loss-of-function studies in Xenopus and zebrafish, using antisense morpholinos, demonstrated a role for GATA6 in the differentiation of the cardiac lineage, in the maturation of cardiac progenitors [20].

Secondary heart field

In the developing mouse and chick heart, in addition to the primary heart field, the existence of a secondary heart field has been identified, and has been found to contribute to the formation of the heart. The secondary heart field is located in the splanchnic mesoderm that underlies the floor of the caudal pharynx. These cells express Nkx2.5, GATA4, and Nkx2.8 [21]. In the chick, the secondary heart field generates the smooth

muscle cells of the distal outflow tract [22]. In the mouse, these cells migrate to the arterial pole [21]. Additionally, these cells were found to contribute to the outflow tract and the right ventricle in the mouse FGF10 enhancer trap line, and in the LacZ knockin mutant of Nkx3.1 [23, 24].

Formation of the heart tube

Anterior-medial migration of cells from the right and left heart fields, and subsequent fusion at the anterior end leads to formation of the cardiac crescent (See Figure 1.1) [9]. The cardiac crescent cells, which initially all have cardiomyogenic potential, become subdivided into ventral myogenic and dorsolateral nonmyogenic populations [25]. The ventral myogenic domain gives rise to the myocardium of the heart tube, while the dorsolateral nonmyogenic subpopulation contribute to the mesocardial and pericardial roof cells [25]. Subsequent folding of the embryo leads to fusion of the cardiac crescent at the midline to generate a linear tube-like structure that consists of an outer myocardial cell layer, and an inner endocardial cell layer [3, 7, 26]. The myocardial and endocardial cell layers are separated by a layer of extracellular matrix called the cardiac jelly.

Heart Looping

At HH stage 10 in the chick, or ~ E9.5-E10 in the mouse, the linear heart tube begins to undergo heart looping (See Figure 1.1). The primitive ventricular region bends toward its ventral side, and simultaneously rotates to the right. In this way, the original

left and right sides of the heart tube become the ventral and dorsal sides of the looped heart. After ventricular looping has started, the primitive outflow tract is displaced to the right. Later, the ventricular portion shifts from its originally cranial position to its final position caudal to the atria, and the conus from its right lateral position to the position ventral to the right atrium [7, 27].

Left-right asymmetry in the heart

The direction of cardiac looping is regulated by an asymmetric axial signaling system that designates the positions of the organs [28]. Several left-right determinants have been identified, and include BMP4, Shh, N-cadherin, beta-catenin, Nodal, Lefty, Pitx2, and FGF8. For example, in the chick, BMP4 is active on the right side of Hensen's node, while Shh is restricted to the left [29]. Additionally, N-cadherin is expressed on the right side, while beta-catenin is found in the left [30]. Lefty is involved in limiting Nodal expression on the left, and preventing spreading of left-sided signals to the right [31]. In the left side, the bicoid-type homeobox gene, *Pitx2,* acts downstream of Nodal. Both overexpression and ablation of Pitx2 cause laterality defects [32-34]. In the mouse, FGF8 appears to be a left determinant [35].

Cardiac valve formation

Concomitant with heart looping, and chamber formation, the endocardial cushions form, and remodel to generate the outflow and atrioventricular valves, as well as portions of the atrial and ventricular septa [3, 7]. Endocardial cushions arise as a result of

swelling of the cardiac jelly due to invasion of endothelial cells. Signaling between the myocardial and endocardial cell layers in the cushion region, mediated by the TGF-β protein family, stimulates the transformation of endocardial cells into mesenchymal cells [36]. These cells migrate into the cushions, and differentiate into fibrous tissues of the valves [3, 7].

1.3 Chamber formation and trabeculation

After cardiac looping, individual cardiac chambers become morphologically distinguishable (Figure 1.2). The morphological and contractile properties, in addition to the patterns of gene expression, differ in each cardiac chamber. The iroquois-related homeobox protein Irx4 labels ventricular progenitor cells in the cardiac crescent [37]. In the chick, Irx4 is involved in establishing chamber-restricted gene expression [38]. The T-box gene, *Tbx5*, marks the atrial compartment of the myocardium [39]. In mice, ablation of Tbx5 results in severe hypoplasia of the atrial and left ventricular chambers, while the right ventricle and outflow tract are unaffected [39]. CoupTFII, a nuclear receptor, is expressed in atrial precursors, and is required for atrial growth [40]. Retinoic acid (RA) also plays a role in chamber formation; RA-deficient quail embryos have oversized ventricles, and hypoplasic atria [41].

One of the hallmarks of ventricular chamber formation is the formation of trabeculae, characteristic finger-like projections, consisting of cardiomyocyte sheets,

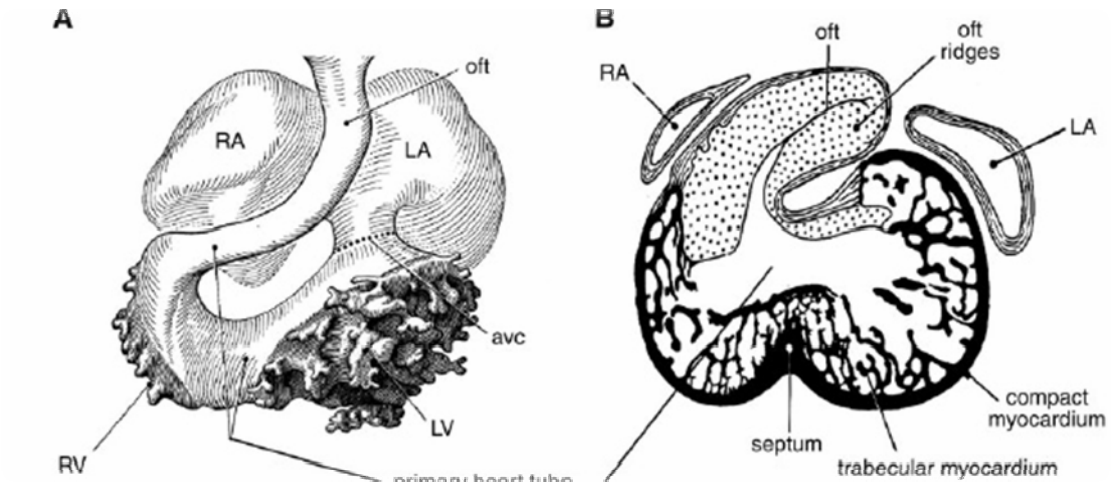
A
oft
RA
LA
avc
LV
RV
B
oft
oft
ridges
RA
LA
compact
myocardium
septum
trabecular myocardium

[27]

Figure 1.2: Chamber formation and trabeculation

A: A “lumen cast” of a human embryonic heart at 4 weeks of development. B: Drawing of a section of the heart at the same stage. The cardiac chambers become morphologically distinguishable after cardiac looping. Myocardial cells in the compact myocardium proliferate and migrate into the ventricular lumen to generate the trabeculae, characteristic finger-like projections indicative of ventricular chamber formation. Coalescence of the trabeculae generates the thickened myocardium, interventricular septum, and future sites of the conduction system. OFT: outflow tract; AVC: atrioventricular canal; RA: right atrium; LA: left atrium; RV: right ventricle; LV: left ventricle

lined by endocardial cells. Trabeculae are generated when myocardial cells in the ventricular segment proliferate, and migrate into the ventricular lumen [42-44]. Coalescence of the trabeculae forms the interventricular septum, thickened myocardium of the ventricles, and future sites of the conduction system [45]. The basic helix-loop-helix transcription factors dHAND/HAND2 and eHAND/HAND1 are differentially expressed in the right and left ventricles, respectively. Deletion of HAND2 in mice results in hypoplasia of the right ventricle [46]. Conversely, over-expression of HAND2 in mice significantly upregulated expression of trabecular markers [47]. Homozygous null mice for neuregulin-1 and its receptors ErbB2 or ErbB4 exhibit defective ventricular chamber formation, and absent trabeculation [48-50]. Injection of NRG-1 into the ventricular chamber of mouse embryos induced trabecular marker expression without increasing cardiomyocyte proliferation [51]. Contrary to neuregulin-1, both BMP10 and the rho-associated coiled-coil kinases (ROCKs) regulate ventricular chamber formation and trabeculation by controlling cardiomyocyte proliferation; inactivation of BMP10 or ROCK causes ventricular hypoplasia and decreased trabeculation due to decreased proliferative activity of cardiomyocytes [52, 53].

1.4 Cardiac conduction system

Components of the conduction system

The specialized tissues of the cardiac pacemaking and conduction system drive and coordinate the rhythmic contractions of the heart. Atrial components of the

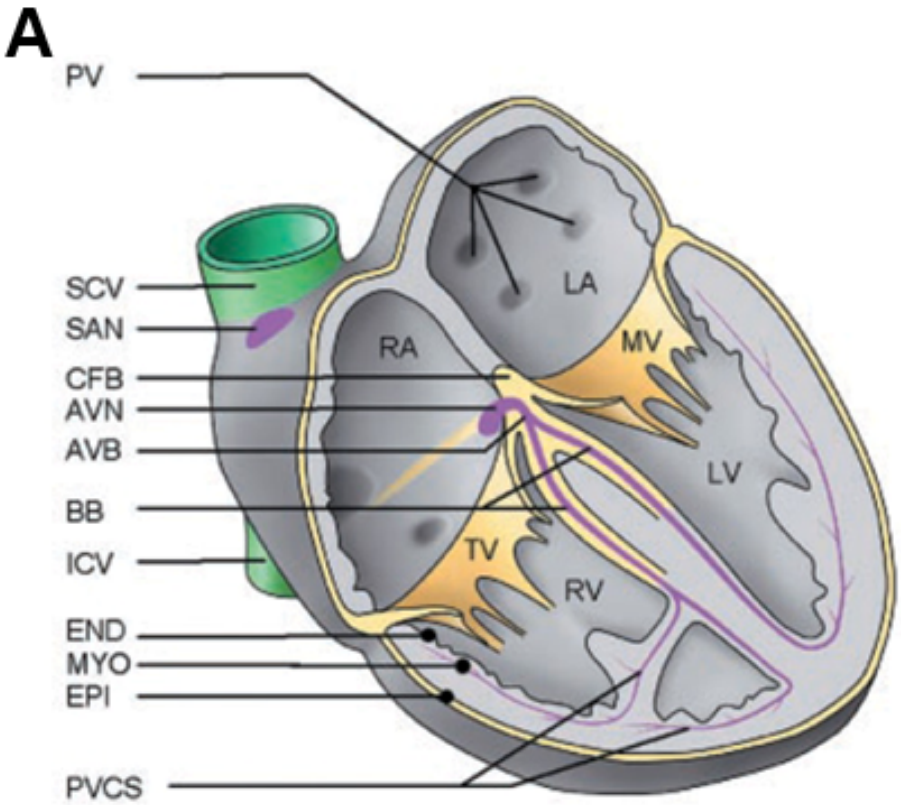
A
PV
SCV
SAN
CFB
AVN
AVB
BB
ICV
END
MYO
EPI
PVCS
LA
RA
MV
LV
TV
RV

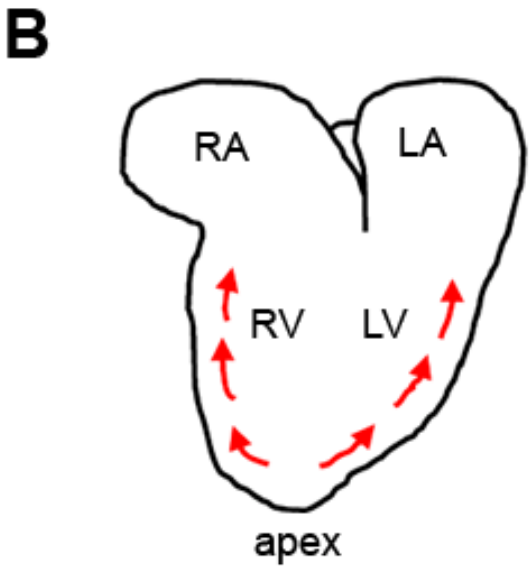
B
RA
LA
RV
LV
apex

[27]

Figure 1.3: Components of the conduction system

A: The working myocardium of the heart consists of the right and left atria (RA, LA) and right and left ventricles (RV, LV). The atrial conduction system is composed of the pacemaking tissues of the sinoatrial node (SAN) and the atrioventricular node (AVN), while the ventricular conduction system consists of the fast-conducting components comprising the atrioventricular bundle (AVB), the left and right bundle branches (BB), and the peripheral ventricular conduction system (PVSC), also known as the Purkinje fibers. B: Schematic drawing showing the apex to base contraction of the heart. The action potential is initiated at the SAN, and then travels to the AVN. After exiting the AVN, the action potential rapidly spreads along the His bundle and its branches. It then spreads throughout the ventricular chambers via a network of fibers, known as Purkinje fibers. PV: pulmonary veins; S/I CV: superior/inferior caval vein; CFB: central fibrous body; MV: mitral valve; TV: tricuspid valve; END: endocardium; EPI: epicardium; MYO, myocardium.

fibers are components of the ventricular conduction system (See figure 1.3) [27, 54]. The intrinsic rhythm of the heart is determined by the cardiac pacemaker, the sinoatrial (SA) node. The SA node sits at the inflow tract of the right atrium. The pacemaker activity is the first element to function in the cardiac conduction system. In the cardiac muscle, cells with the most rapid inherent rhythm set the rate of contraction of the myocardium. The heterogeneous cells of the SA node display the most rapid rhythm, and thereby act as the pacemaker of the heart. The node is richly innervated by both the sympathetic and parasympathetic nervous system. The pace making action potential is produced by a slow depolarization that involves a number of ion channels, including T- and L-type calcium channels [54]. Little is known, however, about the mechanisms that induce and maintain the pacemaker cells of the heart.

Following initiation of a cardiac action potential within the SA node, the electrical impulse is propagated through the muscular tissues of the atria, and focuses into the atrioventricular (AV) node. The AV node sits at the junction of the atria and ventricles, and generates a momentary delay in the propagation of the action potential. Cells of the AV node are interspersed with connective tissue and vasculature. In mammals, a thin layer of atrial myocardium separates the AV node from the endocardium. In the periphery of this region, cells adopt a flat and spindle-like morphology, while fibers found more deeply are irregularly shaped. The AV delay first becomes evident when the looping heart undergoes morphogenic constriction to divide the atrial and ventricular chambers. Myocytes of the AV node express the gap junction protein, connexin45.

These channels are characterized by high voltage sensitivity and low permeability, which contribute to the slow conduction in the AV canal [54]. However, like the SA node, the mechanisms that are responsible for normal AV nodal development remain obscure.

After exiting from the AV node, the action potential rapidly spreads along the His bundle and its distal branches. The action potential finally spreads throughout the ventricular chambers via a network of fibers known as the Purkinje fibers. His first described the bundle of cells that form a connection between the atrial and ventricular chambers in the mammalian heart. The His bundle originates at the posterior right atrial wall, and passes over the upper margin of the ventricular septal muscle. It then bifurcates near the aorta into a right and a left bundle branch. The left and right bundle branches lead into the Purkinje fibers, which are distributed widely throughout the left and right ventricles. The tips of the Purkinje fibers are coupled to muscle cells via gap junctions, and initiates an apex to base contraction of the ventricle in the mature heart [54]. Whether the development of the atrial and ventricular conduction components requires the same molecular pathways, or whether they are independently generated and physically coupled is unknown.

Origins and development of the conduction system

Cells of the conduction system are characterized by reduced numbers of myofibrils, and a higher accumulation of glycogen than working myocytes [55, 56]. Ventricular conduction cells of the avian heart express high levels of connexin 42, a gap

junctional protein, absent or present at lower amounts in cardiac muscle cells [57]. Conduction cells also express genes usually associated with neural and skeletal tissues, including neurofilament antigens [58], HNK-1 [54, 59-62], EAP-300 [63], acetylcholinesterase [64], and a slow skeletal muscle isoform of the myosin heavy chain [65]. The co-expression of both neural and muscle genes have led to the proposal of two possible origins of the conduction system: myogenic and neurogenic. In the chick, from E2-3, neural crest cells initiate migration from the hindbrain, and enter the tubular heart at E4, forming the neuronal and glial elements of cardiac ganglia. Analysis of clonal populations of myocytes tagged with replication-defective retroviral constructs encoding β-galactosidase demonstrated that β-gal$^+$ clonal populations contained both conduction cells and working myocytes [66]. Following microinjection of retrovirus into the neural folds at the hindbrain of HH8-10 embryos, no virally tagged cells could be traced into the conduction cell lineage, excluding the contribution of neural crest cells to the conduction system [67]. This provided compelling evidence for a common lineage for cardiac conduction cells and working myocytes.

Due to the close proximity of conduction cells to arterial vessels, it has been demonstrated that the recruitment of conduction cells from myocardial clones occurs as a result of paracrine signals from endocardial and endothelial cells of the coronary arteries, including endothelin-1 (ET-1) and neuregulin-1 (NRG-1). *In vitro*, cultured chick embryonic myocytes can be induced to express conduction cell markers with endothelin-1, which is produced by endothelial cells lining the coronary arteries [68]. Supporting

these results, co-expression of the ET-1 precursor, preproendothelin, and endothelin converting enzyme-1 (ECE-1) in vivo caused cardiomyocytes to express conduction cell markers [69]. The proteolytic activity of ECE-1 is required to process ET-1, so that it may bind to its receptors. While the receptors are ubiquitously expressed by all myocytes, ECE-1 is expressed specifically in the endothelial cells of coronary arteries and the endocardium [69]. Hemodynamic forces regulate the expression of ECE-1, and are crucial in demarcating the location of conduction cell recruitment [70]. Using a transgenic mouse line in which LacZ delineates the conduction system, it was demonstrated that addition of neuregulin-1 to mouse embryos is sufficient to induce ectopic expression of LacZ. Optical mapping showed electrophysiological changes in activation pattern, upon treatment with neuregulin-1, consistent with additional recruitment of conduction cells [71].

Several transcription factors, including HF-1b, Nkx2.5, Tbx5, and Id2, have been shown to play important roles in conduction system development. Mice deficient in HF-1b, a SP1-related transcription factor, exhibit sudden death, associated with ventricular tachycardia and AV block, due to defective differentiation of conduction cells [72, 73]. Nkx2.5 knockout mice display a hypoplastic atrioventricular (AV) node, and ventricular conduction defects associated with decreased conduction cells [74, 75]. Similarly, Tbx5 haploinsufficiency in mice exhibited defects in the atrioventricular and bundle branch conduction systems, due to a maturation failure of conduction cells. Electrophysiological testing revealed the presence of right-bundle-branch block consistent with failed

maturation of the AV node [76]. Recently, the generation of mice with compound haploinsufficiency of Tbx5 and Nkx2.5 or Tbx5 and Id2 revealed defective conduction system formation due to inhibition of ventricular conduction cell specification, placing these genes in a molecular pathway that coordinates specification of myocytes into the conduction cell lineage [77].

1.5 The Notch Signaling Pathway

The Notch signaling pathway is an evolutionarily conversed mechanism used by many organisms to regulate a broad spectrum of critical processes, including cell differentiation, proliferation, survival and migration, during embryogenesis and in post-natal development [78-80]. The *notch* gene was first identified in *Drosophila*, where the first mutant allele gave rise to notches on the margins of the wing blades. The *notch* gene encodes a cell surface type I single-pass transmembrane protein receptor (See figure 1.4). Vertebrates have four Notch receptors (Notch1-Notch4). The conserved Notch proteins consist of an extracellular portion (NECD) that contains 29-36 tandem epidermal growth factor (EGF)- like repeats, and an intracellular portion (NICD) which consists of several domains: two nuclear localization signals, a RAM domain, multiple ankyrin repeats, a transactivation domain (TAD), and a C-terminal PEST sequence. In the ER and Golgi, Fringe and other glycosyltransferases mediate a series of glycosylation events that modify NECD. In the trans-Golgi network, proteases of the Furin family process

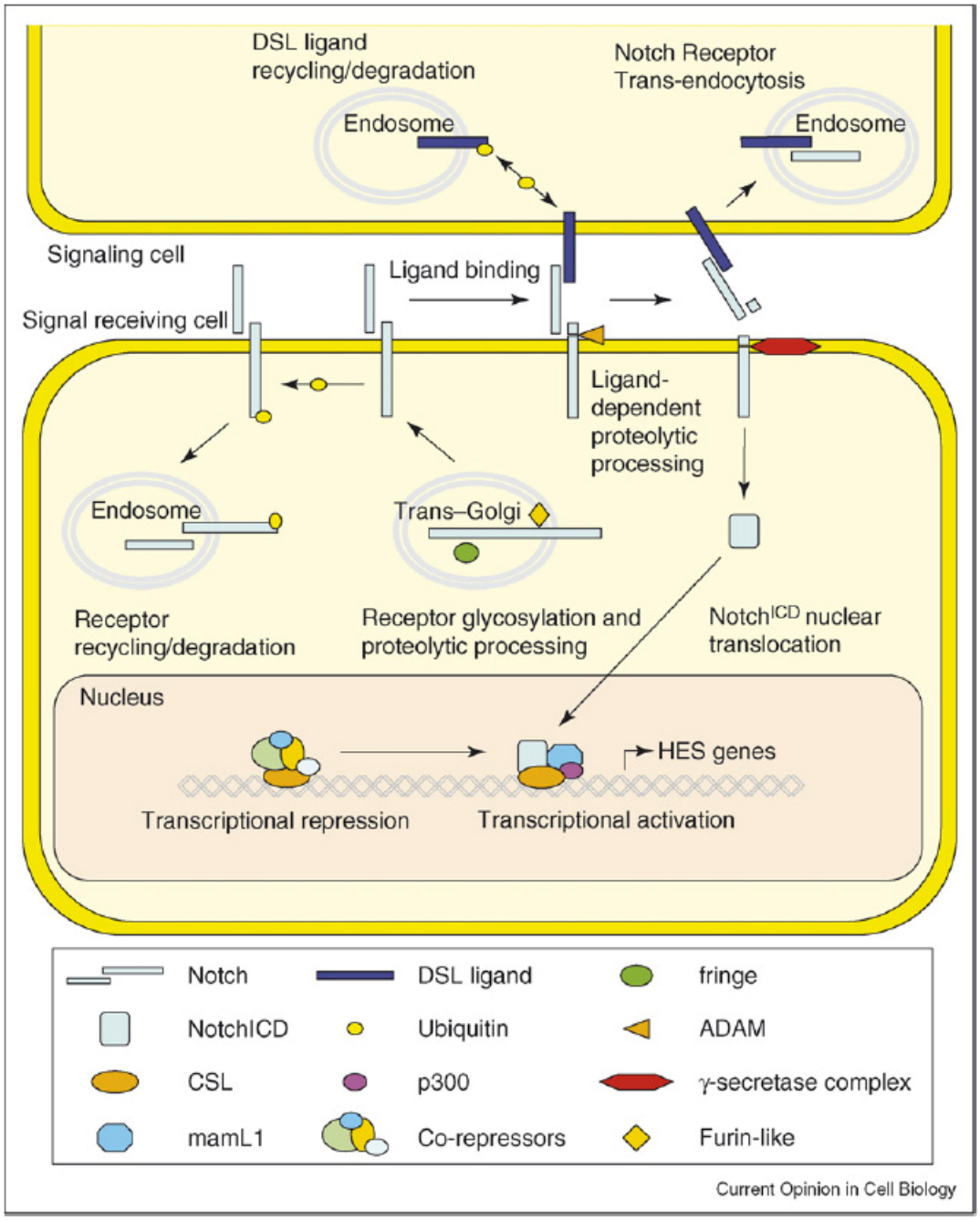
DSL ligand
recycling/degradation
Notch Receptor
Trans-endocytosis
Endosome
Endosome
Signaling cell
Ligand binding
Signal receiving cell
Ligand-
dependent
proteolytic
processing
Endosome
Trans–Golgi
Receptor
recycling/degradation
Receptor glycosylation and
proteolytic processing
Notch^ICD nuclear
translocation
Nucleus
HES genes
Transcriptional repression
Transcriptional activation
Notch
DSL ligand
fringe
NotchICD
Ubiquitin
ADAM
CSL
p300
γ-secretase complex
mamL1
Co-repressors
Furin-like
Current Opinion in Cell Biology

[78]

Figure 1.4: Overview of Notch signaling

Notch receptors are composed of an extracellular domain (NECD) containing numerous EGF-like repeats, a small transmembrane region (NTM), and an intracellular domain (NIC). In the ER and Golgi, NECD is modified by a series of glycosylation events mediated by Fringe and other glycosyltransferases. Furin proteases process Notch molecules in the trans-Golgi. Upon ligand binding, NECD is removed through cleavage by the ADAM/TACE/Kuzbanian family of metalloproteases. NECD remains bound to the ligand, and both proteins may be endocytosed by the ligand presenting cell. The receptor then undergoes a second series of cleavage events mediated by the γ-secretase complex to release NIC. NIC translocates to the nucleus and associates with a CBF1/Su(H)/Lag-1 (CSL) family transcriptional regulator. The CSL protein family acts as transcriptional repressors in the absence of NIC. Upon Notch binding, co-repressors are exchanged for co-activators, including Mastermind, leading to the activation of target genes, including HES family members.

newly synthesized Notch molecules. Subsequently, Notch inserts at the plasma membrane as a heterodimer consisting of an extracellular domain (NECD), and a membrane tethered intracellular domain (NTM), which interact non-covalently in a Ca^{2+}-dependent manner.

Two families of type I single-pass transmembrane proteins, Delta and Serrate (also known as Jagged in vertebrates), have been identified as Notch ligands. In vertebrates, five ligands for the Notch receptor have been identified (Delta1, Delta3, Delta4, Serrate1/Jagged1, and Serrate2/Jagged2). The ligands contain extracellular regions that differ in the number of EGF-like repeats. Additionally, the extracellular regions of Jagged ligands also contain a cysteine-rich region.

Notch signaling is initiated upon cell-to-cell contact as a result of interactions between Notch receptors and their ligands expressed on neighboring cells. Upon ligand binding, the Notch receptor undergoes a series of successive proteolytic cleavages. The first cleavage occurs extracellularly, close to the transmembrane domain, and is mediated by metalloproteases of the ADAM/TACE/Kuzbanian family. This releases the extracellular domain of Notch, and generates a membrane bound form of Notch (NEXT). NECD remains bound to the ligand, and are endocytosed by the ligand presenting cell. NEXT undergoes two more cleavages, which occurs within the transmembrane domain, and is mediated by a multi-protein complex with γ-secretase activity consisting of presenilin, nicastrin, APH-1, and PEN-2 proteins. This second cleavage releases the

intracellular domain of the receptor to translocate into the nucleus, where it assembles into a ternary complex with the transcription factor CSL/CBF1/Suppressor of Hairless (Su(H))/RBP-Jκ through the RAM domain and ankyrin repeats. In the absence of NICD, CSL proteins are part of a repressor complex. NICD also binds to the Mastermind (MAM)/Lag-3 co-activator through the ankyrin repeats, thus converting CSL from a transcriptional repressor into a transcriptional activator. This complex binds specific regulatory DNA sequences, and activates the transcription of CSL/Notch target genes, including the basic-helix-loop-helix (bHLH) protein families, Hes and Herp (also known as Hey, Hesr, HRT, CHF, and gridlock) [78-80].

Notch signaling and differentiation

The most well documented role of the Notch signaling pathway is in cell fate specification and differentiation. In most cases, Notch signaling acts in a binary cell fate decision, where it blocks differentiation towards a primary differentiation fate in a cell, and instead drives the cell to a second differentiation program. Notch signaling requires cell-cell interaction, and its effects on binary cell fate decisions are often mediated via a mechanism called lateral inhibition. In an initially homogenous cell population, stochastic changes are amplified leading to the differential expression of ligand and receptor in opposing cells. The cell that adopts the primary fate expresses high levels of ligand, and low levels of receptor. The juxtaposing cell takes on the secondary fate, and in contrast, expresses high levels of receptor, and low levels of ligand. Initial small differences in ligand and receptor expression become amplified via a

feedback mechanism between Notch and Delta. The ligands and receptors mutually repress each others' expression on neighboring cells. The mechanism of Delta downregulation may be mediated by CSL/CBF1/Suppressor of Hairless (Su(H))/RBP-Jκ-induced upregulation of bHLH proteins. These proteins function as transcriptional repressors, and in conjunction with Groucho, down-regulate expression of Achaete-Scute, which is necessary for Delta expression.

A classic example of Notch signaling in influencing a binary cell fate decision stems from the developing peripheral nervous system in *Drosophila*. Mechanosensory bristles develop from a pool of pluripotent progenitor cells called sensory organ precursor cells (SOPs). A SOP cell generates two different cell types (IIa and IIb), which in turn give rise to either hair and socket cells (from IIa cells) or neuron and sheath cells (from IIb cells). Notch is required at both stages for the specification of particular cell fates; it first specifies the IIa cell fate from the SOP cells, and then specifies the identities of the socket cell and the sheath cell [81].

In vertebrates, Notch signaling has also been shown to influence neurogenesis; Notch signaling promotes glial cell fate by inhibiting neuronal cell fate. Both gain-of-function and loss-of-function approaches have demonstrated the role of Notch in cell fate specification during neurogenesis. Retroviral delivery of activated Notch1 into the mouse forebrain upregulated glial cell markers, and promoted radial glia identity [82]. Activation of Notch signaling with soluble Delta ligand in neural crest stem cells

promoted the expression of glial markers [83]. Similarly, expression of activated Notch1 in the rat retina blocked neuronal cell differentiation, and led to the upregulation of Muller glial markers [84, 85]. Conversely, conditional inactivation of Notch1 in midbrain-hindbrain neuroepithelial cells led to premature neurogenesis, and failed differentiation of glial cells [86]. During later steps of neurogenesis, Notch signaling acts to specify astrocyte cell fate; transient activation of Notch signaling in neurospheres promotes the differentiation of astrocytes, at the expense of neuronal and oligodendrocyte differentiation [87]. Likewise, activated Notch1 promotes the differentiation of astroglia from rat adult hippocampus-derived multipotent progenitors [88]. Therefore, Notch signaling acts on neural stem cells in two steps: by initially inhibiting neuronal fate, while allowing for glial cell fate, and then promoting astrocyte differentiation, while inhibiting differentiation to both neurons and oligodendrocytes.

During hematopoiesis, both loss-of-function and gain-of-function studies have demonstrated the essential role of Notch1 for T-cell lineage commitment [89, 90]. Conditional inactivation of Notch1, or inhibition of Notch signaling via inducible inactivation of RBP-Jκ, in bone marrow progenitors leads to a block in T-cell development and promotes B-cell differentiation in the thymus, suggesting that Notch1 plays a role in the differentiation of early lymphoid progenitors [89, 91, 92]. Overexpression of NIC in bone marrow progenitors resulted in a reciprocal phenotype characterized by ectopic T-cell development in the bone marrow at the expense of B-cell development [90]. In addition to its function in the T-cell lineage, Notch signaling is also

important in later stages of B-cell development. Immature bone marrow-derived B-cells enter the spleen, where they differentiate into either follicular B-cells (FoBs) or marginal zone B-cells (MZBs). B-cell specific inactivation of RBP-Jκ leads to a loss of MZBs, accompanied by an increase in follicular B-cells [93].

In the pancreas of Delta-like1 or RBP-Jκ knockout mice, there is an excess of endocrine cells, suggesting that Notch signaling inhibits endocrine-lineage differentiation from common exocrine and endocrine progenitors during pancreatic development [94]. Consistent with this result, activation of Notch in the developing pancreas resulted in a disorganized pancreatic epithelium due to reduced numbers of endocrine cells [95]. These studies demonstrate that Notch signaling is not only used in many different organ systems to regulate cell differentiation, but also reiteratively during the maturation of an individual organ.

Notch signaling and cell migration

Cell migration plays a key role in embryogenesis. Precise coordination of cell migration is required for proper formation of organs. Not all cells are allowed to leave their place of birth. Cells that are selected to move must convert from a static to a motile state, loosen their contacts to the surrounding tissue, and respond to environmental cues that ensure the proper onset, directionality, and speed of their movement [96, 97]. Actin dynamics at the leading edge provides the key driving force during cell migration, while contraction of actin and myosin II filaments moves the cell body. At the trailing edge,

microtubule-dependent targeting of dynamin and endocytosis promotes disassembly of adhesion complexes [98-100].

In addition to its key roles in cell fate specification, Notch signaling also influences cell migration during organogenesis. The role of Notch in cell migration has been most frequently studied in *Drosophila*, where inactivation of Notch signaling leads to aberrant migration phenotypes. For example, temperature-sensitive Notch mutants display aberrant peripheral glial cell migration [101]. Notch signaling has been shown to regulate the movement of anterior boundary cells via the cytoskeletal linker protein, Shot [102]. Additionally, inactivation of Notch signaling, via expression of dominant-negative Kuzbanian, causes failed border cell migration due to the inability of these cells to detach from the follicular epithelium [103, 104].

Examples of Notch signaling in cell migration in vertebrates include Delta1 null mice with delayed and non-segmental migration of neural crest cells [105]. Additionally, conditional ablation of Jagged1 in the midbrain-hindbrain boundary in mice causes delayed migration with accumulation of cells in the external germinal layer [106]. These studies illustrate the requirement for Notch signaling in migration. However, Notch signaling has also been shown to limit cell migration. In zebrafish, morpholinos directed against Suppressor-of-Hairless/RBP-Jκ and Delta-like 4 increased cell migration and proliferation during blood vessel sprouting [107].

Notch signaling and cardiogenesis

In the heart, Notch signaling plays key roles in regulating cardiogenic differentiation, proliferation, and epithelial-to-mesenchymal transition (EMT) during development. The expression pattern of Notch receptors in the cardiovascular system varies from one receptor to another, in different organisms. Around embryonic day 8.5 (E8.5) in the mouse, Notch1 is expressed mainly in the endocardial layer of the outflow tract in the primary heart tube [108]. Later, expression is also found in the atrioventricular canal, the aorta, the epicardium, and the trabeculae of the ventricles. Notch2 is expressed in the atrioventricular canal, overlapping with Notch1 expression, the pulmonary arteries, and the aorta. Mouse Notch3 is expressed in the aorta, and the pulmonary artery. Whereas, Notch4 is present in the endothelium of the aorta [108]. Jagged1, Jagged2, and Delta-like4 are all expressed in endothelial cells [109].

In mouse, null mutations in Notch1 and RBP-Jκ cause embryonic lethality and pericardial edema [110, 111]. Additionally, mice carrying hypomorphic mutations in Notch2 also exhibit embryonic lethality, and pericardial edema [112]. In humans, genetic Notch1 haploinsufficiency causes aortic valve disease characterized by calcification [113]. Additionally, mutations in Jagged1 causes Alagille syndrome, an autosomal dominant disorder characterized by liver, heart, eye, kidney, skeletal and craniofacial defects [114]. These studies suggest a role for Notch signaling during cardiac development.

The expression of Notch1 in the endocardium indicates a role for Notch signaling in endocardial development. Notch signaling regulates EMT during formation of the cardiac valve primordia by downregulating expression of E-cadherin [115, 116]. RBP-Jκ null mice exhibit impaired EMT due to attenuated expression of Snail, a repressor of E-cadherin [115]. Moreover, the downstream targets of Notch signaling, Hesr1 and Hesr2, play crucial roles in cardiac development. Hesr2-null mice exhibit defects in AV valve formation, and atrial and ventricular septal defects [117-120]. Hesr1/Hesr2 double knockout mice show defective trabeculation and septation of the heart due to impaired EMT [121].

Recently, it has been demonstrated that Notch signaling regulates the formation of the ventricles, by controlling cell proliferation. Notch1 and RBP-Jκ knockout mice exhibit defective ventricular formation due to attenuated expression of BMP10, which is necessary for cell proliferation [122].

Notch signaling has been reported to play suppressive roles during myocardial cell specification in a number of different species. In *Xenopus*, interaction of Notch with its ligand Serrate suppresses myogenesis, and establishes myocardial and non-myocardial domains within the early heart field [123]. Similarly, Notch activity in the *Drosophila* heart prevents myocardial cell fate determination [124]. RBP-Jκ-null embryonic stem cells show increased cardiomyogenic differentiation [125]. Consistent with these results, constitutive activation of Notch in the mesodermal cell lineage, in mouse, causes

deformities of the ventricles and atrioventricular canal due to suppression of myocardial differentiation [126].

Our work demonstrates an additional role for Notch signaling in regulating cell fate specification during cardiac conduction system development. Loss-of-function and gain-of-function studies demonstrate that Notch signaling promotes cardiac conduction cell differentiation, at the expense of cardiac muscle cell differentiation. Additionally, optical mapping studies show that constitutive activation of Notch signaling causes abnormal conduction propagation consistent with defective cardiac cell differentiation.

During ventricular chamber formation, characteristic finger-like projections, known as trabeculae, are generated. Trabeculae are formed when myocardial cells in the ventricular segment proliferate and migrate into the ventricular lumen. Coalescence of the trabeculae generates the interventricular septum, the thickened myocardium, and future sites of the conduction system. Our results show that Notch signaling regulates the migration of cardiac cells during cardiac development. In vivo studies show that Notch signaling regulates the distribution of cardiac cells within the heart, suggesting a role for Notch in cell migration. In vitro studies further demonstrate that Notch signaling regulates cardiac cell migration by influencing delamination and increasing cell motility. Additionally, in vitro studies demonstrate that the effects of Notch on cell migration are independent of its effects on differentiation.

CHAPTER II: Notch signaling plays a key role in cardiac cell differentiation

2.1 Abstract

Results from lineage tracing studies indicate that precursor cells in the ventricles give rise to both cardiac muscle and conduction cells. Cardiac conduction cells are specialized cells responsible for orchestrating the rhythmic contractions of the heart. Here, we show that Notch signaling plays an important role in the differentiation of cardiac muscle and conduction cell lineages in the ventricles. Notch1 expression coincides with a conduction marker, HNK-1, at early stages. Misexpression of constitutively active Notch1 (NIC) in early heart tubes in chick exhibited multiple effects on cardiac cell differentiation. Cells expressing NIC had a significant decrease in expression of cardiac muscle markers, but an increase in expression of conduction cell markers, HNK-1, and SNAP-25. However, the expression of the conduction marker connexin 40 was inhibited. Loss-of-function study, using a dominant-negative form of Suppressor-of-Hairless, further supports that Notch1 signaling is important for the differentiation of these cardiac cell types. Functional studies show that the expression of constitutively active Notch1 resulted in abnormalities in ventricular conduction pathway patterns.

2.2. Introduction

The cardiac conduction system is a specialized tissue responsible for setting, maintaining, and coordinating the rhythmic contractions of the heart [54, 127, 128]. Precisely timed electrical impulses are generated at the sinoatrial node, spread through the atrial myocytes,and are received at the atrioventricular node. This impulse is then rapidly propagated along the His bundles and its branches, spreading into the ventricular muscle via the Purkinje fiber network. Although much progress has been made in the understanding of heart development [7, 129], the mechanism underlying the development of the cardiac conduction system is only partially understood.

Cardiac conduction cells are distinguished by their unique gene expression pattern. Antibodies to Leu-7 (HNK-1) have been used widely to delineate the developing conduction system in mammals and in chicken [54, 59-62]. The HNK-1 antibody recognizes a complex sulfate-3-glucuronyl carbohydrate moiety, which is present on a series of molecules involved in cell adhesion and extracellular matrix interaction. The antibody to SNAP-25 protein, a component of the SNARE complex, has also been used to mark the elements of the ventricular conduction system in chick [62]. Among the gap junction protein connexins, Connexin40 (Cx40) or the chicken homolog Cx42, has been used as a marker for the conduction system in many species [57, 130-132].

Retroviral lineage analyses have provided compelling evidence that conduction cells are derived from precursor cells in the heart, sharing a common lineage with working cardiomyocytes [66, 67]. Clonally related cells are found in both cardiac muscle cells and in the conduction system. Following microinjection of replication-defective retrovirus into the cardiac neural crest, however, no virally tagged cells could be traced into the Purkinje fiber lineage, excluding contribution from the neural crest.

It has been demonstrated that the selection of conduction cells within myocardial clones occurs as a result of paracrine signals from endocardial cells and endothelial cells from coronary arteries, including endothelin-1 (ET-1) in chick and Neuregulin-1 in mouse [69-71, 133]. Coexpression of preproendothelin (preproET-1) and endothelin converting enzyme (ECE-1) in the embryonic myocardium induced myocytes to express Purkinje fiber markers [69, 70]. Addition of neuregulin-1 to embryo cultures of CCS-lacZ mice, in which lacZ delineates the cardiac conduction system, increased lacZ expression [71]. Several transcription factors, including Nkx2.5, Tbx5, and HF-1b have also been shown to play an important role in the development of the cardiac conduction system [72, 74-76, 134-136]. Mouse mutants deficient in either of the transcription factors HF-1 b, Tbx5 or Nkx2.5 exhibit defects in the development and function of the conduction system.

The Notch signaling pathway is an evolutionarily conserved mechanism used by metazoans to control cell fate decisions through local cell interactions [137]. The notch

gene encodes a single-pass transmembrane protein receptor that interacts with its ligands, Delta and Serrate/Jagged. Upon binding of the ligand, the intracellular domain of Notch (NIC) undergoes proteolytic cleavage, and is translocated to the nucleus. In the nucleus, NIC binds to its major downstream effector, Suppressor-of-Hairless [Su(H)]. Su(H) binds to the regulatory sequences of the Enhancer-of-Split [E(spl)] locus, upregulating the expression of basic helix-loop-helix (bHLH) proteins, which in turn regulate the expression of downstream target genes. Signals transmitted through the Notch receptor, in combination with other cellular factors, influence differentiation of various cell types, in the nervous system, immune system and pancreas [137].

The Notch pathway has been previously shown to influence cardiogenesis. In Xenopus, it is suggested that the interaction of Notch1 with its ligand Serrate1 apportions myogenic and non-myogenic cell fates within the early heart field [123]. In mouse, null mutations in both notch1 and RBP-J, the mammalian homolog of Suppressor-of-Hairless, leads to embryonic lethality and pericardial edema [110, 111]. The absence of RBP-J in mouse ES cells causes an increase in cardiac muscle development suggesting that Notch/RBP-J signaling is required for the specification of cell fates within the heart field by suppressing cardiomyogenesis [125]. Recently, mutations in Notch1 in humans have been shown to cause aortic valve defects and activation of Notch1 in mouse leads to abnormal cardiogenesis characterized by deformities of the ventricles and atrioventricular canal [113, 126]. Additionally, mutations in various Notch signaling pathway genes, including Jagged1, mind bomb 1, Hesr1/Hey1, and Hesr2/Hey2, result in cardiac defects,

such as pericardial edema, atrial and ventricular septal defects, cardiac cushion, and valve defects [117-121, 138-140].

Here, we demonstrate a role for Notch1 in the differentiation of cardiac cell types in the ventricles. *Notch1* mRNA transcripts are expressed in the ventricular conduction cell lineage at early stages. Forced expression of constitutively active Notch1 in progenitor cells inhibits muscle marker expression but promotes expression of conduction marker HNK-1 and SNAP-25. Cells expressing constitutively active Notch were localized predominantly in the trabeculae where conduction cells are concentrated, and not in the future myocardial compact zone. Loss-of-function study further demonstrates the requirement for Notch in this lineage decision. By optical mapping, we have further shown that expression of constitutively active Notch1 resulted in abnormal conduction patterns in the heart consistent with a defect in cardiac cell differentiation.

2.3 Results

To study the mechanism of cardiac cell differentiation, we analyzed the expression of the notch1 gene by in situ hybridization. At embryonic days 6 (E6), in situ hybridization on heart sections showed that notch1 was expressed in the ventricles and the atria, concentrated in a subset of cells in the trabecular myocardium, and atrioventricular canal (Figs. 2.1A, B, and data not shown). Some very weak signals were also detected in the endocardium (Fig. 2.1B).

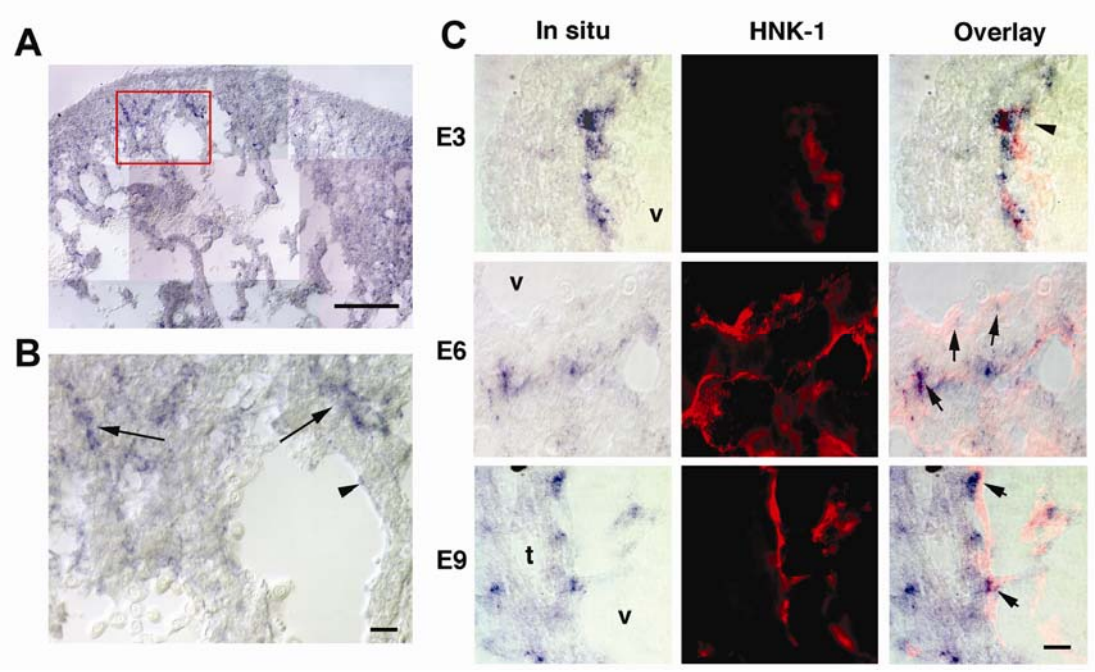
A
B
C
In situ
HNK-1
Overlay
E3
E6
E9
v
v
t
v

Figure 2.1. Expression patterns of *notch1* mRNA in the embryonic chick heart, by in situ hybridizations on heart sections at embryonic days 3 (HH19), 6 (HH29), and 9 (HH35) (E3, E6, E9). A. *notch1* expression at E6 is shown at a low magnification in the ventricles. B. The boxed area in A is shown at a higher magnification. Note the expression of *notch1* in the myocardium (arrows), in addition to very weak signals in the endocardium (arrowhead). C. To identify the cells expressing *notch1*, we immunostained the heart section with the antibody HNK-1 (red), after the completion of in situ hybridization. Note that *notch1* in situ signals appear to be closely associated with cells positive for HNK-1 staining on the plasma membrane at E3 and E6 (arrows). The HNK-1 staining appears subendocardial. The sections shown are of oblique angles. At E9, many *notch1*-positive cells are no longer associated with HNK-1 staining. v: ventricles; t: trabecula. Scale bars in B, C=20 μm; in A=200 μm.

To determine which cardiac cell type in the myocardium expressed notch1 mRNA, we performed in situ hybridization on heart sections using the chick notch1 probe, followed by immunostaining with markers for different cardiac cell types. From E3 to E6, the notch1 in situ signals in the ventricles were largely associated with staining by HNK-1 (Fig. 2.1C). HNK-1 antibody recognizes a complex carbohydrate moiety on the cell surface and has been used extensively as a marker for the ventricular conduction system in many species including chick, rat, rabbit and human [59-62, 141-146], and overlaps with another conduction system marker, Cx40 (Supplementary Fig. 2.1S). As in situ signals are localized in the cytoplasm whereas HNK-1 staining is found on the plasma membrane, the association of the expression patterns suggests that these cells may be expressing HNK-1 and notch1. By E9, however, notch1 in situ signals in the ventricles appeared to be concentrated in the grooves between the trabeculae, with limited association to HNK- 1 staining (Fig. 2.1C). This result suggests that notch1 is expressed in the ventricular conduction cell lineage at early stages.

To define the role of notch1 in heart development, we first took a gain-of-function approach by expressing a constitutively active form of Notch1 in a replication-competent avian retrovirus (RCAS-NIC) (Fig. 2.2A). The truncated protein consisting only of the intracellular domain of Notch1 is known to localize largely in the nucleus, and elicits a constitutively active phenotype [147]. RCAS-NIC, or a control virus RCAS-GFP, encoding green fluorescent protein (GFP), was injected into the early heart tube at HH 9. As shown in Fig. 2.2B, by co-staining with the anti-myc and anti-viral GAG antibodies,

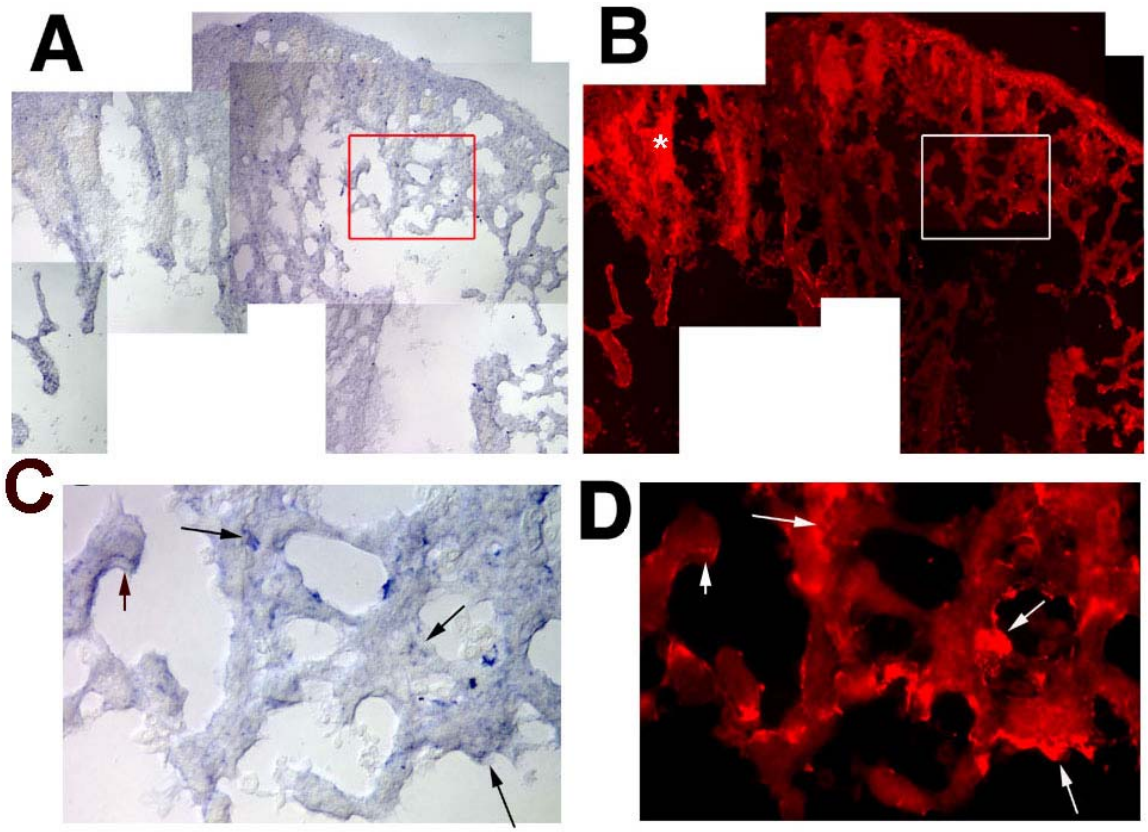
A
B
*
C
D

Figure 2.1S. In situ hybridization was performed on E6 chick heart sections by using the chick Cx40 RNA probe, followed by immunostaining with the antibody HNK-1. (A) The in situ hybridization result is shown at a low magnification in the ventricular region. (B) The boxed area in A is shown at a higher magnification. The HNK-1 staining patterns in the same areas in A, C are shown in B, D, respectively. Note that the HNK-1 staining appears largely fiberous in the trabeculae regions. There is a close association of the *Cx40*-positive cells and the HNK-1 staining. Note that a perfect overlap of the two signals cannot be expected due to the fact that the blue precipitates from the in situ hybridization block fluorescent signal, and HNK-1 staining is on the plasma membrane whereas the *Cx40* transcripts are localized in the cytoplasm. Scale bars in C=20 μm; in A=200 μm.

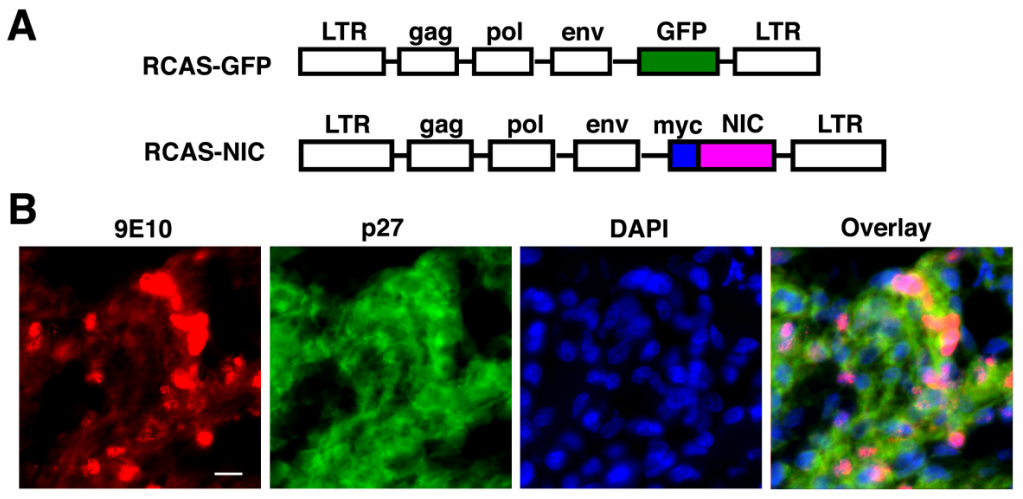
A
LTR
gag
pol
env
GFP
LTR
RCAS-GFP
LTR
gag
pol
env
myc
NIC
LTR
RCAS-NIC
B
9E10
p27
DAPI
Overlay

Figure 2.2. Expression of constitutively active Notch1 (NIC) via a retroviral construct in embryonic chick heart. (A) Retroviral constructs, RCAS-GFP and RCAS-NIC. LTR: Long terminal repeat; gag: gene encoding the viral capsid proteins; env: gene encoding viral envelop protein; pol: gene encoding viral reverse transcriptase. (B) RCAS-NIC injected chick hearts were harvested at E6, sectioned and immunostained with p27 (anti-viral GAG protein, green) to identify infected cells, and an antibody against the myc tag, 9E10 (red). DAPI (blue) was used to stain for the nuclei. Note that the myc-tag staining coincides with the nuclear stain. Scale bar, 10 μm.

NIC protein was observed in the nuclei of the infected cardiac cells. However, not all infected cells appeared positive for the anti-myc antibody staining, possibly due to low detection sensitivity with a single copy of myc-tag present on the NIC protein. Because most of the embryos injected with RCAS-NIC died around E5, we analyzed some embryos at E4.5. For later analyses at E6 or E10, we injected diluted viral stocks to improve survival. Because some molecular markers are more specific in the ventricles, we focused our analysis within the ventricles.

To determine the effect of constitutively active Notch on cardiac muscle differentiation, we co-immunostained the samples with anti-viral GAG p27 antibody to visualize the infected areas, and an antibody that recognizes the sarcomeric myosin heavy chain band, MF20. We did not use myc staining for quantitative analyses because it is difficult to ascertain whether the cell type markers are expressed in the same cells positive for myc in the nuclei, among the densely packed cells. Control RCAS-GFP-infected cells appeared to be mostly positive for MF20 staining, similar to wild type uninjected hearts (Fig. 2.3A upper panels, and B). The majority of the RCAS-NIC-infected cells, however, appeared to have much decreased MF20 staining (Fig. 2.3A, middle and bottom panels). Loss of MF20 staining was more apparent in samples with wide spread infection, nearly 100% of the ventricular cells in some cases (Fig. 2.3A, bottom panels). At higher magnification by using confocal microscopy, the control RCAS-GFP-infected cells showed a strong sarcomeric banding pattern with MF20 staining, and exhibited typical rod-shaped cardiomyocyte morphology (Fig. 2.3C).

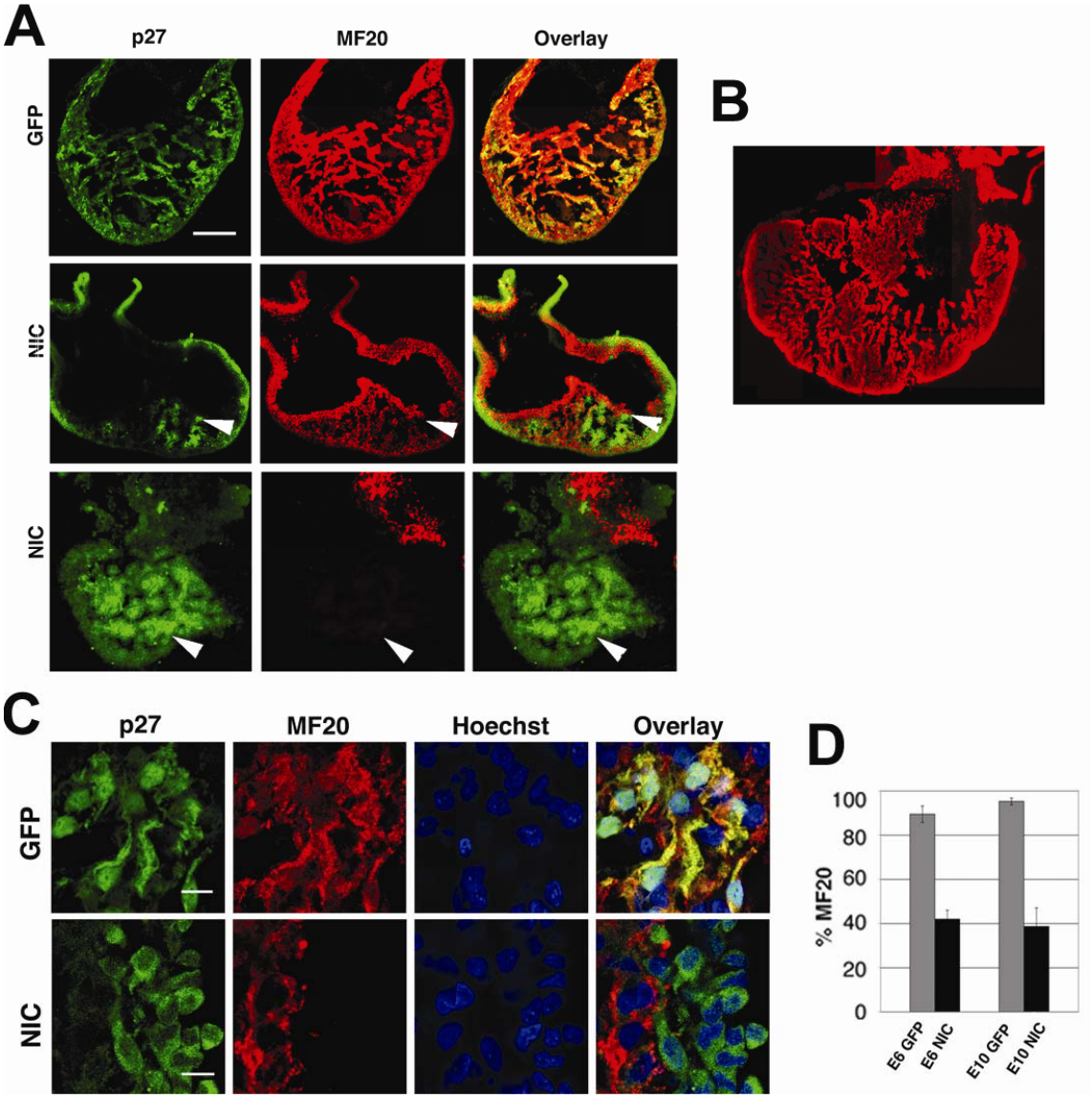
A
p27
MF20
Overlay
GFP
NIC
NIC
B
C
p27
MF20
Hoechst
Overlay
GFP
NIC
D
% MF20
100
80
60
40
20
0
E6 GFP
E6 NIC
E10 GFP
E10 NIC

Figure 2.3. Constitutively active Notch1 (NIC) inhibits cardiac muscle cell differentiation. RCAS-NIC or control RCAS-GFP injected hearts were harvested at E4.5 (A) and E6 (C), sectioned and immunostained with p27 (green) and the anti-sarcomeric myosin heavy chain marker, MF20 (red). Hoechst dye 34580 (blue) was used to stain for the nuclei. (A) E4.5 stained heart sections were analyzed at low magnification on an epifluorescence microscope. Note that, in the RCAS-GFP-infected sample (top panel), MF20 staining is widely distributed throughout the heart. RCAS-NIC-infected patches, however, show a substantial decrease in MF20 staining (arrowheads). In some heavily infected hearts, little MF-20 staining was seen in the ventricles (bottom panel). (B) Staining pattern of MF20 on a wildtype E6 heart is shown. (C) To quantify the results, E6 heart samples were analyzed on confocal microscopy. Note that the control RCAS-GFP infected cells are mostly positive for MF20, showing characteristic banding patterns, whereas many RCAS-NIC infected cells are negative for MF20 staining. (D) Quantification of the results by scoring for the percent of infected cells stained with MF20 at E6 and E10, respectively. Note that RCAS-NIC infected expressed significantly less MF20, $p < 0.001$, Student's t-test. Scale bar in A common to B=500 μm, C=10 μm.

However, RCAS-NIC-infected cells lacked this muscle cell morphology, appeared more rounded, and the majority of the cells lacked MF20 staining (Fig. 2.3C). In the hearts with limited infection, only RCAS NIC-infected cells appeared negative for MF20 staining, while neighboring uninfected cells were positive for MF20, suggesting that the effect of the NIC protein is likely cell-autonomous (Fig. 2.3C). The results of partially infected E6 samples were quantified by scoring randomly chosen infected cells on the confocal microscope. Heart sections infected with the RCAS-NIC virus showed a marked decrease in the percentage of MF20-positive cells, compared to the control RCAS-GFP-injected samples (mean ± std: 41.9 ± 4.0% and 89.4 ± 3.7%, respectively; $p < 0.001$, Student's t-test) (Fig..3D). To determine whether the decrease of MF20 staining is due to a delay in cardiomyocyte differentiation by constitutive Notch1 activity, we examined RCAS NIC- infected hearts at a later stage, E10. We observed similar results at E10: RCAS-NIC infected hearts displayed a similar decrease in the number of MF20 positive cells (38.6 ± 8.4 vs. 95.2 ± 1.5% in control cells, $p < 0.001$) (Fig.2.3D). Furthermore, we analyzed the expression of another muscle marker a-actin in the RCAS-NIC infected cells and a similar inhibitory effect was observed (data not shown). These results suggest that persistent Notch activity inhibits cardiomyocyte differentiation.

We next examined the effects of constitutively active Notch1 on the differentiation of conduction cells. In the control RCAS-GFP injected samples similar to uninjected wild type samples, conduction marker HNK-1 staining was observed in the areas of the trabeculae and interventricular septum (Fig. 2.4A and B). At higher

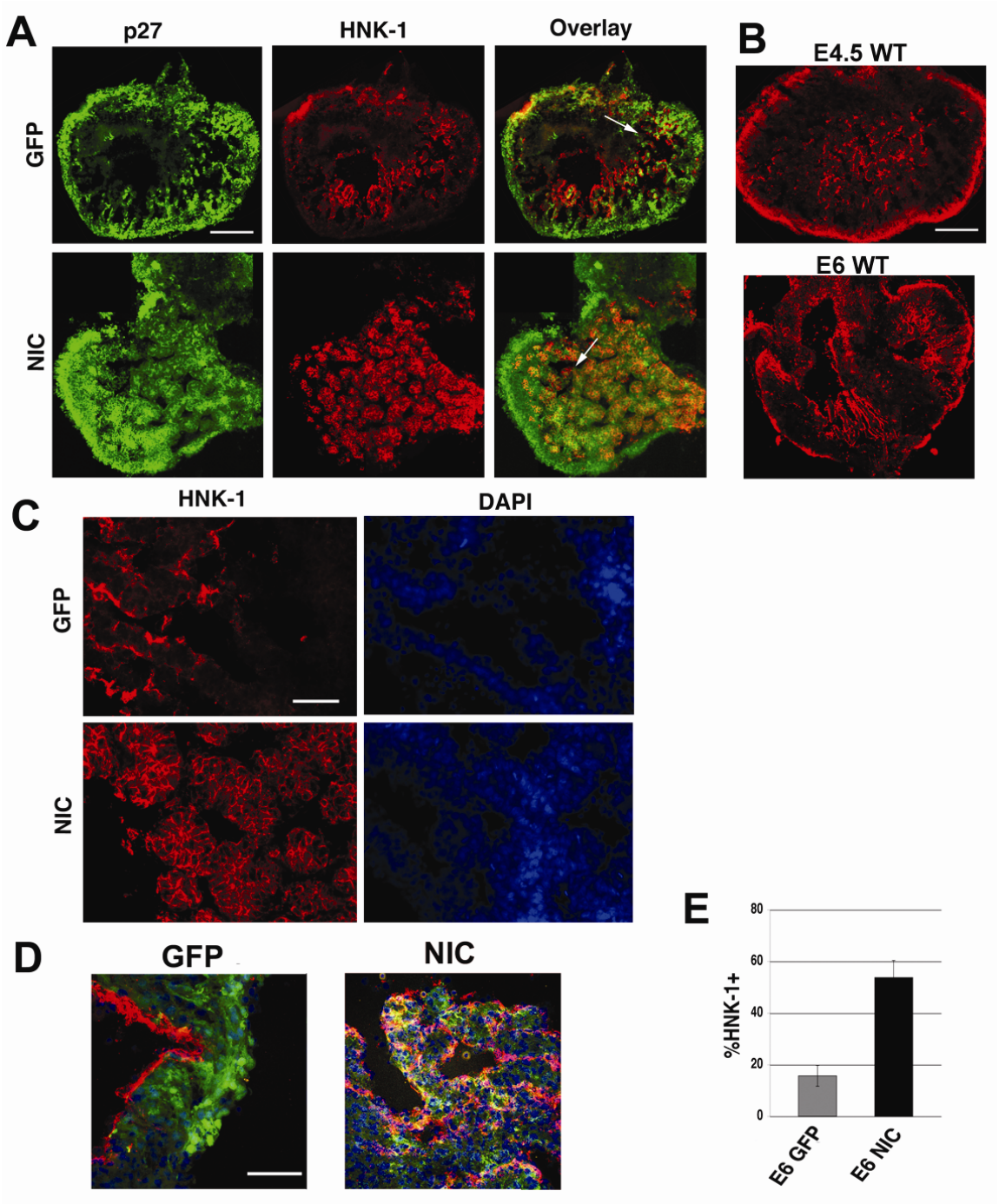
A
p27
HNK-1
Overlay
GFP
NIC
B
E4.5 WT
E6 WT
C
HNK-1
DAPI
GFP
NIC
D
GFP
NIC
E
%HNK-1+
80
60
40
20
0
E6 GFP
E6 NIC

Figure 2.4. RCAS-NIC increases expression of the conduction system marker, HNK-1. RCAS-GFP or RCAS-NIC injected hearts were harvested at E4.5(A, C) or E6 (D), sectioned and immunostained with p27 (green), to identify infected cells, and the conduction lineage marker HNK-1 (red). Hoechst dye 34580 or DAPI (blue) were used to stain for the nuclei. (A) E4.5 stained heart sections were analyzed at low magnification on an epifluorescence microscope. Note that the RCAS-NIC infected sample shows a significant increase in HNK-1 staining as compared to the RCAS-GFP infected heart. (B) The staining patterns of HNK-1 in wild type E4.5 and E6 hearts are shown. Note that HNK-1 staining is concentrated around the trabeculae. (C) The areas of the hearts marked by arrows in (A) are shown in a higher magnification. The RCAS-NIC infected sample shows HNK-1 staining around almost every cell within the trabeculae, while HNK-1 staining mostly outlines the trabeculae in the RCAS-GFP infected heart. (D) The overlay images of the infected hearts at E6 are shown (red, HNK-1; green, P27; blue, Hoechst dye). Note that the trabeculae partially infected with RCAS-NIC has an increase in HNK-1 expression, especially within the trabeculae. (E) Quantification of the percentage of the cells infected with RCAS-GFP or RCAS-NIC expressing HNK-1 at E6. Note that significantly more RCAS-NIC infected cells express HNK-1, $p < 0.001$, Student's t-test. Scale bar in A common to B=500 μm; C=100 μm; D=100 μm.

magnification, HNK-1 staining appeared to line the trabeculae with limited staining inside the trabeculae (Fig. 2.4C). However, in hearts heavily infected with RCAS-NIC, the expression of HNK-1 was found in nearly all of the ventricular myocardium (Fig. 2.4A). Instead of a normal pattern lining the trabeculae, HNK-1 staining appeared to surround every cell in the RCAS-NIC injected samples (Fig. 2.4C). Similar increase in HNK-1 staining was observed in the E6 samples, despite the fact that these samples were not well-infected by injection with diluted viral stocks. By scoring randomly chosen infected areas on the confocal microscope, a significant increase was observed in the proportion of RCAS-NIC-infected cells at E6 expressing HNK-1, compared to RCAS-GFP-infected cells (53.8 ± 6.6 and $15.7 \pm 4.0\%$, respectively; $p < 0.001$) (Fig. 2.4D and E). These results support our notion that constitutively active Notch1 increases the expression of HNK-1.

To determine the effect of Notch signaling on other known conduction cell lineage markers, we examined the expression of SNAP-25 and connexin 40 in the RCAS-NIC injected hearts. SNAP-25 is a component of the SNARE complex that is involved in exocytosis on synaptic terminals. The antibody of SNAP-25 has been shown to label components of the ventricular conduction system in the chick embryo [62]. At low magnification on an epifluorescence microscope, SNAP-25 expression in E6 wild type hearts was found to be concentrated in the trabeculae, in areas similar to HNK-1 staining. But unlike HNK-1 staining which lines the trabeculae, SNAP-25 staining was found inside the trabeculae (Fig. 2.5A and B). At higher magnification, SNAP-25 staining was

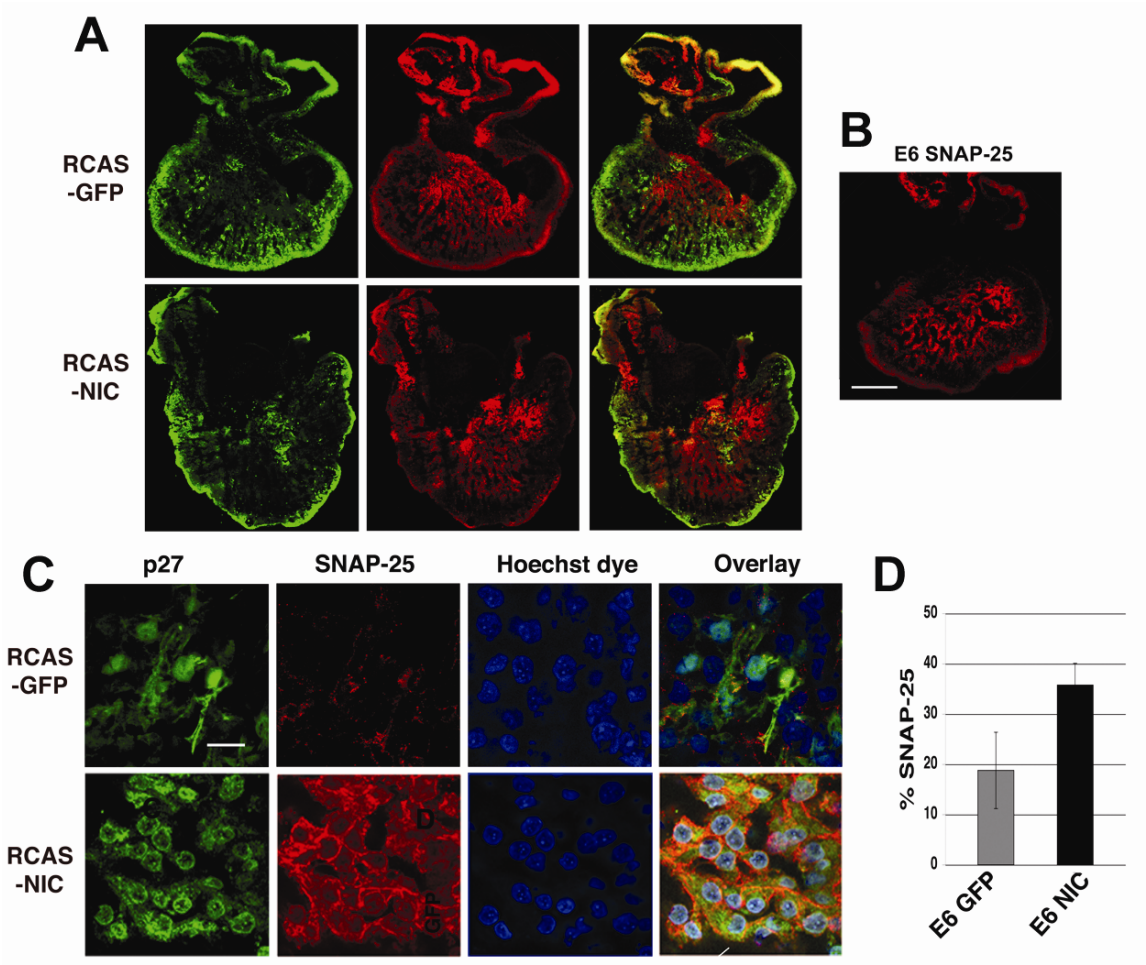
A
RCAS
-GFP
RCAS
-NIC
B
E6 SNAP-25
C
p27
SNAP-25
Hoechst dye
Overlay
RCAS
-GFP
RCAS
-NIC
D
% SNAP-25
50
40
30
20
10
0
E6 GFP
E6 NIC

Figure 2.5. Increase in proportion of the RCAS-NIC infected cells expressing SNAP-25. RCAS-GFP or RCAS-NIC injected hearts were harvested at E6, sectioned and immunostained with anti-GAG antibody p27 (green), and the conduction marker SNAP-25 (red). Hoechst dye 34580 (blue) was used to stain for the nuclei. (A) At low magnification, RCAS-NIC-infected cells are found to be largely localized to the trabeculae region where SNAP-25 expression is enriched. (B) The staining pattern of SNAP-25 antibody is shown on wild type E6 heart section. Note that the SNAP-25 antibody stains the tips of the trabeculae. (C) Stained heart sections were analyzed at higher magnification by confocal microscopy. Many RCAS-NIC-infected cells are SNAP-25 positive. High levels of expression of SNAP-25 were observed on the membrane and the cytoplasm of the RCAS-NIC expressing cells with some punctate staining among the myocardial fibers (top panels). (D) Quantification of the percentage of the cells infected with RCAS-GFP or RCAS-NIC expressing SNAP-25. Note that significantly more RCAS-NIC infected cells express SNAP-25, $p < 0.01$, Student's t-test. Scale bar in A common to B=500 μm, in C=10 μm.

visible in the cytoplasm and plasma membrane of the conduction cells, in addition to punctate staining amidst the muscle cell fibers (Fig. 2.5C). Because SNAP-25 is not expressed in the ventricles until E6, we could not analyze the effect of NIC on SNAP-25 in heavily infected E4.5 hearts. When we scored randomly selected RCAS-NIC-infected cells at E6 on a confocal microscope, a significant increase in the percentage of SNAP-25-positive cells was observed, compared to the control samples (35.8 ± 4.2 and $18.8 \pm 7.6\%$ of the infected cells, respectively; $p < 0.01$) (Fig. 2.5D). At lower magnification, these NIC-expressing cells were found to localize to the trabeculae region, which is normally enriched with SNAP-25 positive cells (Fig. 2.5A, bottom panels). In contrast, the control RCAS-GFP-positive cells were largely distributed in the myocardium destined for the future compact zone (Fig. 2.5A, top panels).

Another conduction system marker, connexin 40 (also called Cx42 in chick), encodes a gap junction protein [54, 57, 148]. By in situ hybridization, we found low levels of Cx40 expression in cardiomyocytes in addition to intense staining in conduction system cells, in uninjected samples or the control samples injected with RCAS-GFP (Fig. 2.6A). This pattern has been reported previously [149, 150]. By in situ hybridization on heart sections infected with RCAS-GFP or RCAS-NIC virus using the chick Cx40 probe, followed by immunostaining with the anti-GAG antibody, we found that RCAS-NIC-infected areas appeared to have decreased Cx40 in situ signals (Fig. 2.6C and D). Few strongly stained cells were observed and the overall weak staining in the cardiomyocytes

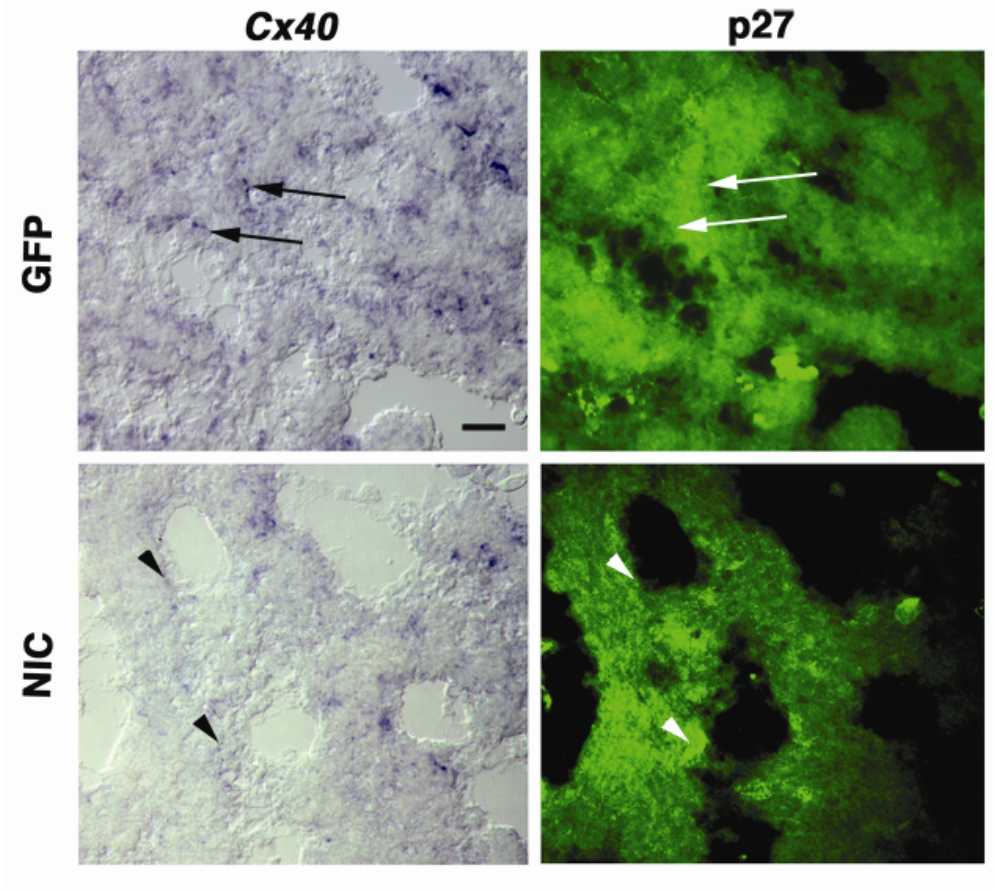
Cx40
p27
GFP
NIC

Figure 2.6. The expression of the conduction system marker *connexin 40* (*Cx 40*) is decreased by constitutively active Notch. RCAS-GFP (A, B) or RCAS-NIC (C, D) infected heart sections were analyzed by in situ hybridization with the *Cx40* probe. Trabeculae areas were shown for both samples. Note the dark subendocardial *Cx40* signals were not decreased by RCAS-GFP expression (arrows). The entire area shown was infected by RCAS-GFP. Because the dark precipitates of the in situ signals quench the fluorescence, small non-fluorescent areas overlapping exactly with the in situ signals are likely infected. In contrast, the RCAS-NIC-infected areas correlated with decreased *Cx 40* in situ signals, both in the subendocardial cells (arrowheads) and myocardial cells. Scale bar, 20 μm.

was further reduced. This result demonstrates that constitutively active Notch1 decreases the expression of Cx40.

We next took a loss-of-function approach by expressing a dominant-negative form of the Suppressor-of-Hairless through retroviral infection, RCAS-Su(H)DN. The dominant-negative form of Suppressor-of-Hairless has been shown to interfere with transcriptional activation of target genes by the Notch1 protein, thereby inhibiting Notch1 function [83, 151]. The injected hearts were harvested at E4 and E6 and processed similarly as in our gain-of-function study. In contrast to the control hearts which show high levels of Cx40 expression in the subendocardial cells in addition to low level expression in the myocardial cells (Fig. 2.6A and B), expression of Su(H)DN resulted in loss of cells expressing high levels of Cx40 (Fig. 2.7A). However, low-level of Cx40 expression in myocardial cells was unaltered.

For MF20, HNK-1 and SNAP-25 markers, we found reversed phenotypes with the RCAS- Su(H)DN-expressing cells as compared to those expressing constitutively active Notch1 (RCAS-NIC). At E4, we found a small but significant increase of RCAS-Su(H)DN-infected cells showing MF20 staining, compared to RCAS-GFP-infected cells (98.4 ± 0.8 vs. $90.0 \pm 1.2\%$ in control, $p < 0.001$) (Fig. 2.7A and B). Additionally, expression of Su(H)DN also appeared to significantly decrease the percentage of HNK-1 expressing cells (4.7 ± 1.1 vs. $13.5 \pm 1.9\%$ in controls, $p < 0.001$) (Fig. 2.7A and B). We found similar results at E6 as those at E4; a significant increase of

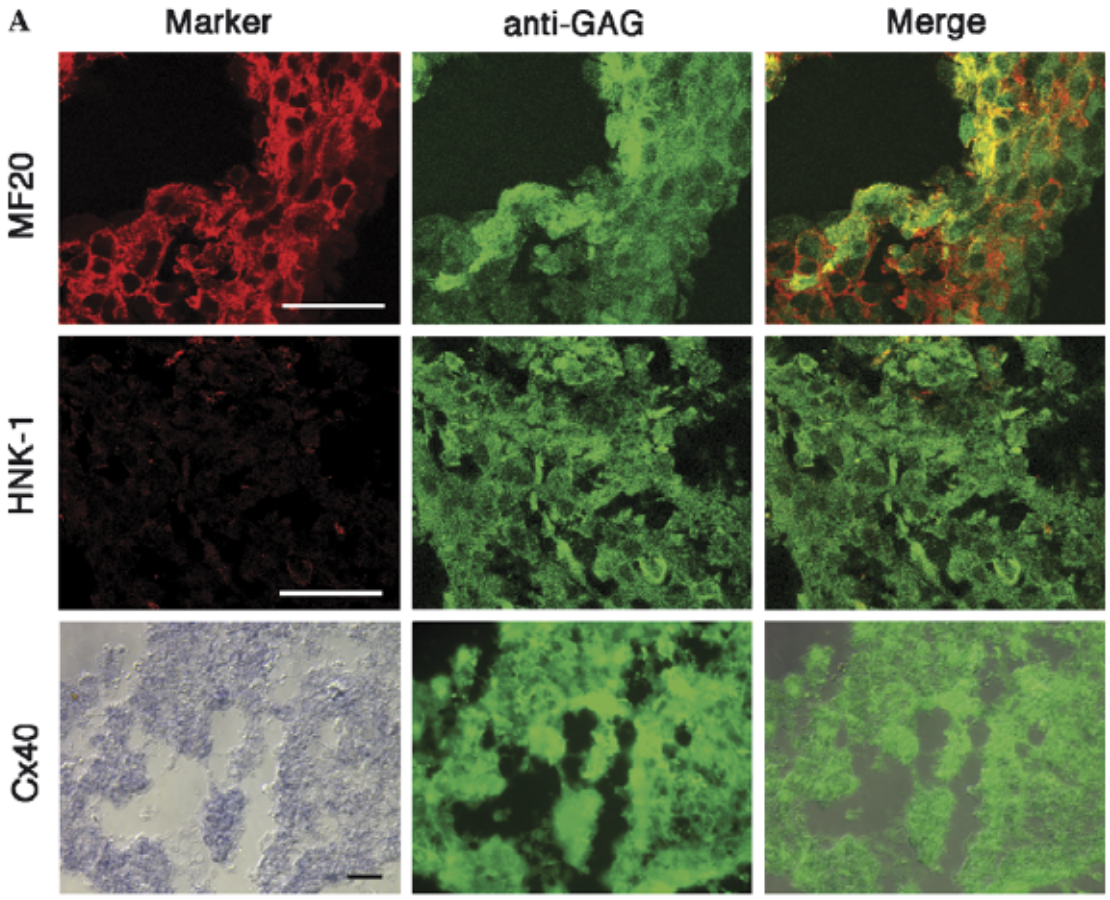
A
Marker
anti-GAG
Merge
MF20
HNK-1
Cx40

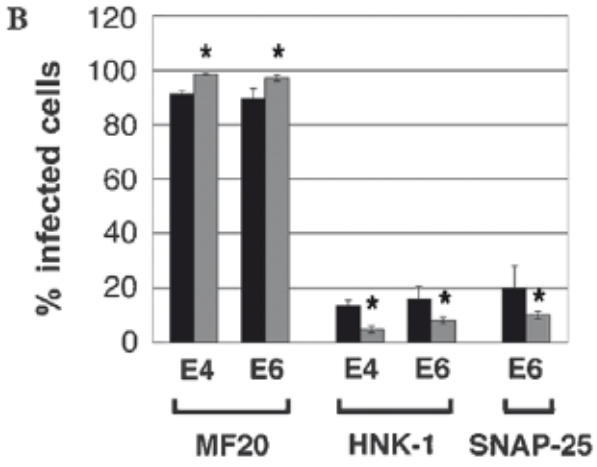
B
% infected cells
120
100
80
60
40
20
0
*
E4
E6
E4
E6
E6
MF20
HNK-1
SNAP-25

Figure 2.7. Expression of the dominant-negative form of Suppressor-of-Hairless alters the expression of cardiac cell type markers. Chick embryos were injected with the control virus, RCAS-GFP, or with the RCAS-Su(H)DN virus. (A) Hearts were harvested at E6 and E4 (not shown), sectioned and immunostained with anti-viral GAG antibody, and various cell type specific markers. Note that most of the RCAS-Su(H)DN infected are positive for MF20, but negative for HNK-1. Expression of Cx40 was also analyzed by in situ hybridization on the infected heart sections, followed by staining with anti-GAG antibody. In the RCAS-Su(H)DN infected areas, the Cx40 expression appears to be at a low level uniformly, unlike the control hearts which show relatively high levels of Cx40 in some subendocardial cells (Fig. 6A, B). Scale bars, 20 lm. (B) Quantification of the results by scoring the percentage of the RCAS-Su(H)DN infected cells that express various markers. Note that, compared to the GFP control (black bar), expression of Su(H)DN (gray bar) increased the percentage of cells positive for MF20, and decreased the percentage of cells positive for HNK-1 or SNAP-25, $p < 0.001$ for MF20, $p < 0.001$ for HNK-1 and SNAP-25. Asterisks indicate statistical significance.

RCAS-Su(H)DN-infected cells showing MF20 staining, compared to RCAS-GFP-infected cells, and a significant decrease in the percentage of RCAS-Su(H)DN-infected cells positive for HNK-1 and SNAP-25 (Fig. 2.7B).

To determine the effect of constitutive Notch signaling on the functional development of the ventricular conduction system, we utilized an optical mapping technique to visualize the propagation pathway of action potentials across the ventricular myocardium. High-speed imaging was performed on uninjected control, RCAS-GFP injected and RCAS-NIC-injected hearts. The hearts were dissected, stained with a voltage sensitive fluorescent dye, di-4-ANEPPS, and recorded for both the dorsal and ventral sides. After recording, hearts were fixed, sectioned, and the degree of infection was determined by anti-GAG staining. As the fluorescent signal decreases with an increase in membrane voltage, the most rapid decrease in fluorescent signal corresponds to an action potential. Custom software was developed to compute absolute values of rates of fluorescent change at each 5X5 pixel area of the entire ventricular surface and the maximum slope of the action potential was displayed as red in the color scale. Five beat series were analyzed for each heart and the patterns appeared consistent from beat to beat. Because a great majority of RCAS-NIC injected embryos died by E5 and hearts younger than E4.5 were difficult to handle because of their small size and fragility, we imaged live hearts at E4.5-5. Seven out of 12 uninjected control hearts at this stage exhibited an immature, unidirectional propagation pattern (Fig. 2.8A, upper sequence). After activation of the atrium, the impulse travels along the myocardial wall in a

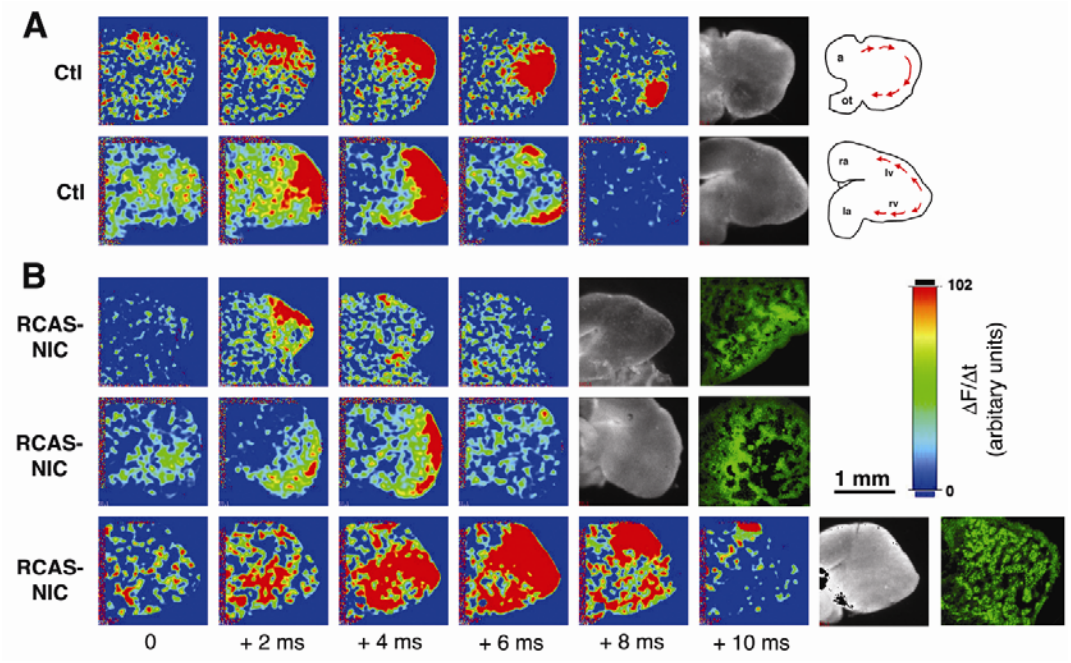
A
Ctl
Ctl
a
ot
ra
lv
rv
la
B
RCAS-NIC
RCAS-NIC
RCAS-NIC
102
ΔF/Δt
(arbitary units)
0
1 mm
0
+ 2 ms
+ 4 ms
+ 6 ms
+ 8 ms
+ 10 ms

Figure 2.8. Constitutively active Notch1 alters the conduction propagation pattern in embryonic chick hearts. (A) Optical mapping was performed on uninjected control hearts at E4.5-5. Images were collected at 2 milliseconds per frame, and processed using a custom software. The first derivative was computed and the maximum upstroke velocity was defined as dF/dt max and depicted as red in the color scale. Note, in the top panel, the impulse propagates along the myocardial wall from the atrium towards the outflow tract in the immature propagation pattern (red arrows) in about 8-10ms. Also note, in the bottom panel, the impulse travels from the apex to the base (red arrows) within 8ms in the mature activation sequence. (B) Optical mapping was similarly performed on RCAS-NIC-injected hearts at E4.5-5. After imaging, the hearts were fixed, sectioned and stained with anti-P27 to visualize the extent of infection (shown in green fluorescence). Note, the impulse fails to advance towards the base and dissipates within 4ms in the top two panels, and a diffuse activation pattern in the bottom panel. The heart in the bottom panel was more extensively infected with the RCAS-NIC virus.

unidirectional fashion towards the outflow tract. The action potential travels across the heart within 8-10 ms. The rest of the uninjected hearts (5 out of 12) displayed a mature, apex to base sequence of activation within a similar time frame (Fig. 2.8A, lower sequence), suggesting that the transition from an immature to a mature activation pattern occurs at around E4.5-5. These results are consistent with previous optical mapping studies in chick showing similar mature and immature activation patterns [60, 70, 152]. In 5 out of 24 hearts injected with RCAS-NIC, we observed an altered apex-to-base pattern in which the breakthrough impulse at the apex failed to advance towards the base. Instead of a normal 8-10 ms propagation time from apex to base, the activation sequence dissipated within 4 ms (Fig. 2.8B, upper and middle sequence). Upon analysis of the samples after imaging, we found that these hearts expressed NIC in a relatively wide spread area (approx. 20-50%) (Fig. 2.8B, green fluorescence images in top and middle panels). Another abnormal pattern found in the hearts injected with RCAS-NIC was a relatively diffuse activation pattern where the impulse at the apex of the heart traveled across the majority of the ventricular surface to the base (5 out of 24) (Fig. 2.8B, bottom sequence). These hearts appeared to be infected most broadly in the myocardium but not in the epicardium (approx. 70-95%) (Fig. 2.8B, green fluorescence image in bottom panel). The rest of the RCAS-NIC injected hearts had largely normal conduction patterns in the ventricle. These hearts were not as well infected, with only small patches of infection (data not shown). We also examined the activation patterns of RCAS-GFP-injected hearts (n = 14). These hearts displayed normal activation patterns within the same time frame as the control uninjected hearts (14 of 14), suggesting that viral

infection alone did not affect the conduction patterns. Taken together, these data suggest that expression of a constitutively active Notch resulted in an abnormality in the functional development of the cardiac conduction system.

Delta1 is a well-characterized ligand known to bind to the Notch receptor and activate the Notch signaling pathway. We analyzed the expression of Delta1 by performing in situ hybridization on chick heart sections. As shown in Fig. 2.9A, Delta1 transcripts were detected widely in myocardial cells in the ventricles at E3 and E6, but the signal was reduced at E9. It has been previously shown that Delta1 expression can be negatively regulated by Notch signaling through downstream basic helix-loop-helix (bHLH) transcription factors [86, 153, 154].

To test whether a similar feedback loop is also at work in this system, expression of Delta1 transcripts was analyzed in control RCAS-GFP or RCAS-NIC-infected hearts. As shown in Fig. 2.9B, the expression of Delta1 was decreased in areas infected with RCAS-NIC, but not in areas infected with control RCAS-GFP. These results suggest that Delta1 may act as a ligand for the Notch receptor and a negative feedback loop may also be present during cardiac differentiation.

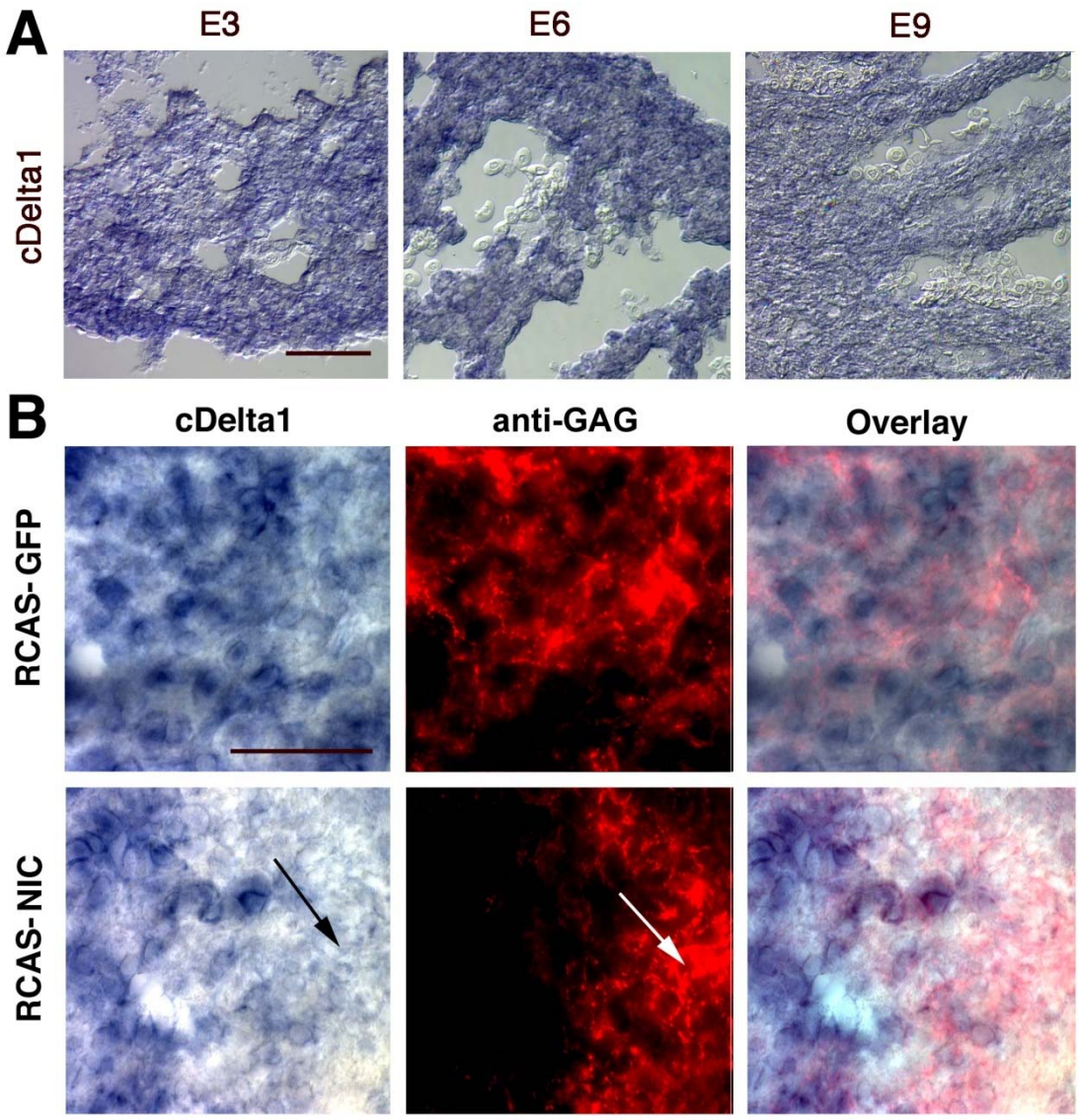
A
E3
E6
E9
cDelta1
B
cDelta1
anti-GAG
Overlay
RCAS- GFP
RCAS- NIC

Figure 2.9. Expression of Delta1 is decreased in the cells infected with RCAS-NIC. (A) Expression of chick *Delta1* transcripts in the developing heart. In situ hybridization was performed on cardiac sections of E3, E6, and E9 chick embryos. Note that *Delta1* is widely expressed in the myocardium. (B) Expression of *Delta1* is reduced in the areas infected with the RCAS-NIC virus. Heart tubes were injected with control RCAS-GFP or RCAS-NIC virus at HH9-10 and the infected hearts were harvested at E6. In situ hybridization was performed on the infected tissues with the *Delta1* probe, and the infected areas were detected by anti-viral GAG staining. Note that *Delta1* transcript expression was inhibited by the expression of NIC (arrows), but not GFP. Scale bars, 50 μm.

2.3. Discussion

In this paper, we show that Notch signaling plays an important role in cardiac cell differentiation. Notch1 transcripts are expressed in the early conduction lineage but not in cardiomyocytes in the ventricles. Expression of constitutively active Notch inhibits the expression of cardiac muscle proteins including sarcomeric myosin heavy chain and a actin. The effects of constitutively active Notch on the conduction cell markers are more complex: there was an increase in the expression of conduction lineage markers, HNK-1 and SNAP-25, but a decrease in the expression of Cx40. By using a Su(H)DN construct, we found that reducing Notch signaling resulted in an increase of MF20 expression and a decrease of conduction markers including HNK-1, SNAP-25, and a high level of Cx40 expression. These results suggest that Notch signaling plays a role, along with the inductive signals, in the genetic network regulating cardiac cell type specification and determination.

Multiple functions have been reported for the Notch pathway in heart development, in specification of the cardiogenic field in Xenopus and mouse [123, 125]. Mutations in the genes in the Notch signaling pathway result in various cardiac defects including pericardial edema, defects in formation of valves, atrial and ventricular septa, and in endocardial cushions [115, 117-121, 138-140]. We injected retroviruses after the completion of early cardiogenesis. Thus, initial cardiogenic processes in the RCAS-NIC injected samples were unaffected and the hearts retained largely normal morphology.

Our study thus provides evidence for an additional, later role of Notch1 in heart development, in the differentiation of ventricular cell types. The following evidence supports the notion that inhibition of cardiac muscle marker expression by RCAS-NIC is due to specific effects of Notch signaling, and not nonspecific effects of the virus. First, samples infected with a control virus expressing GFP displayed normal expression of myocardial and conduction cell markers, and have a normal conduction pathway, suggesting that the virus itself does not cause non-specific effects on cardiac differentiation. This type of virus has been widely used to study the development of many organ systems, and no significant adverse effects have been reported. Second, a significantly higher proportion of the RCAS-NIC-infected cells expressed the conduction cell markers, HNK-1 and SNAP-25. Third, the retrovirally expressed dominant negative Su(H) gave rise to the opposite effects of those with RCAS-NIC, suggesting that these effects on marker expression are likely due to specific effects of the transgenes, not nonspecific effects of viral infection. Fourth, the effects of constitutively activated Notch1 on cell differentiation are also consistent with its endogenous expression pattern; Notch1 is expressed in the conduction cell lineage at early stages, but not in myocardial cells.

Notch activity has been shown to influence various cell differentiation processes, by selecting a subset of cells from an initially homogenous precursor population [137]. This is mainly achieved through a process termed “lateral inhibition”, in which a small

difference in signaling among the cells is amplified through a feedback mechanism. A key element of this mechanism is that the expression of Delta is repressed by Notch signaling through downstream basic helix-loop-helix (bHLH) transcription factors [153, 154]. We have shown that Delta1 is similarly downregulated by constitutively activated Notch, suggesting that a feedback loop is possibly at work in cardiac differentiation.

Because our cell type markers are on the plasma membrane (HNK-1) or sarcomeric (MF-20), and the cells are large and densely packed, we used cytoplasmic staining of GAG rather than the nuclear myc staining for scoring. Although not all GAG-positive cells are positive for myc due to low sensitivity of a single copy myc, we think NIC is expressed by most of the GAG-positive cells. This is evident in the well-infected samples such as those shown in Figs. 2.4A and 2.3A, that nearly all the ventricular cells are positive for HNK-1 and negative for MF-20, respectively. Our results of constitutively active Notch on the expression of myocardial markers, MF20 and a-actin, and conduction markers, HNK-1 and SNAP-25, support that Notch1 is involved in cardiac differentiation by inhibiting cardiomyocyte but promoting early conduction cell differentiation. This is reminiscent of the role of Notch1 in the nervous and immune systems, where Notch inhibits neural and B cell fates, and promotes glial and T cell differentiation, respectively. However, the effect of Notch signaling on another conduction marker, Cx40, is more complex. Decreasing Notch signaling by using a dominant negative Su(H) construct shows that the high level of Cx40 expression is diminished but the low level of Cx40 expression in the myocardium remains unchanged.

Because conduction cells express high levels of Cx40 whereas the myocardial cells express low levels of Cx40, this result is consistent with our model that reduction of Notch signaling increases myocardial but decreases conduction cell differentiation. However, because Cx40 is a relatively later marker, Notch signaling may need to be turned down before high levels of Cx40 can be expressed in the conduction cells. Prolonged expression of constitutive active Notch may inhibit the expression of Cx40 in both the myocardial and conduction cells. This is consistent with our observation that Notch1 is only transiently expressed in the conduction cells (Fig. 2.1 and data not shown). Additional signals may also be required with the Notch signaling to turn on the maturation program of the conduction cells including high levels of Cx40 expression. Previous works have shown that paracrine factors released by the endocardium and endothelial cells of the coronary arteries, endothelin in chick and Neuregulin-1 in mouse, can increase the expression of conduction markers and cause a change in conduction pathway that is consistent with excess recruitment of functional Purkinje cells [69-71, 133]. Therefore, our current model is that transient Notch activity may be required for the initial separation of myocardial and conduction lineages by inhibiting cardiomyocyte differentiation and promoting early conduction cell differentiation, possibly through regulating the responsiveness of the cells
to paracrine factors.

Although HNK-1 has been shown as a conduction cell marker in chick and other species, it has also been used as a neural crest marker. However, we believe that the

HNK-1 expression induced by NIC indicates an increase in the conduction lineage cells rather than the neural crest cells for the following reasons. First, NIC increases the expression of another conduction marker SNAP-25 in addition to HNK-1. SNAP-25 has not been shown as a neural crest cell maker, which argues against an increase in neural crest cells. Second, expression of NIC through a non-viral vector by electroporation resulted in a similar increase of HNK-1 expression (data not shown). Because this vector cannot replicate, cells entering the heart after the initial electroporation, such as neural crest cells, will not be infected. Third, in some heavily infected hearts, nearly 100% of the ventricular cells are positive for HNK-1, but negative for MF-20. This is unlikely to be an exclusive effect on neural crest cells.

Our optical mapping studies show that approximately 41% of the RCAS-NIC injected mutants had obvious abnormality in the conduction pathway. Because optical mapping analyzes the pattern of action potential in epicardial cells, it is less likely to be affected by factors which may affect heart rate or contractility. For each heart, we analyzed at least five beat series to confirm that the abnormality is present consistently in each beat. In addition, the degree of abnormality correlated well with the degree of infection by the RCAS-NIC virus. The altered conduction system function revealed by optical mapping is consistent with our model that cells expressing constitutively active Notch are not fully differentiated functional conduction cells. These results are different from the phenotype observed in chick hearts with excess production of endothelin or mouse hearts treated with neuregulin-1, which induced alterations in activation patterns

consistent with additional recruitment of Purkinje cells [70, 71]. Optical mapping studies of the (Cx40) knockout mice indicated some delay or block in conduction velocities in the right bundle branch, and more diffuse breakthrough sites in the left ventricle [155, 156]. Chimeric mice generated from stem cells deficient for connexin 43, a gap junction predominantly expressed in the ventricular myocardium, displayed conduction delay [157]. Thus, reduced expression of gap junction proteins can lead to conduction abnormalities. Because constitutively active Notch down-regulates the expression of Cx40, we speculate that the conduction abnormalities of the RCAS-NIC-injected hearts may be in part due to decreased expression of Cx40. In the hearts moderately infected with RCAS-NIC, a general correlation of blocked pathway with the area of infection was observed, suggesting a block in the infected areas. In the hearts highly infected by RCASNIC, Cx40 expression may be downregulated throughout the myocardium, causing the electrical impulse to disperse across the epicardial surface. Because our optical mapping protocol detects electrical propagation across the epicardial surface, we therefore observed a diffuse activation pattern.

Retroviral lineage analyses have shown that the central and peripheral conduction systems may arise separately although they both share lineages with cardiomyocytes [66, 67]. In chick, two different conduction cell localizations have been described: subendocardial and periarterial [127]. Because most of the well-infected RCAS-NIC embryos died around E5, prior to the formation of periarterial conduction cells, our current study has been focused on subendocardial conduction cells in the ventricles.

However, at early stages such as E3 and E4.5, cells expressing Notch1 and HNK-1 appear not always associated closely with the endocardium. This possibly represents an early pattern prior to the establishment of more defined subendocardial localization, as we have observed this pattern in multiple samples in multiple experiments. It is also interesting to note, that Notch1 appears to be expressed in vascular endothelial cells in the coronary vessels after E9.

While our results support a role for Notch1 in cardiac cell differentiation in the ventricles, we currently do not have evidence whether it is involved in atrial cell differentiation. We focused our study on ventricles because some of the cell type markers we used are not as specific in the atria as they are in the ventricles. Although Notch1 expression was reported in the outflow tract, the atrioventricular canal, the trabeculae of the ventricles, the epicardium, the aorta [108], and the endocardium [115, 158, 159], the expression of Notch1 has yet to be reported in myocardium in mouse. The differences in expression patterns of Notch1 reported in the heart likely reflect dynamic and transient nature of the expression patterns of Notch1. Mutant mice with a targeted deletion of the Notch1 gene die before E11. Although severe pericardial edema was reported for these mutant mice, these mice have a beating heart at E10.5 [111]. It is likely, therefore, that the central conduction system is differentiated to a certain extent by this stage. It is possible that Notch1 function is not required for the differentiation of the central conduction system, or other Notch receptors expressed in the heart may compensate for the loss of the Notch1 receptor. It has been reported that the Notch2 and

Notch3 genes are also expressed in the developing heart [112, 160]. With the characterization of Notch function in chick conduction system development, further study on the role of Notch in the murine conduction system development is warranted.

2.5. Experimental procedures

Whole-mount and section in situ hybridization

Standard specific pathogen-free white Leghorn chick embryos from closed flocks were provided fertilized by Charles River Laboratories (North Franklin, Connecticut). Eggs were incubated inside a moisturized 38°C incubator. The embryos were staged according to Hamburger and Hamilton [161]. Because our analyses were focused on embryos at relatively late stages, we chose to describe the ages of embryos by embryonic days rather than Hamburger-Hamilton stages. E3, E4.5, E6, E9 are equivalent to Hamburger and Hamilton stages 20, 25, 29, and 35, respectively. The hearts were dissected and fixed in 4% paraformaldehyde at 4°C for 12-24 h. Cryosections of 20 μm thickness were prepared from tissue OCT blocks on a cryostat (Leica, Deerfield, IL) and collected on Superfrost Plus slides (Fisher Scientific, Pittsburgh, PA). Whole-mount and section in situ hybridization were performed as previously described in [38, 162] and [159]. cDNA plasmids used for generating the Digoxigenin-labeled Notch1 and Delta1 probes were provided by Dr. D. Henrique. Full length chicken connexin 42 cDNA was obtained from the chicken EST database (MRC Geneservice).

Immunofluorescence staining and data analysis

Immunofluorescence staining was carried out on cryosections of the heart. Sections were fixed in 4% paraformaldehyde, and blocked in 10% calf serum DME with 0.2% Triton X-100. Primary and secondary antibodies were diluted in block, and incubated for 1h at room temperature or overnight at 4°C. Viral infection was confirmed by using the mouse polyclonal anti-gag antibody, p27 (SPAFAS, Norwich, CT). The mouse monoclonal antibody of the muscle marker, MF20, was obtained from the Developmental Studies Hybridoma Bank (University of Iowa, Iowa City, IA). HNK-1 was obtained from ATCC (Manassas, VA), a-actin antibody was obtained from Dako Cytomation (Carpinteria, CA), and SNAP-25 was obtained from Sternberger Monoclonals, Inc. (Lutherville, MD). The nuclear stain, DAPI and Hoechst Dye 34580 were obtained from Roche (Indianapolis, IN), and Molecular Probes (Eugene, OR), respectively. Stained sections were analyzed and scored using the Leica TBS SP2 confocal microscope and software. A total of 500 randomly selected cells were scored from each heart, and a total of four different hearts were examined for each marker. The percentage of infected cells expressing the observed marker was used for statistical analysis by unpaired Student's t test.

Viral constructs

The mouse Notch intracellular domain (NIC) construct was obtained from Dr. Jeffrey Nye. NIC insert was released from the plasmid and cloned into the avian replication-competent retrovirus, RCAS. G-coat viruses were prepared by transient transfection as

previously described in [39]. Early heart tubes of HH stage 9 embryos were injected with the viral stocks. Because the embryos injected with the undiluted viral stock had high rate of mortality, we diluted the viral stocks 1:2 to increase the chances of survival. The dominant-negative form of Suppressor-of-Hairless was a gift from Dr. Nathan Lawson (UMass Medical School,Worcester, MA). The 2.5 kb fragment was cloned into the ClaI site of RCAS. RCAS virus was similarly prepared and used for injection into the heart tubes of HH 9 embryos.

Optical mapping

Optical mapping technique was modified from previously published procedures [152]. Hearts were dissected from uninjected control, RCAS-GFP injected, and RCAS-NIC-injected E4.5 embryos, and stained by submerging in a 0.002% solution of voltage sensitive fluorescent dye, di-4-ANEPPS (Molecular Probes), in Tyrodes-HEPES buffer, pH 7.4, for 4 min at room temperature. The hearts were then transferred to oxygenated 37ºC Tyrode's solution imaged on a custom-built upright wide-field epifluorescence microscope equipped with a 128 X 128 pixel, high-speed, 100% imaging duty cycle electron multiplying CCD camera (Cascade 128+, Photometrics, Tucson, AZ). The laser shutter, camera control and image storage were managed by Metaview software (Universal Imaging, Philadelphia, PA). Hearts were imaged using an Olympus 2X objective lens, with an overall magnification of 10 l/pixel. As the contraction of the heart at this stage did not appear to interfere with the imaging, no motion inhibitors were used. The dye was excited with the 514 nm line of an argon laser, and the emitted fluorescence

was imaged onto the camera through a 580 nm long pass emission filter. A simple image streaming protocol was set up in Metaview and used for all image acquisitions. For each sequence, the laser shutter was opened and 4000 images were streamed directly to system memory at 500 frames/sec (2 ms exposure per image frame). The data were processed using a custom software program as follows. Images were first smoothed using a 5 X 5 box filter, and the first time derivative was computed by subtracting successive images ($dF_i \backslash dt \approx | F_i - F_{i-1} | \backslash 2$ ms, where F is the average fluorescence measured in each smoothed picture element). The maximum upstroke velocity was defined as dF/dt max and depicted as red in the color scale accompanying the sequence of difference images. For most of the hearts, the difference images were analyzed for five beat sequences to confirm the results. In all cases, we found that the activation patterns are consistent from beat to beat, despite some minor differences.

Chapter III: Notch activation increases cardiac cell migration by regulation of cell-cell adhesion and motility

3.1 Abstract

Cell migration is of paramount importance for animal development, essential for morphogenesis and cell differentiation. Many cells initiate migration with a process of delamination, or detachment from their neighboring cells, and become motile. However, the molecular and cellular mechanisms underlying migration processes during embryonic development remain poorly understood. To address the role of Notch signaling in cell migration, we expressed a constitutively active Notch construct and a dominant negative Suppressor-of-Hairless [Su(H)] construct to decrease Notch signaling, in a limited number of cardiac cells in a largely wild type environment in vivo. We found that Notch activation is both necessary and sufficient to promote cardiac cell migration. By developing a 3D gel culture assay combined with marker analysis and time-lapse microscopy, we found Notch activity affects cardiac cell migration by increasing delamination/emigration as well as increasing cell motility. Furthermore, we show that the increase of cell migration by activated Notch is independent of its effects on cell differentiation. We provide evidence that Notch activity decreases the expression of N-cadherin, a predominant adhesion molecule in cardiomyocytes, which may underlie its effect on delamination.

3.2 Introduction

Cell migration is one of the most important processes in animal development, integral to morphogenesis and cell differentiation [96, 97]. Selected cells are signaled to convert from a static to motile state and leave their place of birth in a highly controlled manner. Cells loosen their attachment to the surrounding tissues, and start to migrate with specific direction, velocity, and towards specific destinations. Despite the importance of cell migration in development and tumorigenesis, the mechanisms underlying the control of cell migration remain poorly understood.

The Notch signaling pathway is an evolutionarily conserved mechanism best characterized in controlling cell fate decisions through local cell interactions [78-80]. The Notch gene encodes a 300 kDa single-pass type I transmembrane receptor that consists of a large extracellular domain and an intracellular domain (NIC). Two families of membrane bound proteins, Delta and Serrate/Jagged, have been identified as ligands for the Notch receptors. Upon interaction with its ligands at the extracellular region, the Notch receptor undergoes a series of proteolytic cleavages to release the intracellular domain. Nuclear translocation of NIC allows heterodimerization with the Suppressor-of-Hairless [Su(H)] protein (also called RBPJk/CBF1), which activates downstream target genes. In the nervous system, Notch signaling has been shown to play a key role in the differentiation between neurons and glial cells [82, 83, 85, 86, 163]. During lymphocyte

development, constitutive activation of Notch1 promotes T cell development at the expense of B cells [90].

In addition to its roles in cell fate determination, Notch signaling has been implicated in cell migration during organogenesis. Conditional ablation of Jagged1 in mice leads to granule cell migration defects during embryonic cerebellar development [106]. Similarly, Delta-1 null mice exhibit abnormal migration of neural crest cells due to disruption in the normal distribution of ephrin molecules [105]. In zebrafish, embryos injected with morpholino oligonucleotides against Suppressor of Hairless [Su(H)] to decrease Notch signaling exhibit increased migration and proliferation of endothelial cells during blood vessel sprouting [107]. However, as Notch activation usually causes multiple effects including cell proliferation, differentiation, apoptosis, along with cell migration, the underlying mechanisms by which Notch influences cell migration remains to be characterized.

Highly regulated patterns of cell migration, proliferation and differentiation are fundamental processes of heart development. During development, myocardial cells in the ventricular segments proliferate and migrate inwardly toward the ventricular lumen to form trabeculae, characteristic finger-like protrusions (Fig. 3.1A) [7, 42, 43]. Subsequent fusion of the trabeculae contributes to the formation of the thickened myocardium, interventricular septum, and future sites of the conduction system [45]. Conduction cells are specialized cells responsible for setting and coordinating rhythmic heart beating, and

are known to be derived from common progenitor cells with cardiac muscle cells [66, 67]. Mouse mutants lacking *BMP10*, *neuregulin-1* or neureulin-1 receptors ErbB2, 4 exhibit defective trabeculation and hypoplastic ventricular growth [52, 53]. Injection of neuregulin-1 into mouse embryos promoted trabeculation without increasing cell proliferation [51].

We have previously found that Notch signaling plays a key role in the cell fate decision between cardiac myocytes, and conduction cells, two predominant cell types derived from common progenitor cells [164]. Constitutively active Notch signaling promotes the expression of conduction cell markers and inhibits the differentiation of cardiac muscle cells. In this study, we demonstrate that Notch signaling increases cardiac cell migration both by *in vitro* and *in vivo* approaches. Our results indicate that the effects of Notch on cell migration are two-fold: increasing cell delamination/emigration by decreasing the expression of N-cadherin and additionally increasing the motility of cardiac cells. We provide further evidence that its effects on cell migration are independent of its effects on cell differentiation.

3.3 Results

We have previously shown that *notch1* gene is expressed in a dynamic pattern in the developing ventricles, in undifferentiated precursor cells and newly differentiated conduction cells [164]. To characterize the role of Notch1 signaling in developing cardiac cells, we injected HH9 (~E1.5) chick heart tubes with a replication competent

retrovirus, encoding the intracellular domain of Notch1 (RCAS-NIC) (Fig. 3.1B). The intracellular domain of Notch1 has been previously shown to elicit a constitutively active phenotype [147]. A retrovirus RCAS-GFP encoding the green fluorescent protein was similarly injected as a control (Fig. 3.1B). After injection, the embryos were allowed to develop in ovo until embryonic day 4.5 (E4.5). Heart sections were stained with an anti-viral gag antibody (green), to identify infected cells. As most of the embryos infected heavily with RCAS-NIC died around E4.5, embryos survived to that stage tended to have limited infection rate.

Trabeculae are known to arise from proliferation and centripetal migration of myocardial cells from the compact layer (Fig. 3.1A). To assess the role of Notch in cardiac cell migration, we analyzed the distribution patterns of cells infected by RCAS-NIC or RCAS-GFP in partially infected hearts. Heart sections were double-stained by anti-viral GAG to visualize infected cells, and the antibody HNK-1, to label the conduction cells normally localized beneath the endocardium. Cells expressing control GFP are distributed through the entire thickness of the heart including the future compact zone and trabeculae, similar as reported in lineage tracing studies (Fig. 3.1C) [43, 44]. However, cells infected with RCAS-NIC appeared to distribute more centrally within the heart in the trabeculae area away from the compact zone (Fig. 3.1D). As we previously reported that cells expressing NIC are promoted toward conduction cell differentiation [164], RCAS-NIC-infected cells but not the control RCAS-GFP-infected cells are largely positive for HNK-1 (Fig. 3.1C and D). To quantify the results, we analyzed cell

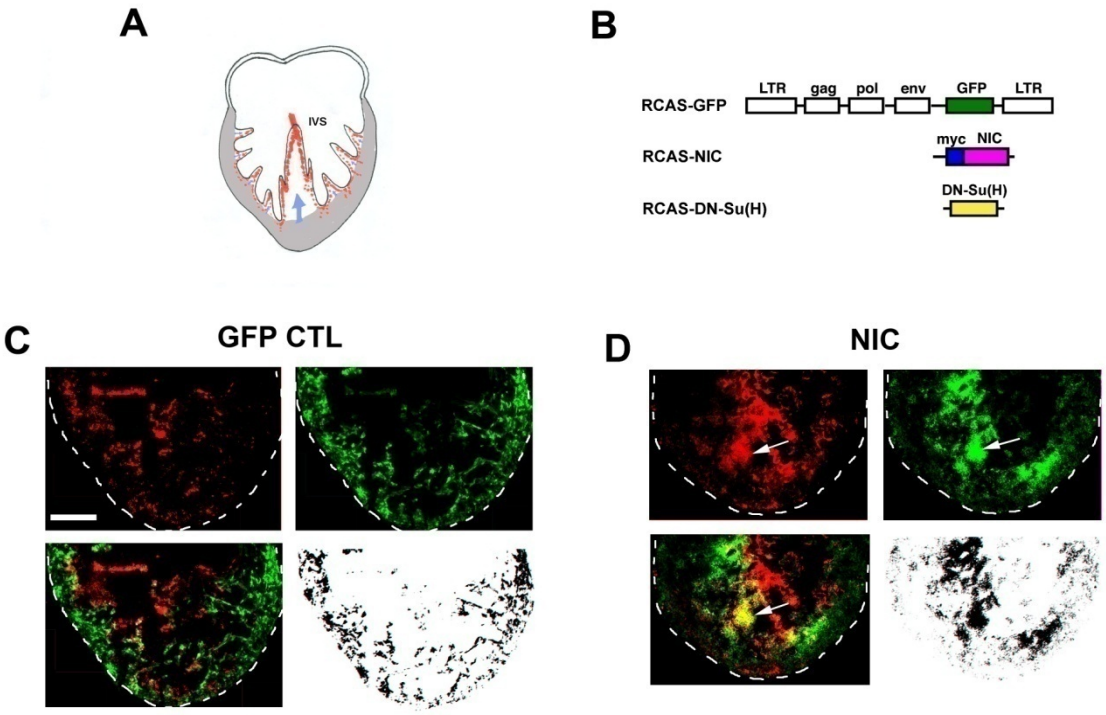
A
IVS
B
LTR
gag
pol
env
GFP
LTR
RCAS-GFP
myc
NIC
RCAS-NIC
DN-Su(H)
RCAS-DN-Su(H)
C
GFP CTL
D
NIC

Figure 3.1. Constitutively active Notch (NIC) causes disproportionate localization of the infected cells in the center region of the heart. **A.** Diagram of a cross section of the heart. Proliferation and centripetal migration (blue arrow) of the cardiac cells from the outerlayer (future compact zone, grey shaded area) of the heart resulted in formation of trabeculae. Fusion of trabeculae contributes to the formation of interventricular septum (IVS) and the peripheral conduction system (red) is closely associated with the trabeculae. **B.** Viral constructs encoding for control GFP, constitutively active Notch (NIC), and dominant negative Su(H) [DN-Su(H)]. **C, D.** RCAS-NIC or control RCAS-GFP-injected hearts were harvested at E4.5, sectioned, immunostained with anti-GAG (green) to show the infected cells and the conduction marker HNK-1 (red). Merged images and binary images (black and white image) are also shown. White dashed lines mark the outer edge of the heart. Note that the RCAS-GFP-infected cells are distributed throughout the entire thickness of the heart, whereas the RCAS-NIC-infected cells localize more centrally within the heart. Additionally, RCAS-NIC-infected areas also largely co-localize with HNK-1 staining (arrow). Scale bar in B and C = 500 μm.

localization by using NIH Image J software which allowed us to convert the fluorescent images to binary images (black and white images in Fig. 3.1C, D, and Fig. 3.2A, B) and calculate the average distance of the infected cells from the edge of the heart (see Method). A total of 4 hearts and 2 sections per heart were analyzed and calculated for each experimental condition. We found that the RCAS-NIC-infected cells were a significantly greater distance away from the edge of the heart as compared to control RCAS-GFP-infected cells, with an average of 523 ± 243 μm vs. 150 ± 54 μm, respectively (Fig. 3.2C). These results suggest that expression of constitutively active Notch in the ventricles causes disproportionate localization of cells in the trabeculae.

To determine whether Notch signaling is required for the proper localization of cardiac cells, we injected HH9 (~E1.5) heart tubes with a retroviral construct encoding the dominant-negative form of Suppressor-of-Hairless [RCAS-DN-Su(H)] (Fig. 3.1B). Dominant negative Su(H) interferes with activation of target gene expression in response to Notch signaling, thus inhibiting Notch signaling [83, 151]. As we previously reported [164], the RCAS-DN-Su(H)-infected cells were largely negative for conduction marker HNK-1 expression (Fig. 3.2B). Embryos with heavy infection rate died early before E4.5. In hearts with more limited infection, DN-Su(H)-infected cells tended to localize at the outer edge of the compact layer and less in the trabeculae than the control GFP-infected cells (Fig. 3.2A, B). Quantification shows that the cells expressing dominant negative Su(H) traveled shorter distances as compared to those expressing GFP control, 83 ± 11 μm vs. 150 ± 54 μm, respectively (Fig. 3.2C). These results suggest that Notch1

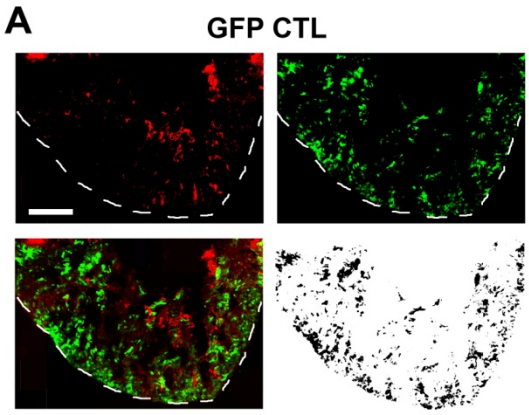
A
GFP CTL

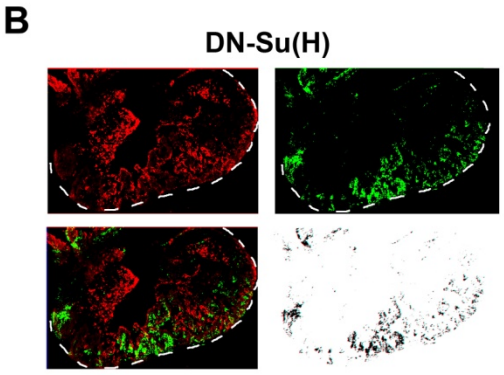
B
DN-Su(H)

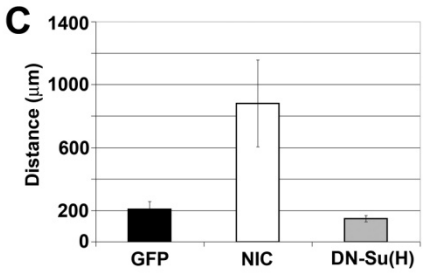
C
1400
1000
600
200
0
Distance (µm)
GFP
NIC
DN-Su(H)

Figure 3.2. Dominant-negative Suppressor of Hairless [DN-Su(H)] causes cells to localize preferentially at the periphery of the heart. RCAS-DN-Su(H) or control RCAS-GFP-injected hearts were harvested at E4.5, sectioned, immunostained with anti-GAG (green) and the conduction marker HNK-1 (red), and analyzed at low magnification on an epiflourescence microscope. **A**. RCAS-GFP-infected cells are found throughout the thickness of the heart as seen in the green immunofluorescent image, and the binary image (black and white image). **B.** In contrast to RCAS-GFP-infected cells, RCAS-DN-Su(H)-infected cells localize at the periphery of the heart, at the base of the prospective compact layer. Additionally, RCAS-DN-Su(H)-infected cells lack HNK-1 staining. Merged images and binary images (black and white image) were shown. White dashed lines mark the outer edge of the heart. **C.** Quantification of the migration distance traveled by infected cells within infected patches from the edge of the heart to the center of the patch, $p < 0.01$, Student's t-test. Scale bar = 500 μm.

signaling is also required for proper localization and migration of cardiac cells in the ventricles. Generation of trabeculae requires the coordination of cellular proliferation and migration. To determine if constitutive activation of Notch1 can increase proliferation, we injected RCAS-GFP, and RCAS-NIC viruses at E1.5, and labeled the embryos in ovo at E4.5 with BrdU. As shown in Fig. 3.3A and B, no significant difference was observed in the number and distribution of $BrdU^+$ cells in the control GFP- versus NIC-expressing cells. This result suggests that, under this experimental condition, constitutively active Notch1 does not significantly increase myocardial cell proliferation.

To further characterize the effects of Notch signaling on cardiac cell migration, we developed an explant culture system designed to assay cell migration in a collagen gel. E4.5 ventricles were dissected, cut into small pieces, and embedded in a collagen gel. Care was taken not to include the atrioventricular junction, because the atrioventricular junction is known to undergo epithelial-mesenchymal transformation. The explants appeared viable and contracting and a subset of myocardial cells migrated out of the uninfected control, and control RCAS-GFP-infected explants (Fig. 3.4A, B). Cell migration appeared to continue for 48 hours in the gel culture. However, a substantially higher number of cells migrated out from ventricular explants infected with RCAS-NIC (Fig. 3.4C). The numbers of cells migrated were scored in three independent experiments, each experiment including 20 explants from 4 hearts, and the data were normalized to control. RCAS-GFP-infected explants displayed a similar number of cells

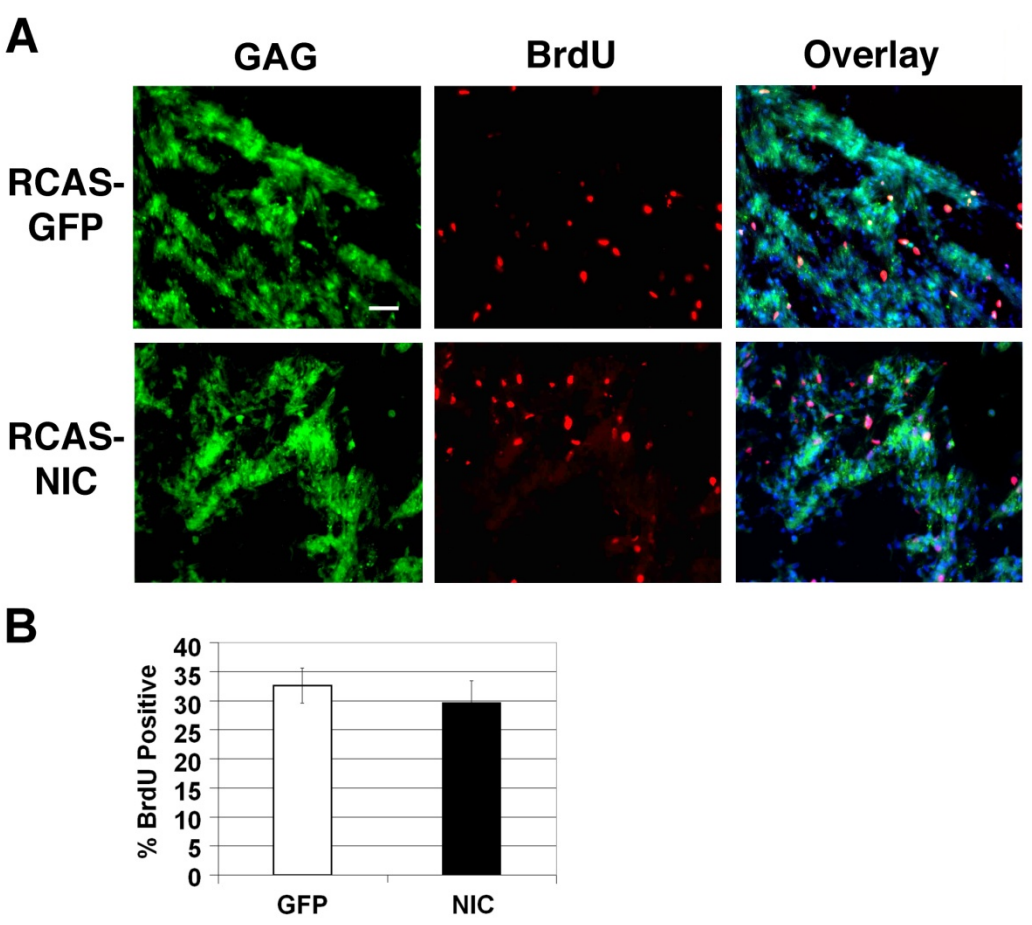
A
GAG
BrdU
Overlay
RCAS-GFP
RCAS-NIC
B
% BrdU Positive
40
35
30
25
20
15
10
5
0
GFP
NIC

Figure 3.3. Constitutively active Notch does not increase myocardial proliferation. E4.5 RCAS-NIC or control RCAS-GFP-injected hearts were labeled with BrdU for 3 hours, harvested, sectioned, and immunostained with anti-GAG (green) and anti-BrdU (red). **A.** Distribution of proliferating cells in RCAS-GFP and RCAS-NIC-infected hearts. Note that RCAS-NIC-infected hearts do not appear to have an increased number of $BrdU^+$ cells. **B.** Quantification of the percentage of RCAS-GFP or RCAS-NIC-infected cells that are $BrdU^+$. Scale bar, 20 μm

\

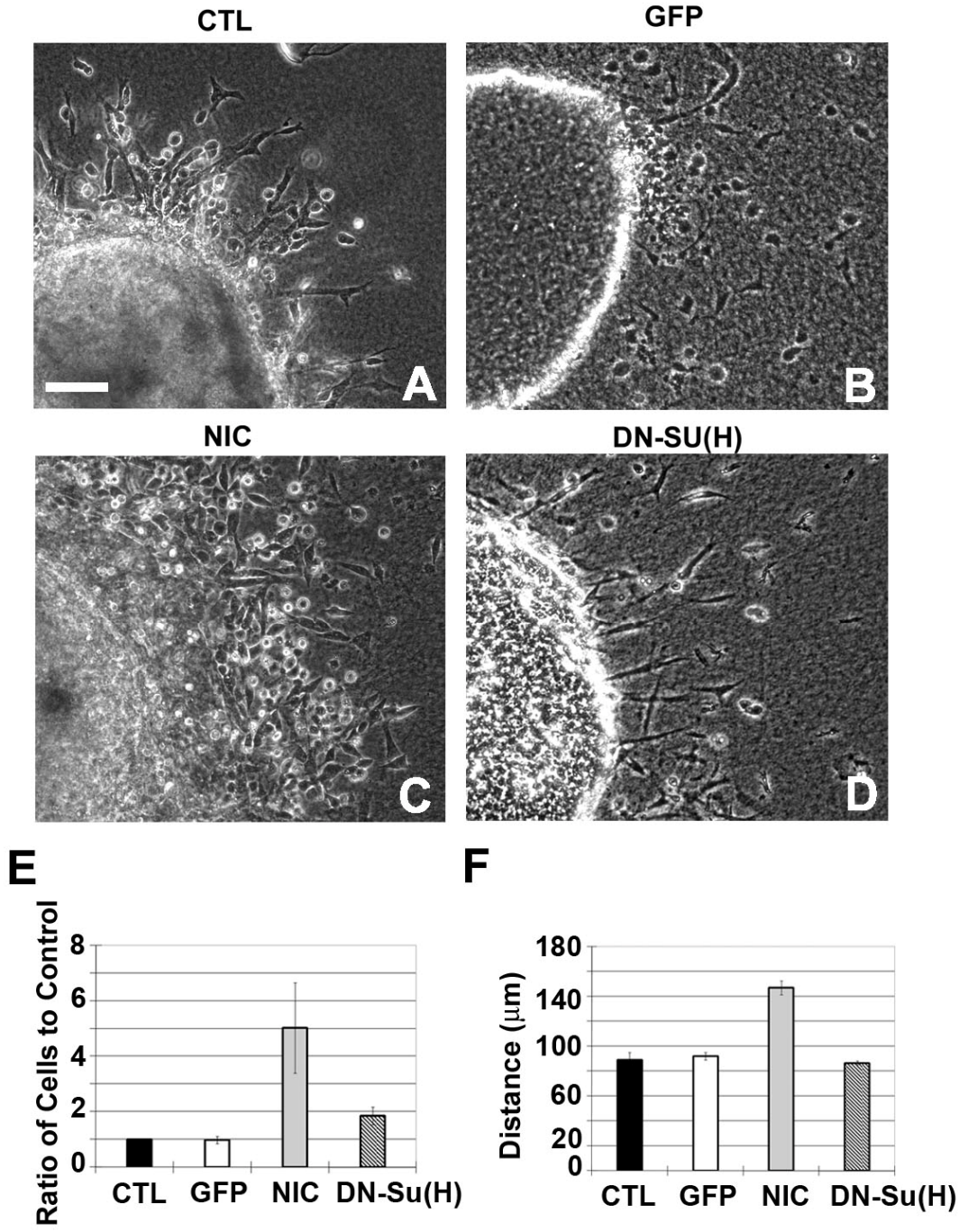
CTL
GFP
A
B
NIC
DN-SU(H)
C
D
E
Ratio of Cells to Control
8
6
4
2
0
CTL
GFP
NIC
DN-Su(H)
F
Distance (μm)
180
140
100
60
20
0
CTL
GFP
NIC
DN-Su(H)

Figure 3.4. Notch signaling regulates cell migration in explant culture. E4.5 chick ventricular explants were prepared from control uninjected (**A**), RCAS-GFP- (**B**), RCAS-NIC- (**C**), or RCAS-DN-Su(H)- (**D**) injected hearts, and cultured in collagen gel for 48 hours. **E.** Quantification of the number of cells migrating from the cardiac explants. **F.** Quantification of the migration distance traveled by cells from the edge of the explant to the rim of the ring formed by most of the migrated cells, $p < 0.01$. Scale bar in A common to B, C and D= 50 μm

that migrated from the explants as compared to control, suggesting that retroviral infection has no effect on migration in vitro. The number of cells migrated from the RCAS-NIC-infected explants was increased to 5.0 ± 1.6 fold compared to that of the uninfected control (Fig. 3.4E). Additionally, as the cells migrated out and formed a ring around the explant, we measured the distance from the rim of the rings to the edge of the explants: 147 ± 5.6 μm in RCAS-NIC-injected samples, versus 88.9 ± 6.0 μm in the uninfected controls, and 92.2 ± 3.0 μm in the GFP-infected controls (Fig. 3.4F). These results suggest that persistent Notch signaling increases the number of cells that migrated out and the migration distance of the cardiac cells in the explant gel culture assay. Similar collagen gel assays were performed on hearts infected with RCAS-DN-Su(H). An increase in the mean number of cells migrated away from RCAS-DN-Su(H)-infected explants was observed (Fig. 3.4E) compared to control uninfected explants (Fig. 3.4D). However, cells in the RCAS-DN-Su(H)-infected explants traveled a similar distance away from the explants as compared to control (Fig. 3.4F).

To identify the infected cells within the explants, we stained the collagen gel explants with an anti-viral GAG antibody. The majority (~ 80%) of cells that migrated away from RCAS-NIC-infected explants was positive for anti-GAG staining, indicating that these cells were expressing constitutively active Notch1 (Fig. 3.5G). Strikingly, none of the cells migrated away from RCAS-DN-Su(H)-infected explants were positive for GAG, suggesting that these cells were not infected with the RCAS-DN-Su(H) retrovirus (Fig. 3.5J). After analyzing 15 explants from three independent experiments,

we found that the RCAS-DN-Su(H)-infected cells only remained within the explants and did not migrate out (Fig. 3.5J). Fewer cells migrated away from the explants infected heavily with RCAS-DN-Su(H) compared to control samples. However, higher number of cell migrated away from those less heavily infected explants. These results confirmed the observations from in vivo experiments that Notch1 signaling is important for migration of cardiac cells.

Previously, we found that Notch1 signaling plays a role in the cell fate decision between cardiac muscle and conduction cell lineages. Constitutively active Notch signaling increases certain conduction marker expression, including HNK-1 and SNAP-25 [164]. To determine whether the role of Notch1 in cellular migration results from increased conduction marker expression, we stained collagen gel explants with the antibody, HNK-1. Interestingly, all of the cells that migrated away from the explants lacked HNK-1 staining, while some cells within the explants exhibited HNK-1 staining (Fig. 3.5B). Absence of HNK-1 staining in migrated cells was observed in cultures derived from all samples, including uninfected, and RCAS-GFP-, RCAS-NIC-, and RCAS-DN-Su(H)-infected explants (Fig. 3.5B, E, H, K). Factor(s) present within the explant but not in the collagen gel, may be required to maintain the expression of HNK-1.

We also analyzed another conduction cell marker, SNAP-25, which we have previously shown to be upregulated by Notch signaling [164]. Similar gel culture experiments followed by immunofluorescent staining showed that SNAP-25 expression

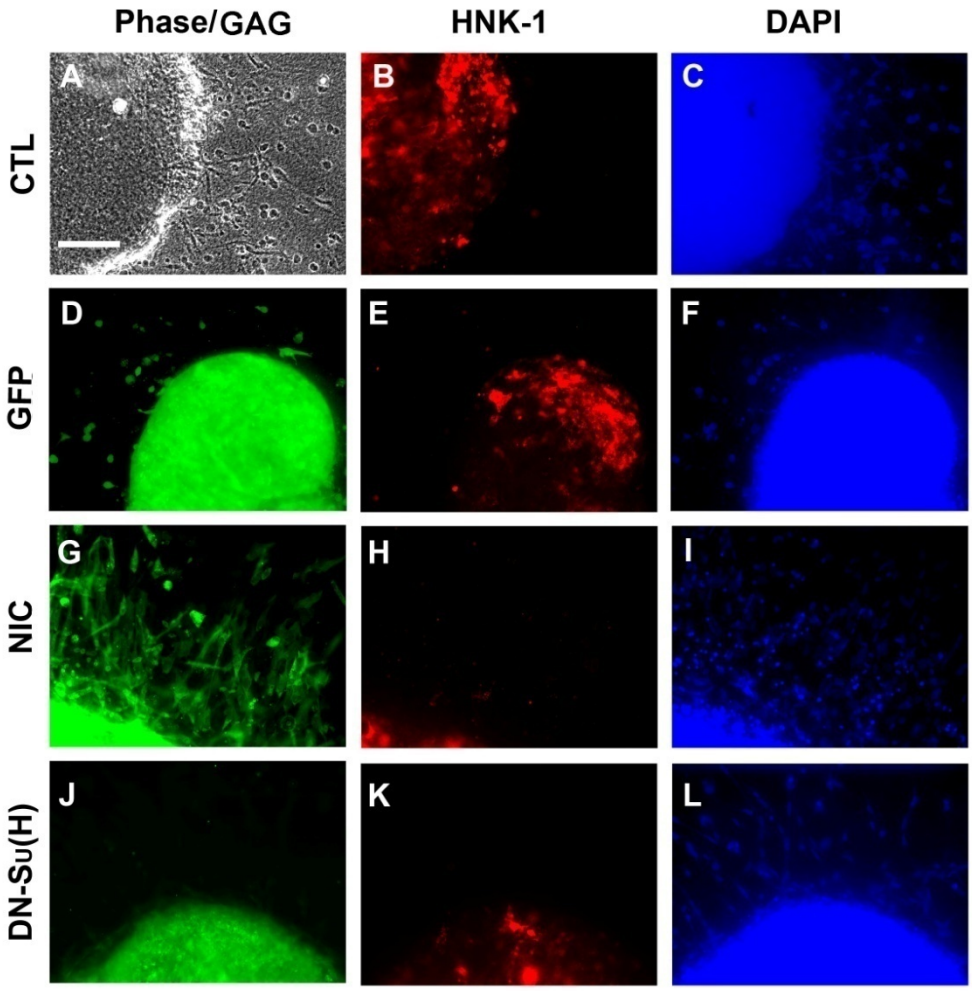
Phase/GAG
HNK-1
DAPI
CTL
GFP
NIC
DN-Su(H)
A
B
C
D
E
F
G
H
I
J
K
L

Figure 3.5. The effects of Notch signaling on cell migration do not require expression of the conduction marker HNK-1. E4.5 cardiac explant gel cultures were immunostained with anti-GAG (green), conduction marker HNK-1 (red), and the nuclear dye, DAPI (blue). Explant cultures were prepared from control uninjected (**A**-**C**), RCAS-GFP- (**D**-**F**), RCAS-NIC- (**G**-**I**) or RCAS-DN-Su(H)- (**J**-**L**) injected ventricles. Note that HNK-1 staining was confined inside the explants but not on any of the migrated cells regardless of the samples (B, E, H, K). The majority (~80%) of cells migrated from RCAS-NIC-infected explants are positive for anti-GAG staining (**G**). However, none of the cells infected by RCAS-DN-Su(H) migrated out of the explants (**J**). Scale bar in A common to all panels = 50 μm.

was absent in the control explant cultures (Fig. 3.6), likely due to the fact that SNAP-25 expression is late and does not turn on until E6 in vivo (Fig. 3.6B). In RCAS-NIC-infected explants, most cells did not express SNAP-25, with the exception of a few cells located in the migrated cell population and within the explants (Fig. 3.6E, H). These results indicate that cell migration in gel culture does not require the expression of conduction cell markers, including HNK-1 and SNAP-25, and the effect of Notch on cell migration is not secondary to increased conduction cell marker expression.

To further characterize the effect of Notch signaling on cell migration, we performed time-lapse microscopy on cardiac cell explants in the gel culture. Cardiac explants from control and RCAS-NIC-infected hearts were embedded in collagen gels and cultured for 20-24 hours before filming. Explants were filmed for 1-12 hours in a temperature, and CO_2-controlled setting. Because the migration patterns of the cell did not appear to change substantially over time, we analyzed only the first 30 minutes of the movies for simplicity. The first frames taken at the beginning of filming were aligned with the frames corresponding to the 30 minute time-point to determine the extent of cell migration. Only cells that had migrated from the explants and were not in contact with more than one other cell were analyzed for motility, speed and directionality (Fig. 3.7A). 49.1% of cells that had migrated from wildtype explants were motile during the first 30 minute time frame of the movies. However, a significant increase in the percentage of motile cells (70.5%) was observed in RCAS-NIC-infected explants (Fig. 3.7B). The velocity of the motile cells in the RCAS-NIC-infected explants, however, did not

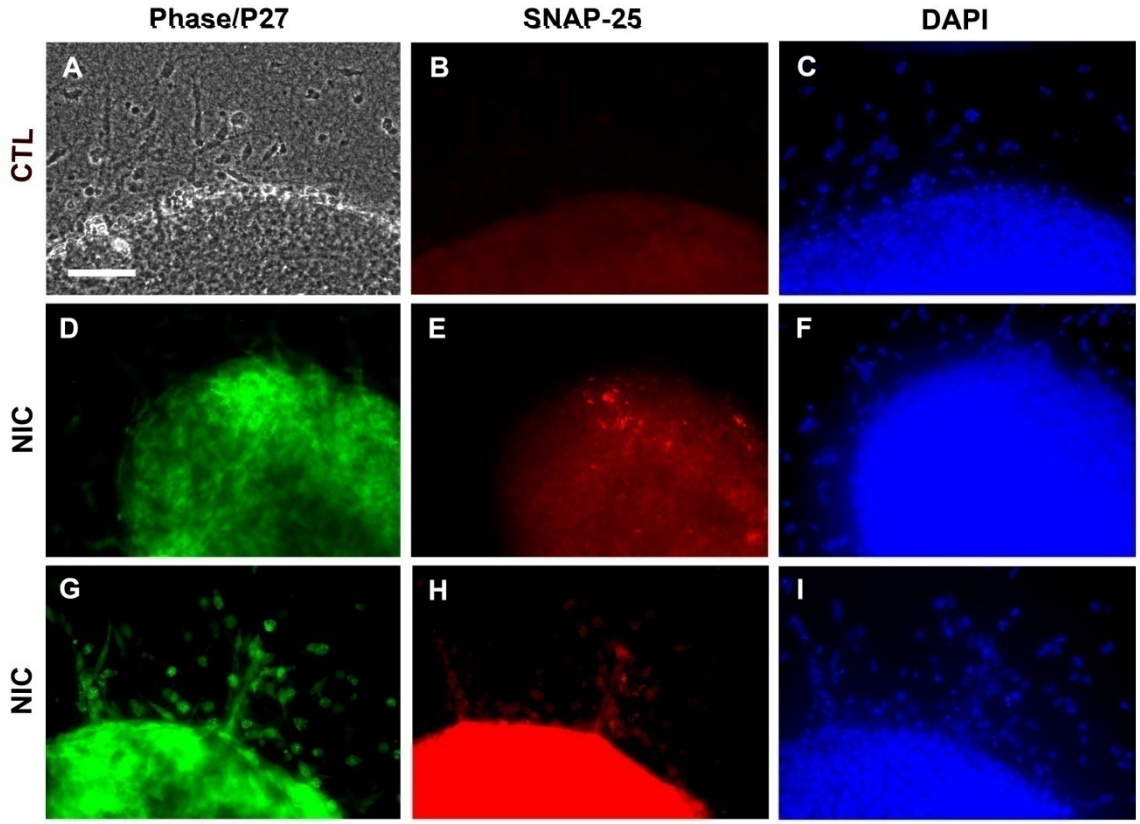
Phase/P27
SNAP-25
DAPI
CTL
NIC
NIC
A
B
C
D
E
F
G
H
I

Fig.3.6. Migration of cells in constitutively active Notch infected explants does not require expression of the conduction marker SNAP-25. E4.5 cardiac explant gel cultures were immunostained with anti-GAG (green), conduction marker SNAP-25 (red), and the nuclear dye, DAPI (blue). (A-C) Expression of SNAP-25 does not usually turn on until E6, and is absent from control uninjected explants. (D-I) In RCAS-NIC-infected explants, a few cells within the explant or migrated cells are positive for SNAP-25 expression. Note that the majority of the migrated cells lack SNAP-25 expression. Scale bar, 50 μm.

significantly differ from the motile cells in the wild type explants (7.12 ± 0.49 μm/h vs. 7.91 ± 0.65, respectively) (Fig. 3.7C). Additionally, the direction of movement of the motile cells was analyzed. In both wild type and RCAS-NIC-infected explants, the majority of the cells moved forward, away from the explants (55 ± 4.7% vs. 62.7 ± 4.0%, respectively) (Fig. 3.7D). The remainder of the cells migrated either back towards the explants, or laterally. A similar percentage of cells were found to move back towards the explants or laterally in the RCAS-NIC-infected explants, compared with the control (Fig. 3.7D). These results suggest that Notch activity increases the percentage of cardiac cells that are motile but did not affect the velocity or the direction of migration.

Because constitutively active Notch can increase the number of cells migrated out from the explants, we analyzed the expression of N-cadherin, the predominant cell-cell adhesion molecule among cardiomyocyte cell junctions [165]. Co-immunofluorescent staining with anti-N-cadherin and anti-GAG antibodies was carried out on tissue sections derived from the injected hearts and results were analyzed by confocal microscopy. Control RCAS-GFP-infected cells did not have visible effect on the intensity or distribution of N-cadherin staining (Fig. 3.8A-C), with normal levels of N-cadherin localized on the plasma membrane of cardiomyocytes compared to the uninjected samples (Fig. 3.8A-C). In contrast, N-cadherin expression was greatly diminished in cells expressing RCAS-NIC (Fig. 3.8D-F). While 81.5 ± 6.29 % of GFP-infected cells exhibited N-cadherin staining, only 22.5 ± 9.17 % of NIC-infected cells expressed normal levels of N-cadherin compared to the uninfected neighboring cells (Fig. 3.8J). On

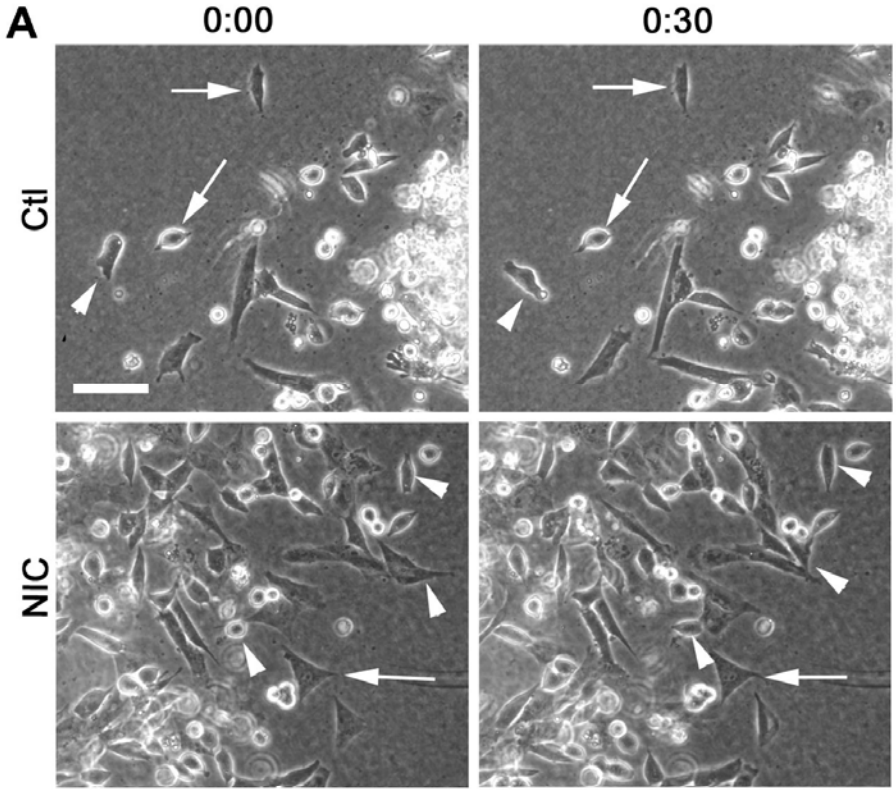
A
0:00
0:30
Ctl
NIC

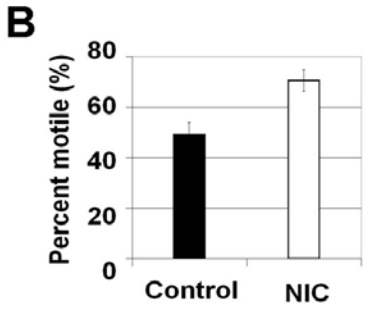
B
Percent motile (%)
80
60
40
20
0
Control
NIC

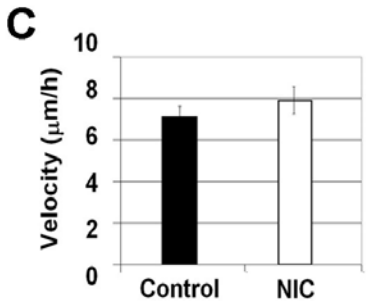
C
Velocity (μm/h)
10
8
6
4
2
0
Control
NIC

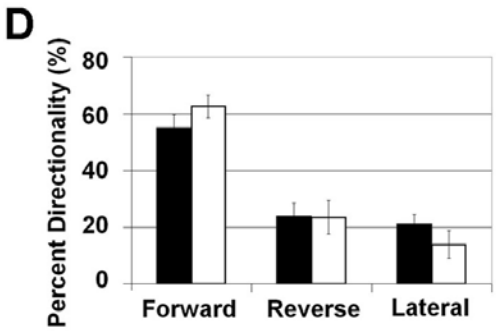
D
Percent Directionality (%)
80
60
40
20
0
Forward
Reverse
Lateral

Fig.3.7. Constitutively active Notch increases the motility of myocardial cells. Gel culture explants were filmed for 1-12 hours. (A) Time-lapse images of control uninjected and RCAS-NIC-infected explants at the start of filming (0:00) and at the 30 inute time-point (0:30) were analyzed for motility, speed and directionality. Note that more cells were motile (arrowheads) in RCAS-NIC-infected explants, while many cells remained stationary (arrows) in control uninjected explants. (B) Quantification of the number of motile cells, $p < 0.01$. (C) Quantification of the speed. (D) Distribution of the directionality of motile cells in control uninjected and RCAS-NIC-infected explants. Note that NIC expression increased the motility of the cardiac cells, but did not affect the speed or directionality of motile cells. Scale bar, 20 μm

the other hand, RCAS-DN-Su(H)-infected cells appeared to have an increased level of N-cadherin expression when compared to the neighboring uninfected cells (Fig. 3.8G-I). We found that 77.8 ± 2.15 % of RCAS-DN-Su(H)-infected cells exhibited visibly higher N-cadherin staining compared to neighboring uninfected cells (Fig. 3.8K). This result supports that Notch signaling may influence cell migration, by regulating the expression of N-cadherin.

3.4 Discussion

In this paper, we characterized the effect of Notch signaling in the regulation of myocardial cell migration. By in vivo mosaic expression using incomplete retroviral infection, we demonstrate that cells expressing constitutively active Notch localized more centrally within the heart, whereas interference of Notch signaling resulted in more peripheral localization. By using 3D gel culture assay, we show that the effects of Notch on cardiac cell migration are two-fold: by increasing the ability of cells to delaminate/emigrate from the explant and by increasing the motility of the cell. Furthermore, we show that the effects of Notch on cardiac cell migration are independent of its effects on cell differentiation.

Incomplete retroviral infection created mosaic patches of cells expressing either the constitutively active Notch (NIC), or dominant-negative Su(H) construct to disrupt Notch function. This allowed us to examine both the gain-of-function and loss-of-

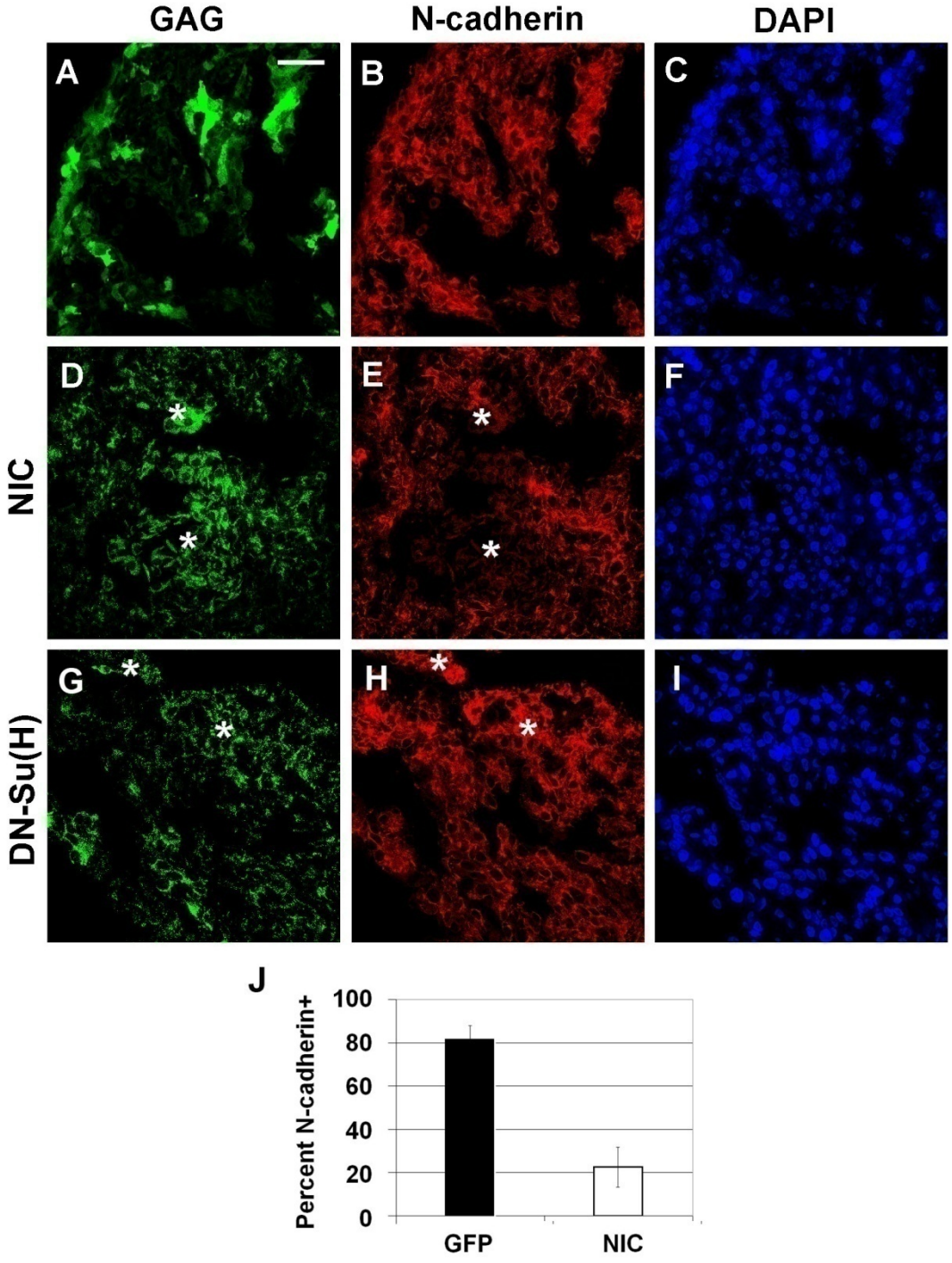
GAG
N-cadherin
DAPI
A
B
C
D
E
F
G
H
I
NIC
DN-Su(H)
J
Percent N-cadherin+
100
80
60
40
20
0
GFP
NIC

Figure 3.8. Notch signaling regulates the expression of N-cadherin. RCAS-NIC-, RCAS-DN-Su(H)- or control RCAS-GFP-injected hearts were harvested at E4.5, sectioned, immunostained with anti-GAG (green), anti-N-cadherin (red), and the nuclear dye DAPI (blue), and analyzed on a confocal microscope. (A-C) N-cadherin localizes on the plasma membrane of cardiomyocytes in control RCAS-GFP-infected hearts. (D-F) RCAS-NIC-infected cardiomyocytes show decreased staining of N-cadherin (asterisks). (G-I) In contrast, N-cadherin staining appears to be increased in RCAS-DN-Su(H)-infected cells, as compared to neighboring uninfected cells (asterisks). (J) Quantification of the percentage of RCAS-GFP- or RCAS-NIC-infected cells that express N-cadherin, $p < 0.01$. Scale bar in A common to all panels = 10 μm

function phenotypes of Notch in a largely normal environment. We injected virus inside the linear heart tube prior to the formation of trabeculae. Most of the clones in control GFP-injected samples appeared cone-shaped and extended through the entire thickness of the ventricular myocardium, similarly as reported earlier using a retrovirus expressing β-galactosidase [43, 44]. However, in samples injected with RCAS-NIC, the infected clones were largely distributed at the tips of the trabeculae without contacting the outer surface of the heart. On the contrary, the infected clones by RCAS-DN-Su(H) were preferentially distributed at the base of the myocardium. Centripetal migration of cardiomyocytes has been demonstrated by earlier studies using retroviral injection [42, 43]. The disproportionate distribution of the clones thus suggests that Notch may play a role in cardiac cell migration during heart development.

We have previously shown that Notch signaling regulates the cell fate decision between cardiac muscle and conduction cells. Expression of constitutively active Notch increased the expression of conduction cell type markers, including HNK-1 and SNAP-25 [164]. Because HNK-1 antibody recognizes a complex sulfate-3-glucuronyl carbohydrate moiety, which is present on a series of molecules involved in cell adhesion and extracellular matrix interactions [166-169], it is possible that the effect of cell migration is secondary to the upregulation of conduction cell markers including HNK-1. By developing a 3D collagen gel culture, we observed that cells migrated from the explants were completely negative for the expression of HNK-1. It is not clear why the cells that migrated away from the explants are negative for HNK-1. One possibility is

that HNK-1 is present on proteins of the extracellular matrix which dissipates from the dissociated cells in the culture media. The other possibility is that HNK-1 expression requires certain signals that are not present in enough amounts in the emigrated cells but remain inside the explants. Nevertheless, the effect of Notch on cell migration in the gel culture is clearly independent of HNK-1 expression. Further examination of SNAP-25 expression, another conduction cell marker, supports the notion that the effect of cell migration by Notch is independent of conduction cell marker expression. The expression of SNAP-25 usually does not come up until E6 in control samples. With the exception of a limited number of cells, most of the NIC-expressing cells were negative for SNAP-25, suggesting that the migration effects by Notch also do not require the expression of the conduction cell marker SNAP-25.

Several lines of evidence suggest that the effect of Notch on cardiomyocyte migration under our experimental conditions is also independent of altered cell proliferation. First, the clone size of RCAS-NIC-infected patches appeared similar to that of the control RCAS-GFP patches (data not shown). Second, we show that the expression of constitutively active Notch did not increase the percentage of cells labeled by BrdU, suggesting that Notch activation did not increase myocardial proliferation. This appears in conflict with a recent paper indicating that mouse null mutants of *Notch1* or *RBPJk* show impaired trabeculation and decreased myocardial proliferation due to attenuated expression of *EphrinB2*, *NRG1*, and *BMP10* [122]. However, the effect of Notch activation on cell proliferation appears variable in different studies, ranging from

decrease of proliferation, no effect, or increase of proliferation [170-172]. In addition, expression of constitutively active Notch under different experimental conditions may yield different results on cell proliferation, possibly due to the timing of transgene expression. For example, constitutive activation of Notch in the embryonic chicken pancreas increased proliferation of pancreatic epithelial cells [173]. However, transgenic mice with knock-in of constitutively active Notch in pancreatic progenitor cells did not display increased proliferation [174]. In our case, we injected retrovirus relatively late at the linear heart tube stage, and therefore may have missed the time window during which Notch signaling may regulate proliferation. Earlier expression of NIC could possibly increase the proliferation of cardiomyocytes.

Additionally, our study demonstrates that the effects of Notch signaling on the migration of cardiac cells are two-fold, increasing delamination and cell motility. In the gel culture assay, constitutively active Notch expression significantly increased the number of cells that emigrated from the explants. Strikingly, the dominant negative Su(H)-expressing cells completely failed to migrate out. It has been shown that N-cadherin is the predominant cadherin expressed in cardiomyocytes [165]. Cadherins are a family of adhesion molecules involved in homophilic cell-cell interaction [175]. Our results indicate that Notch signaling plays an important role in regulation of N-cadherin expression in cardiac cells. Activation of Notch signaling decreased, while interfering with Notch signaling by expressing DN-Su(H) increased, expression of N-cadherin. Regulation of N-cadherin expression may underlie the effect of Notch in cell

delamination/emigration from the outer layer of the heart. We found that cells that migrated away from the explants tended to have low N-cadherin expression on plasma membrane compared to those inside the explant (data not shown). This is analogous to epithelial to mesenchymal transition (EMT), as loss of *E-cadherin* has been shown to be essential prior to cell delamination. Notch signaling has also been shown to be required for downregulation of E-cadherin in EMT in the process of cardiac valve primordia formation [115, 116].

Inhibition of Notch activity via injection of a dominant negative form of Suppressor of Hairless resulted in an increase in the mean number of migrating cells compared with the control samples (Fig. 3.4E). Although explants with a heavy infection rate exhibited decreased numbers of cells migrating into the gel relative to control, less well infected samples appeared to have an increased number of cells migrating into the gel. It is possible that a feedback mechanism similar to "lateral inhibition" is at work between the RCAS-DN-Su(H)-infected and neighboring uninfected cells, resulting in activation of Notch signaling in the uninfected cell. These cells with activated Notch signaling then migrated into the collagen matrix gel. However, none of the cells expressing the DN-Su(H) were observed to migrate out themselves.

The effects of Notch in cell migration has been observed mainly by analyzing phenotypes with Notch loss-of-function mutants [101-103, 105-107]. However, the mechanism by which Notch affects cell migration in these studies is less clear. The

interpretation may be further complicated by the fact that Notch is also involved in cell proliferation, differentiation and apoptosis. In *Drosophila*, Notch signaling has been found to affect the detachment of border cells from the epithelium [104]. Additionally, Notch has been shown to regulate the movement of boundary cells via regulation of the cytoskeletal linker protein, Shot [102]. In our study, by time-lapse microscopy, we show that Notch activity increased motility, but did not alter the velocity or directionality of migration. It is not clear why only about half of the wild type cells are motile within 30 minute time period. Nor is it known of the mechanism by which Notch increases cell motility. The actin cytoskeleton is the major driving force required for cell migration. Actin dynamics provide a protrusive force at the leading edge, while movement of the cell body is driven by actin and myosin II filament contractility. At the trailing edge, microtubule-dependent targeting of dynamin and endocytosis of adhesion molecules promotes adhesion disassembly [98-100]. Further studies will be necessary to determine the downstream mechanisms by which Notch regulates cell migration..

3.5 Experimental Procedures

Chick embryos and Viral constructs

Standard specific pathogen-free white Leghorn chick embryos from closed flocks were provided fertilized by Charles River Laboratories (North Franklin, Connecticut). Eggs were incubated inside a moisturized 38°C incubator. The embryos were staged according to Hamburger and Hamilton [161]. The hearts were dissected and fixed in 4%

paraformaldehyde at 4°C for 12–24 h. Cryosections of 20 μm thickness were prepared from tissue OCT blocks on a cryostat (Leica, Deerfield, IL) and collected on Superfrost Plus slides (Fisher Scientific, Pittsburgh, PA).

The mouse Notch1 intracellular domain (RCAS-NIC), and dominant negative Suppressor of Hairless [RCAS-DN-Su(H)] constructs were previously described [164]. G-coat viruses were prepared by transient transfection [38] and early heart tubes of HH stage 9 embryos were injected with the viral stocks as previously described in [164].

Immunofluorescence staining and data analysis

Immunofluorescence staining was carried out on cryosections of the heart. Sections were fixed in 4% paraformaldehyde, and incubated in block solution containing 10% calf serum in 1X PBS with 0.2% Triton X-100. Primary and secondary antibodies were diluted in block solution, and incubated for 1 h at room temperature or overnight at 4°C. To stain the gel cultures, the gel was scraped off the culture dish, and holes were poked throughout the gel to increase the access of antibodies to the tissues. The cultures were then fixed in 4% paraformaldehyde for 1 hour, and incubated in block solution for 1 day at room temperature. Primary and secondary antibodies were diluted in block, and incubated for 2 days at room temperature. Viral infection was confirmed by using the mouse polyclonal anti-GAG antibody, p27 (SPAFAS, Norwich, CT). The mouse monoclonal conduction cell antibody HNK-1 was obtained from ATCC (Manassas, VA), and SNAP-25 was obtained from Sternberger Monoclonals, Inc (Lutherville, MD). The

nuclear stain, DAPI, was obtained from Roche (Indianapolis, IN). The mouse monoclonal antibody against N-cadherin was obtained from Sigma (Clone CH-19, St.Louis, MO).

To analyze the in vivo distribution of infected cells, we utilized the NIH Image J software to generate binary images (black and white images) of the fluorescent signals. The software allowed us to determine the center of mass for each infected patch, as the average position for the patch. We then calculated the average distance of each patch to the periphery of the ventricles by using the equation $D= \sqrt{(X_1-X_2)^2+(Y_1-Y_2)^2}$, (X_1, Y_1), (X_2, Y_2) being the coordinates for the center of mass and the point at the heart periphery which gives the shortest distance from the center of mass, respectively. The average distance of cell migration in each heart is calculated by the equation: $d=(A_1\times D_1+A_2\times D_2+ \cdots +A_n\times D_n)/(A_1+A_2+ \cdots +A_n)$; A is the area for each patch; n is the total number of patches in the section. We analyzed a total of four hearts, two sections per heart, for each of the constructs. Statistical analysis was performed by using Student's *t*-test.

BrdU labeling and detection

BrdU labeling and detection protocols were modified from [176, 177]. BrdU dissolved in water (3mg/ml) was applied directly onto the amniotic membranes of embryos *in ovo*. 50 mg was used for one E4 embryo, increasing by 25 mg each embryonic day. Embryos were incubated for 3 hours before being sacrificed, and processed for cryostat sectioning. Sections were fixed with 4% paraformaldehyde,

incubated with 0.05% trypsin in 0.1% $CaCl_2$ pH 7.8 for 1 hour, 2N HCl for 30 minutes, followed by 1% H_2O_2 for 30 minutes. Sections were blocked with 10% calf serum DME with 0.2% Triton X-100. Primary and secondary antibodies were diluted in block. Anti-BrdU antibody (diluted 1:250) was purchased from Dako (Carpinteria, CA).

Collagen gel explant culture

E4.5 chick ventricles were dissected and cut into small pieces. Care was taken not to include the atrioventricular junction areas. Ventricular pieces were transferred onto a 35mm cell culture dish. Bovine type I collagen (BD Biosciences,San Diego, CA) neutralized with 1 M $NaHCO_3$ and 10X DMEM was added to the explants and allowed to gel for 30–40 min at 37°C. Culture media (DMEM supplemented with 10% FBS and penicillin/streptomycin) was added, and the explants were incubated at 37°C, 5% CO_2. After 48 h, the cultures were fixed with 4% paraformaldehyde, and stained. Gel culture explants were performed in three independent experiments with 4 different hearts each time, and 5 explants for each heart. The number of cells that emigrated from the explants was scored, and the data were normalized against control. Cells migrated into the matrix gel, and formed a ring around the explants. The migration distance was obtained by measuring the distance from the edge of the explants to the rim of the rings, and averaged.

Time-lapse microscopy

20–24-hour of explant cultures were filmed by using a Zeiss Axiovert microscope with temperature and CO_2 control, coupled to an Axiocam MRM CCD camera. Time-lapse microscopy was carried out for 1-12 hours at 5 min intervals. Movie files were generated using the Axiovision software. To analyze the motility of the cells, the first frame was overlaid with the frame from 30 minutes into filming using Adobe Photoshop. The files were then exported to Axiovision to determine the distance and directionality. Only cells that had migrated from the explants and were not in contact with more than one other cell were analyzed. Using Axiovision, the distance moved by the cells was measured by comparing the center of the cell at the beginning with the center of the cell 30 minutes later. Data was obtained from 4 different hearts, 2 explants per heart, for each condition.

CHAPTER IV: Discussion and Perspectives

Discussion and perspectives for Chapter II

Retroviral lineage studies have demonstrated that the two major cardiac cell types, cardiac muscle cells, and conduction cells, arise from a common progenitor. Our results show that Notch signaling plays a key role in the binary cell fate decision between these two cell types. Notch transcripts are expressed in cardiac progenitor cells, and in the early conduction cell lineage. Constitutive activation of Notch1 in cardiac progenitor cells, prior to the onset of differentiation, promotes the expression of some conduction cell markers, including HNK-1 and SNAP-25, while inhibiting expression of muscle proteins. Inhibition of Notch activity in progenitor cells produced a reciprocal phenotype; loss of Notch function increases the expression of muscle cell markers, while conduction cell marker expression is decreased. These results suggest a role for Notch signaling in promoting conduction cell differentiation at the expense of cardiac muscle cell specification. Optical mapping studies show that constitutive activation of Notch induces abnormal electrical conduction propagation patterns consistent with defective conduction cell differentiation.

Our results demonstrate that Notch1 is involved in cardiac differentiation by inhibiting cardiomyocyte specification and promoting early conduction cell differentiation. Constitutive activation of Notch increases the expression of some conduction markers, including HNK-1 and SNAP-25, while inhibiting muscle marker expression. However, the effect of Notch signaling on another conduction marker, Cx40,

is more complex. Cardiac conduction cells express high levels of Cx40 whereas myocardial cells express low levels of Cx40. Loss of function studies using a dominant negative Su(H) construct shows that the high level of Cx40 expression is diminished but the low level of Cx40 expression in the myocardium remains unchanged. This result is consistent with our model that reduction of Notch signaling increases myocardial but decreases conduction cell differentiation. However, because Cx40 is a relatively late marker, Notch signaling may be involved in the initial separation of conduction and muscle cell lineages.

Optical mapping studies show that RCAS-NIC-infected mutants had obvious abnormalities in the conduction pathway. The altered conduction system function revealed by optical mapping provides additional evidence that cells expressing constitutively active Notch are not fully differentiated functional conduction cells. These results are different from the phenotype observed in chick hearts with excess production of endothelin-1 or mouse hearts treated with neuregulin-1, which induced alterations in activation patterns consistent with additional recruitment of Purkinje cells [70, 71]. Optical mapping studies of the (Cx40) knockout mice indicated some delay or block in conduction velocities in the right bundle branch, and more diffuse breakthrough sites in the left ventricle [155, 156]. Chimeric mice generated from stem cells deficient for connexin 43, a gap junction predominantly expressed in the ventricular myocardium, displayed conduction delay [157]. Thus, reduced expression of gap junction proteins can lead to conduction abnormalities. Because constitutively active Notch down-regulates

the expression of Cx40, we speculate that the conduction abnormalities of the RCAS-NIC injected hearts may be in part due to decreased expression of Cx40. In the hearts moderately infected with RCAS-NIC, a general correlation of blocked pathway with the area of infection was observed, suggesting a block in the infected areas. In highly infected hearts, Cx40 expression may be downregulated throughout the myocardium, causing the electrical impulse to disperse across the epicardial surface. Because our optical mapping protocol detects electrical propagation across the epicardial surface, we therefore observed a diffuse activation pattern. Therefore, our model is that transient Notch activity may be required for the initial separation of myocardial and conduction lineages by inhibiting cardiomyocyte differentiation and promoting early conduction cell differentiation, possibly through regulating the responsiveness of the cells to other inductive factors.

Additional signals may also be required to cooperate with Notch signaling to induce maturation of the conduction cells. Previous works have shown that paracrine factors released by the endocardium and endothelial cells of the coronary arteries, such as endothelin-1 and neuregulin-1, can increase the expression of conduction markers and cause a change in conduction pathway that is consistent with excess recruitment of functional Purkinje cells [69-71, 133]. It would be important to determine whether Notch regulates the responsiveness of cardiac progenitor cells to inductive factors, and if it works upstream of genes, such as neuregulin-1 and endothelin-1. This can be done by the addition of inductive factors to cardiac progenitor cells lacking Notch signaling.

Additionally, analysis of neuregulin-1 or endothelin-1 expression upon constitutive Notch activation will allow us to determine if Notch acts in a similar pathway, upstream of neuregulin-1 and/or endothelin-1.

Mice deficient for HF-1b, a SP1-related transcription factor, exhibit sudden cardiac death and conduction defects, including ventricular tachycardia and AV block [72, 73]. The phenotypes of HF-1b-deficient mice are restricted to features associated with dysregulation of the electrophysiological properties of ventricular muscle and conduction cells, suggesting that HF-1b may orchestrate the electrophysiological properties of conduction cells. HF-1b acts as a positive regulator for the activation of ion channels and connexins necessary for functional conduction and muscle cells. It is possible that Notch may act upstream of HF-1b to promote differentiation of "immature" conduction cells that can respond to HF-1b activation of gene expression associated with functional conduction cells.

Recently, it has been demonstrated that Nkx2.5, Tbx5, and Id2 cooperate in a molecular pathway that coordinates the specification of conduction cells [77]. Specification of the ventricular conduction system failed in mice with compound haploinsufficiency of Tbx5 and Nkx2.5 or Tbx5 and Id2. Tbx5 and Nkx2.5 cooperatively activate transcription of Id2, a member of a gene family encoding basic helix-loop-helix-containing transcriptional repressors, in the developing ventricular conduction system. Id2 has been shown to block the myogenic activity of MyoD and other myogenic bHLH

proteins, and may distinguish conduction cells from working cardiomyocytes by inhibiting cardiomyocyte specification. The high level expression of Tbx5 and Nkx2.5 in cardiac conduction cells may establish a regionally restricted program of conduction system gene expression, by activating promoters, such as Id2, to suppress cardiomyocyte differentiation. Notch may act cooperatively with Id2 to inhibit cardiomyocyte specification, while promoting the differentiation of conduction cell types. It would be of interest to determine if Notch cooperates with Tbx5, Nkx2.5 and Id2 in a similar molecular pathway. Further studies will be necessary to determine the downstream targets of Notch in regulating the lineage decision between cardiac muscle and conduction cells. Microarray studies utilizing cardiac progenitor cells and "immature" conduction cells with activated Notch signaling will allow the delineation of downstream gene targets. Candidate genes can be further characterized by mutation studies, and co-IP to determine if they interact with Notch.

Our results demonstrate a role for Notch signaling in the development of the avian ventricular conduction system. It is unclear whether conversion of murine embryonic cardiomyocytes into conduction cells occurs through a similar mechanism as in the avian model. Notch transcripts are expressed in the avian ventricular myocardium, in addition to weak signals in endocardial cells. In the mouse, Notch1 expression was reported in the outflow tract, the atrioventricular canal, the trabeculae of the ventricles, the epicardium, the aorta [108], and the endocardium [115, 158, 159]. However, the expression of Notch1 has yet to be reported in the myocardium of murine ventricles. The differences in

expression patterns of Notch1 reported in the heart likely reflect the dynamic and transient nature of the expression patterns of Notch1. Mutant mice with a targeted deletion of the Notch1 gene die before E11. Although severe pericardial edema was reported for these mutant mice, these mice have a beating heart at E10.5 [111]. It is possible that Notch1 may play a similar role in the binary lineage decision between cardiac muscle and conduction cells in the murine cardiac conduction system. Generation of murine models with conditional inactivation or constitutive expression of Notch1 in cardiac progenitor cells will address this question, and allow the elucidation of whether specification of conduction cells in mice occur through a similar mechanism found in avian models.

The best studied function of Notch is in cell fate specification. Notch signaling not only acts in the cell fate specification of many organs, but also reiteratively during the maturation of a single organ. Notch signaling has been previously found to play key roles in heart development, in specification of the cardiogenic field in Xenopus and mouse [123, 125]. Mutations in genes of the Notch signaling pathway result in various cardiac defects including pericardial edema, defects in formation of valves, atrial and ventricular septa, and in endocardial cushions [115, 117-121, 138-140]. Our work provides evidence for an additional role of Notch signaling in later stages of heart development in differentiation of ventricular cell types. This is reminiscent of its roles during neurogenesis, hematopoiesis, and pancreatic development, where it acts during multiple stages of organ development in cell fate specification.

The effects of Notch signaling on cell fate specification are often mediated by a mechanism known as lateral inhibition. In an initially homogenous cell population, initial small differences in ligand and receptor expression on adjacent cells become amplified via a feedback mechanism between Notch and Delta. A key element of this mechanism is that the expression of Delta is repressed by Notch signaling through downstream basic helix-loop-helix (bHLH) transcription factors [153, 154]. We have shown that Delta1 is similarly downregulated by constitutively activated Notch, suggesting that a feedback loop is possibly at work in cardiac differentiation. However, it remains unclear whether Delta1 is the ligand for Notch in regulating differentiation of conduction cells. This can be determined by over-expression of Delta1 in vivo.

However, despite the numerous roles of Notch signaling in regulating differentiation, the mechanisms by which Notch influences differentiation are not clearly understood. Notch signaling may regulate differentiation via a generalized mechanism that is present in all cell types. Perhaps Notch signaling may affect differentiation by stimulating cells to move away from or towards areas containing inductive factors.

Discussion and perspectives for Chapter III

Cell migration plays key roles during organogenesis. During ventricular chamber formation, characteristic finger-like projections, known as trabeculae, are formed when myocardial cells in the ventricular segment proliferate and migrate into the ventricular

lumen. Our work shows that Notch signaling regulates the migration of cardiac cells. Constitutive activation of Notch, in vivo, causes cells to localize more centrally within the heart. Conversely, cells with loss of Notch function remain within the periphery of the heart, and accumulate in the compact myocardium. These results suggest that Notch signaling regulates the distribution of cardiac cells in vivo, and may play a role in migration. To determine if Notch regulates migration, we developed a 3D gel culture migration assay, and found that Notch signaling regulates cell migration by down-regulating expression of N-cadherin, and increasing cell motility. Additionally, we show that the effects of Notch signaling on cell migration are independent of its effects on differentiation.

We have demonstrated that a feedback mechanism exists between Notch and Delta, and may be at work during cardiac differentiation. Furthermore, Delta1 transcripts are expressed in the ventricular myocardium during trabeculae formation. The ligand that interacts with Notch1 in regulating cardiac cell migration is unknown. It is possible that Delta1 may the ligand that interacts with Notch1 due to the presence of Delta1 transcripts during trabeculae formation. Studies involving the addition of soluble Delta1 protein to cardiac explants in gel culture will allow the determination of the interacting ligand. Additionally, over-expression of Delta1 in vivo will address this issue.

Our study demonstrates that the effects of Notch signaling on the migration of cardiac cells are two-fold, increasing delamination and cell motility. Constitutively

active Notch expression significantly increased the number of cells emigrating from cardiac explants in the gel culture assay. Strikingly, dominant negative Su(H)-expressing cells completely failed to migrate out. It has been shown that N-cadherin is the predominant cadherin expressed in cardiomyocytes [165]. Cadherins are a family of adhesion molecules involved in homophilic cell-cell interaction [175]. Downregulation of N-cadherin is necessary prior to migration. Our results indicate that Notch signaling plays an important role in the regulation of N-cadherin expression in cardiac cells. Activation of Notch signaling decreased expression of N-cadherin. Inhibition of Notch signaling produced a reciprocal effect; dominant-negative Su(H)-expressing cells show increased N-cadherin expression. Regulation of N-cadherin expression may underlie the effect of Notch in cell delamination/emigration from the outer layer of the heart. This is analogous to epithelial to mesenchymal transition (EMT), as loss of *E-cadherin* has been shown to be essential prior to cell delamination. Notch signaling has also been shown to be required for downregulation of E-cadherin in EMT during cardiac valve primordia formation [115, 116]. In this context, Notch signaling regulates expression of Snail, a member of the zinc-finger-containing family of transcriptional repressors that target E-cadherin expression. RBP-Jκ null mutants exhibit impaired EMT due to attenuated expression of Snail. It is unclear how Notch regulates the expression of N-cadherin in cardiomyocytes. The snail homologue slug is expressed in AV canal endothelial cells, and mesenchymal cells within the endocardial cushions within the chick heart [178]. Although slug is not expressed in the ventricular myocardium, it is possible that Notch signaling may act via slug to regulate N-cadherin expression during cardiac cell

migration. To determine if Notch signaling regulates N-cadherin expression via slug, the expression of slug can be analyzed in cardiac cells expressing constitutively active Notch1 or dominant-negative Su(H). It is also possible that Notch signaling affects N-cadherin expression via a different mechanism as seen in EMT. Analysis of the effects of Notch signaling on known regulators of N-cadherin will allow the determination of mechanisms by which Notch regulates N-cadherin. Additionally, it is unclear whether downregulation of N-cadherin is necessary and sufficient for the migration of cardiac cells. Studies in which N-cadherin expression is altered can address this issue.

The effects of Notch in cell migration have been observed mainly by analyzing phenotypes with Notch loss-of-function mutants [101-103, 105-107]. However, the mechanism by which Notch affects cell migration in these studies is unclear. Analysis of the aberrant migration phenotypes may be further complicated by the fact that Notch is also involved in cell proliferation, differentiation and apoptosis. In *Drosophila*, Notch signaling has been found to affect the detachment of border cells from the epithelium [104]. Additionally, Notch has been shown to regulate the movement of boundary cells via regulation of the cytoskeletal linker protein, Shot [102]. In our study, by time-lapse microscopy, Notch activity increased cell motility, but had no effect on the speed or directionality of migration. The mechanism by which Notch increases cell motility is not known. Further studies will be necessary to determine the mechanism and downstream target genes through which Notch increases cell motility. Microarray studies comparing the gene expression profiles of stationary and motile cells will allow the elucidation of

mechanisms involved in Notch-mediated cell migration. Additionally, co-IP studies using Notch antibodies and motile cell lysates will allow identification of interacting genes.

Actin dynamics provide the key driving force at the leading edge of migrating cells. During formation of the foregut-associated proventriculus organ in the Drosophila embryo, Notch activity regulates the movement of a population of foregut epithelial cells that invaginate into the endodermal midgut layer. The short stop (Shot) gene encodes a member of the spectraplakin family of cytoskeletal linker proteins, which is required for the movement of the proventricular cells. Furthermore, transcription of Shot is activated in response to Notch signaling in posterior boundary cells; shot protein, in turn, regulates the localization and stability of the Notch receptor, suggesting the presence of a feedback loop between shot and Notch. These results suggest that Notch signaling controls actin cytoskeletal organization via the cytoskeletal linker, Shot, during proventricular cell movement. Therefore, it is possible that Notch may regulate the migration of cardiac cells by controlling actin dynamics via a similar mechanism. Analysis of the actin organization within cardiomyocytes upon over-expression of Notch will provide insight into this question.

Precise coordination of cell migration is required for proper formation of organs. Not all cells are allowed to leave their place of birth. Cells that are selected to move must convert from a static to a motile state, loosen their contacts to the surrounding tissue, and

respond to environmental cues that ensure the proper onset, directionality, and speed of their movement [96, 97]. The factors and environmental cues that select for and guide the migration of cardiac cells are unknown. Our study shows that Notch regulates delamination and cell motility during cardiac cell migration. It does not appear to affect the speed or directionality of migrating cells. Studies screening factors that regulate the speed and directionality of migrating cardiac cells are warranted, and will allow the elucidation of the precise mechanisms regulating cardiac cell migration.

The gel culture assay demonstrates that the effects of Notch on cell migration are independent of its effects on differentiation. Staining of cardiac explants with conduction cell markers indicate that expression of conduction markers is not required for cell migration. However, it is unclear whether migration and differentiation are linked. We speculate that Notch signaling may influence differentiation by inducing the migration of progenitor cells away from or towards inductive factors (See Figure 4.1). In order to address this issue, it is first necessary to determine the mechanisms by which Notch regulates cell migration. Inhibition of migration in vivo followed by assessment of differentiation markers will address this issue.

The precise coordination of cardiac cell differentiation, proliferation and migration is required for proper formation of the heart. Our studies show that the Notch signaling pathway plays key roles in regulating cardiac differentiation and migration during cardiogenesis, and underscore the importance of this signaling pathway during

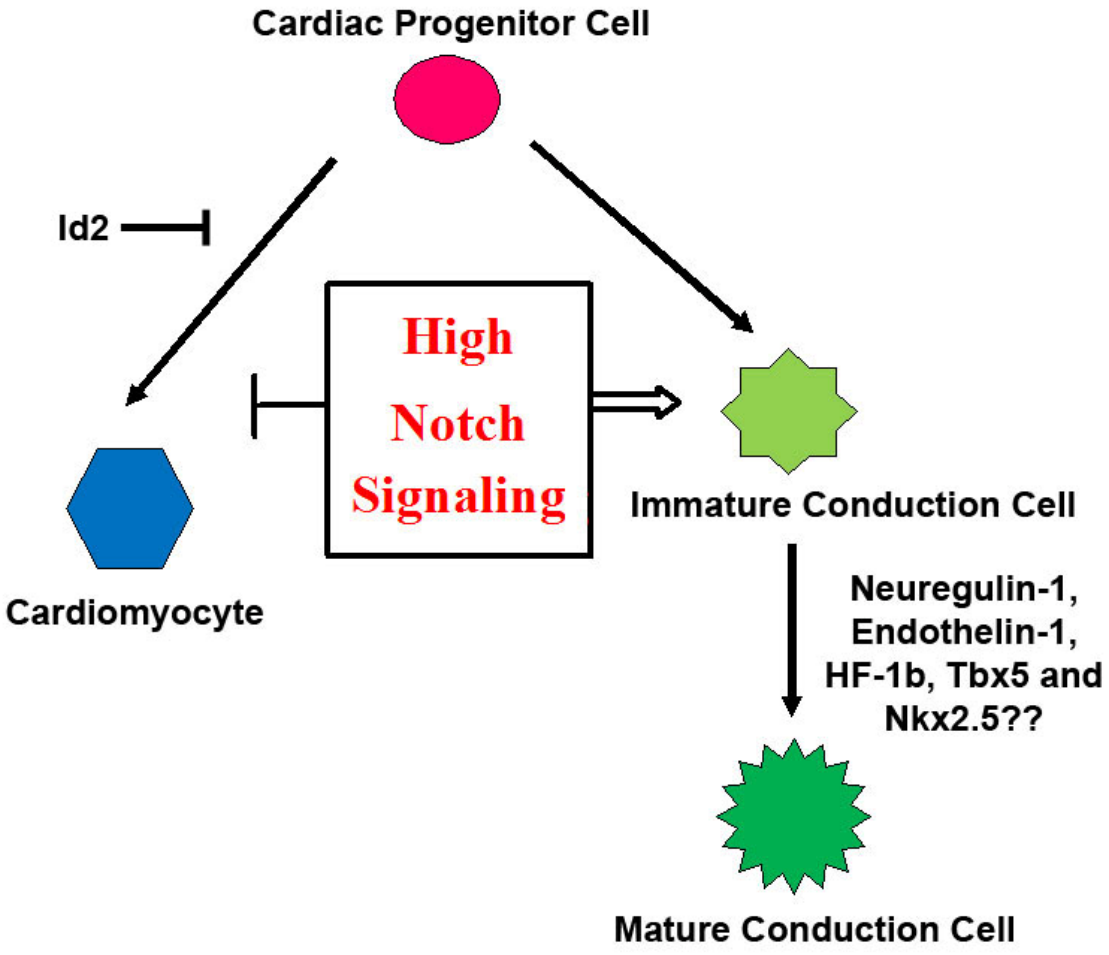
Cardiac Progenitor Cell
Id2
High
Notch
Signaling
Cardiomyocyte
Immature Conduction Cell
Neuregulin-1,
Endothelin-1,
HF-1b, Tbx5 and
Nkx2.5??
Mature Conduction Cell

Figure 4.1 Summary model of Notch activity in cardiac differentiation. Stochastic or environmental factors cause differential expression of Notch receptor and ligands in an initially equivalent pool of cardiac progenitor cells. A feedback mechanism between adjacent cells leads to amplification of the initial differences in receptor and ligand levels. Thus, in cells expressing high levels of the Notch receptor, interaction with its ligand, leads to activation of high Notch signaling activity. Because cardiac muscle and conduction cells arise from a common progenitor, Notch signaling acts in the initial separation of cardiac muscle and conduction cells in this binary cell fate decision. High Notch activity inhibits the differentiation of cardiac muscle cells. Id2, a transcriptional repressor, has been shown to inhibit muscle specification [77]. Thus, Notch may cooperate with Id2, or activate Id2, to inhibit cardiac muscle differentiation. Because Notch activity does not seem to increase expression of late conduction cell markers, Notch activity acts in the initial separation of conduction and muscle cell lineages. Paracrine factors, such as neuregulin-1, and endothelin-1, have been demonstrated to promote the differentiation of conduction cells [70, 71]. These factors may act downstream of Notch to regulate the maturation of conduction cells. Additionally, the transcription factors, HF-1b, Tbx5, and Nkx2.5, have also been demonstrated to play important roles in the specification and maturation of conduction cells [72, 77]. It is possible that these factors become activated after the initial separation of cardiac muscle and conduction cells by Notch. Additionally, it has been demonstrated that conduction cells are recruited to arterial beds by the paracrine factors, neuregulin-1 and endothelin-1 [70, 71]. It is therefore possible that Notch activity may promote the migration of cardiac

progenitor cells to areas containing factors that induce differentiation and maturation of cardiac conduction cells.

embryogenesis. Further studies to elucidate the precise mechanisms by which Notch regulate these key processes will allow understanding of cardiogenesis, and the development of potential therapies for cardiac diseases. Knowledge of these mechanisms in cardiac development may extend to understanding of the many roles played by the Notch pathway in other organ systems.

References

1. Hoffman, J.I. and S. Kaplan, *The incidence of congenital heart disease.* J Am Coll Cardiol, 2002. **39**(12): p. 1890-900.
2. Thom, T., et al., *Heart disease and stroke statistics--2006 update: a report from the American Heart Association Statistics Committee and Stroke Statistics Subcommittee.* Circulation, 2006. **113**(6): p. e85-151.
3. Fishman, M.C. and K.R. Chien, *Fashioning the vertebrate heart: earliest embryonic decisions.* Development, 1997. **124**(11): p. 2099-117.
4. Kitajima, S., et al., *MesP1 and MesP2 are essential for the development of cardiac mesoderm.* Development, 2000. **127**(15): p. 3215-26.
5. Saga, Y., et al., *MesP1 is expressed in the heart precursor cells and required for the formation of a single heart tube.* Development, 1999. **126**(15): p. 3437-47.
6. Saga, Y., S. Kitajima, and S. Miyagawa-Tomita, *Mesp1 expression is the earliest sign of cardiovascular development.* Trends Cardiovasc Med, 2000. **10**(8): p. 345-52.
7. Srivastava, D. and E.N. Olson, *A genetic blueprint for cardiac development.* Nature, 2000. **407**(6801): p. 221-6.
8. Harvey, R.P., *NK-2 homeobox genes and heart development.* Dev Biol, 1996. **178**(2): p. 203-16.
9. Niessen, K. and A. Karsan, *Notch signaling in the developing cardiovascular system.* Am J Physiol Cell Physiol, 2007. **293**(1): p. C1-C11.

10. Gajewski, K., et al., *D-mef2 is a target for Tinman activation during Drosophila heart development.* EMBO J, 1997. **16**(3): p. 515-22.

11. Fu, Y., et al., *Vertebrate tinman homologues XNkx2-3 and XNkx2-5 are required for heart formation in a functionally redundant manner.* Development, 1998. **125**(22): p. 4439-49.

12. Lyons, I., et al., *Myogenic and morphogenetic defects in the heart tubes of murine embryos lacking the homeo box gene Nkx2-5.* Genes Dev, 1995. **9**(13): p. 1654-66.

13. Durocher, D., et al., *The cardiac transcription factors Nkx2-5 and GATA-4 are mutual cofactors.* EMBO J, 1997. **16**(18): p. 5687-96.

14. Gajewski, K., et al., *The zinc finger proteins Pannier and GATA4 function as cardiogenic factors in Drosophila.* Development, 1999. **126**(24): p. 5679-88.

15. Molkentin, J.D., *The zinc finger-containing transcription factors GATA-4, -5, and -6. Ubiquitously expressed regulators of tissue-specific gene expression.* J Biol Chem, 2000. **275**(50): p. 38949-52.

16. Kuo, C.T., et al., *GATA4 transcription factor is required for ventral morphogenesis and heart tube formation.* Genes Dev, 1997. **11**(8): p. 1048-60.

17. Reiter, J.F., Y. Kikuchi, and D.Y. Stainier, *Multiple roles for Gata5 in zebrafish endoderm formation.* Development, 2001. **128**(1): p. 125-35.

18. Morrisey, E.E., et al., *GATA6 regulates HNF4 and is required for differentiation of visceral endoderm in the mouse embryo.* Genes Dev, 1998. **12**(22): p. 3579-90.

19. Koutsourakis, M., et al., *The transcription factor GATA6 is essential for early extraembryonic development.* Development, 1999. **126**(9): p. 723-32.

20. Peterkin, T., A. Gibson, and R. Patient, *GATA-6 maintains BMP-4 and Nkx2 expression during cardiomyocyte precursor maturation.* EMBO J, 2003. **22**(16): p. 4260-73.

21. Kelly, R.G. and M.E. Buckingham, *The anterior heart-forming field: voyage to the arterial pole of the heart.* Trends Genet, 2002. **18**(4): p. 210-6.

22. Waldo, K.L., et al., *Conotruncal myocardium arises from a secondary heart field.* Development, 2001. **128**(16): p. 3179-88.

23. Kelly, R.G., N.A. Brown, and M.E. Buckingham, *The arterial pole of the mouse heart forms from Fgf10-expressing cells in pharyngeal mesoderm.* Dev Cell, 2001. **1**(3): p. 435-40.

24. Schneider, A., et al., *Targeted disruption of the Nkx3.1 gene in mice results in morphogenetic defects of minor salivary glands: parallels to glandular duct morphogenesis in prostate.* Mech Dev, 2000. **95**(1-2): p. 163-74.

25. Raffin, M., et al., *Subdivision of the cardiac Nkx2.5 expression domain into myogenic and nonmyogenic compartments.* Dev Biol, 2000. **218**(2): p. 326-40.

26. Brand, T., *Heart development: molecular insights into cardiac specification and early morphogenesis.* Dev Biol, 2003. **258**(1): p. 1-19.

27. Moorman, A.F. and V.M. Christoffels, *Cardiac chamber formation: development, genes, and evolution.* Physiol Rev, 2003. **83**(4): p. 1223-67.

28. Capdevila, J., et al., *Mechanisms of left-right determination in vertebrates.* Cell, 2000. **101**(1): p. 9-21.

29. Levin, M., et al., *A molecular pathway determining left-right asymmetry in chick embryogenesis.* Cell, 1995. **82**(5): p. 803-14.

30. Garcia-Castro, M.I., E. Vielmetter, and M. Bronner-Fraser, *N-Cadherin, a cell adhesion molecule involved in establishment of embryonic left-right asymmetry.* Science, 2000. **288**(5468): p. 1047-51.

31. Schlange, T., et al., *Chick CFC controls Lefty1 expression in the embryonic midline and nodal expression in the lateral plate.* Dev Biol, 2001. **234**(2): p. 376-89.

32. Campione, M., et al., *The homeobox gene Pitx2: mediator of asymmetric left-right signaling in vertebrate heart and gut looping.* Development, 1999. **126**(6): p. 1225-34.

33. Logan, M., et al., *The transcription factor Pitx2 mediates situs-specific morphogenesis in response to left-right asymmetric signals.* Cell, 1998. **94**(3): p. 307-17.

34. Ryan, A.K., et al., *Pitx2 determines left-right asymmetry of internal organs in vertebrates.* Nature, 1998. **394**(6693): p. 545-51.

35. Meyers, E.N. and G.R. Martin, *Differences in left-right axis pathways in mouse and chick: functions of FGF8 and SHH.* Science, 1999. **285**(5426): p. 403-6.

36. Brown, C.B., et al., *Requirement of type III TGF-beta receptor for endocardial cell transformation in the heart.* Science, 1999. **283**(5410): p. 2080-2.

37. Bruneau, B.G., et al., *Cardiac expression of the ventricle-specific homeobox gene Irx4 is modulated by Nkx2-5 and dHand.* Developmental Biology (Orlando), 2000. **217**(2): p. 266-77.

38. Bao, Z.Z., et al., *Regulation of chamber-specific gene expression in the developing heart by Irx4.* Science, 1999. **283**(5405): p. 1161-4.

39. Bruneau, B.G., et al., *A murine model of Holt-Oram syndrome defines roles of the T-box transcription factor Tbx5 in cardiogenesis and disease.* Cell, 2001. **106**(6): p. 709-21.

40. Pereira, F.A., et al., *The orphan nuclear receptor COUP-TFII is required for angiogenesis and heart development.* Genes Dev, 1999. **13**(8): p. 1037-49.

41. Dersch, H. and M.H. Zile, *Induction of normal cardiovascular development in the vitamin A-deprived quail embryo by natural retinoids.* Dev Biol, 1993. **160**(2): p. 424-33.

42. San Clemente, H., F. Dieterlen-Lievre, and T. Jaffredo, *In vivo diversification and migrations of chick embryo heart muscle cells: a morphometric analysis with ALV- and SNV-based non-replicative vectors.* Development Genes and Evolution, 1996. **206**(3): p. 169-179.

43. Mikawa, T., L. Cohen-Gould, and D.A. Fischman, *Clonal analysis of cardiac morphogenesis in the chicken embryo using a replication-defective retrovirus. III: Polyclonal origin of adjacent ventricular myocytes.* Dev Dyn, 1992. **195**(2): p. 133-41.

44. Mikawa, T., et al., *Clonal analysis of cardiac morphogenesis in the chicken embryo using a replication-defective retrovirus: I. Formation of the ventricular myocardium.* Dev Dyn, 1992. **193**(1): p. 11-23.

45. Sedmera, D., et al., *Developmental changes in the myocardial architecture of the chick.* Anat Rec, 1997. **248**(3): p. 421-32.

46. Srivastava, D., et al., *Regulation of cardiac mesodermal and neural crest development by the bHLH transcription factor, dHAND [see comments] [published erratum appears in Nat Genet 1997 Aug;16(4):410].* Nature Genetics, 1997. **16**(2): p. 154-60.

47. Togi, K., et al., *Essential role of Hand2 in interventricular septum formation and trabeculation during cardiac development.* Biochem Biophys Res Commun, 2006. **343**(1): p. 144-51.

48. Gassmann, M., et al., *Aberrant neural and cardiac development in mice lacking the ErbB4 neuregulin receptor. [see comments].* Nature, 1995. **378**(6555): p. 390-4.

49. Meyer, D. and C. Birchmeier, *Multiple essential functions of neuregulin in development. [see comments]. [erratum appears in Nature 1995 Dec 14;378(6558):753].* Nature, 1995. **378**(6555): p. 386-90.

50. Lee, K.F., et al., *Requirement for neuregulin receptor erbB2 in neural and cardiac development. [see comments].* Nature, 1995. **378**(6555): p. 394-8.

51. Hertig, C.M., et al., *Synergistic roles of neuregulin-1 and insulin-like growth factor-I in activation of the phosphatidylinositol 3-kinase pathway and cardiac chamber morphogenesis.* J Biol Chem, 1999. **274**(52): p. 37362-9.

52. Chen, H., et al., *BMP10 is essential for maintaining cardiac growth during murine cardiogenesis.* Development, 2004. **131**(9): p. 2219-31.

53. Zhao, Z. and S.A. Rivkees, *Rho-associated kinases play an essential role in cardiac morphogenesis and cardiomyocyte proliferation.* Dev Dyn, 2003. **226**(1): p. 24-32.

54. Moorman, A.F., et al., *Development of the cardiac conduction system.* Circ Res, 1998. **82**(6): p. 629-44.

55. Kim, Y. and M. Yasuda, *Development of the cardiac conducting system in the chick embryo.* Anat Histol Embryol, 1980. **9**(1): p. 7-20.

56. Szabo, E., S. Viragh, and C.E. Challice, *The structure of the atrioventricular conducting system in the avian heart.* Anat Rec, 1986. **215**(1): p. 1-9.

57. Gourdie, R.G., et al., *The spatial distribution and relative abundance of gap-junctional connexin40 and connexin43 correlate to functional properties of components of the cardiac atrioventricular conduction system.* J Cell Sci, 1993. **105 (Pt 4)**: p. 985-91.

58. Gorza, L. and M. Vitadello, *Distribution of conduction system fibers in the developing and adult rabbit heart revealed by an antineurofilament antibody.* Circ Res, 1989. **65**(2): p. 360-9.

59. Gorza, L., S. Schiaffino, and M. Vitadello, *Heart conduction system: a neural crest derivative?* Brain Res, 1988. **457**(2): p. 360-6.

60. Chuck, E.T. and M. Watanabe, *Differential expression of PSA-NCAM and HNK-1 epitopes in the developing cardiac conduction system of the chick.* Dev Dyn, 1997. **209**(2): p. 182-95.

61. Nakagawa, M., et al., *Developmental anatomy of HNK-1 immunoreactivity in the embryonic rat heart: co-distribution with early conduction tissue.* Anat Embryol (Berl), 1993. **187**(5): p. 445-60.

62. Verberne, M.E., A.C. Gittenberger-De Groot, and R.E. Poelmann, *Distribution of antigen epitopes shared by nerves and the myocardium of the embryonic chick heart using different neuronal markers.* Anat Rec, 2000. **260**(4): p. 335-50.

63. McCabe, C.F., R.P. Thompson, and G.J. Cole, *Distribution of the novel developmentally-regulated protein EAP-300 in the embryonic chick nervous system.* Brain Res Dev Brain Res, 1992. **66**(1): p. 11-23.

64. Wessels, A., et al., *Spatial distribution of "tissue-specific" antigens in the developing human heart and skeletal muscle. I. An immunohistochemical analysis of creatine kinase isoenzyme expression patterns.* Anatomical Record, 1990. **228**(2): p. 163-76.

65. Gonzalez-Sanchez, A. and D. Bader, *Characterization of a myosin heavy chain in the conductive system of the adult and developing chicken heart.* J Cell Biol, 1985. **100**(1): p. 270-5.

66. Gourdie, R.G., et al., *Terminal diversification of the myocyte lineage generates Purkinje fibers of the cardiac conduction system.* Development, 1995. **121**(5): p. 1423-31.

67. Cheng, G., et al., *Development of the cardiac conduction system involves recruitment within a multipotent cardiomyogenic lineage.* Development, 1999. **126**(22): p. 5041-9.

68. Gourdie, R.G., et al., *Endothelin-induced conversion of embryonic heart muscle cells into impulse-conducting Purkinje fibers.* Proc Natl Acad Sci U S A, 1998. **95**(12): p. 6815-8.

69. Takebayashi-Suzuki, K., et al., *In vivo induction of cardiac Purkinje fiber differentiation by coexpression of preproendothelin-1 and endothelin converting enzyme-1.* Development, 2000. **127**(16): p. 3523-32.

70. Hall, C.E., et al., *Hemodynamic-dependent patterning of endothelin converting enzyme 1 expression and differentiation of impulse-conducting Purkinje fibers in the embryonic heart.* Development, 2004. **131**(3): p. 581-92.

71. Rentschler, S., et al., *Neuregulin-1 promotes formation of the murine cardiac conduction system.* Proc Natl Acad Sci U S A, 2002. **99**(16): p. 10464-9.

72. Nguyen-Tran, V.T., et al., *A novel genetic pathway for sudden cardiac death via defects in the transition between ventricular and conduction system cell lineages.* Cell, 2000. **102**(5): p. 671-82.

73. Hewett, K.W., et al., *Knockout of the neural and heart expressed gene HF-1b results in apical deficits of ventricular structure and activation.* Cardiovasc Res, 2005. **67**(3): p. 548-60.

74. Jay, P.Y., et al., *Nkx2-5 mutation causes anatomic hypoplasia of the cardiac conduction system.* J Clin Invest, 2004. **113**(8): p. 1130-7.

75. Pashmforoush, M., et al., *Nkx2-5 pathways and congenital heart disease; loss of ventricular myocyte lineage specification leads to progressive cardiomyopathy and complete heart block.* Cell, 2004. **117**(3): p. 373-86.

76. Moskowitz, I.P., et al., *The T-Box transcription factor Tbx5 is required for the patterning and maturation of the murine cardiac conduction system.* Development, 2004. **131**(16): p. 4107-16.

77. Moskowitz, I.P., et al., *A molecular pathway including Id2, Tbx5, and Nkx2-5 required for cardiac conduction system development.* Cell, 2007. **129**(7): p. 1365-76.

78. Hurlbut, G.D., et al., *Crossing paths with Notch in the hyper-network.* Curr Opin Cell Biol, 2007. **19**(2): p. 166-75.

79. Schweisguth, F., *Regulation of notch signaling activity.* Curr Biol, 2004. **14**(3): p. R129-38.

80. Kadesch, T., *Notch signaling: the demise of elegant simplicity.* Curr Opin Genet Dev, 2004. **14**(5): p. 506-12.

81. Jan, Y.N. and L.Y. Jan, *Genetic control of cell fate specification in Drosophila peripheral nervous system.* Annu Rev Genet, 1994. **28**: p. 373-93.

82. Gaiano, N., J.S. Nye, and G. Fishell, *Radial glial identity is promoted by Notch1 signaling in the murine forebrain.* Neuron, 2000. **26**(2): p. 395-404.

83. Morrison, S.J., et al., *Transient Notch activation initiates an irreversible switch from neurogenesis to gliogenesis by neural crest stem cells.* Cell, 2000. **101**(5): p. 499-510.

84. Bao, Z.Z. and C.L. Cepko, *The expression and function of Notch pathway genes in the developing rat eye.* Journal of Neuroscience, 1997. **17**(4): p. 1425-34.

85. Furukawa, T., et al., *rax, Hes1, and notch1 promote the formation of Muller glia by postnatal retinal progenitor cells.* Neuron, 2000. **26**(2): p. 383-94.

86. Lutolf, S., et al., *Notch1 is required for neuronal and glial differentiation in the cerebellum.* Development, 2002. **129**(2): p. 373-85.

87. Grandbarbe, L., et al., *Delta-Notch signaling controls the generation of neurons/glia from neural stem cells in a stepwise process.* Development, 2003. **130**(7): p. 1391-402.

88. Tanigaki, K., et al., *Notch1 and Notch3 instructively restrict bFGF-responsive multipotent neural progenitor cells to an astroglial fate.* Neuron, 2001. **29**(1): p. 45-55.

89. Radtke, F., et al., *Deficient T cell fate specification in mice with an induced inactivation of Notch1.* Immunity, 1999. **10**(5): p. 547-58.

90. Pui, J.C., et al., *Notch1 expression in early lymphopoiesis influences B versus T lineage determination.* Immunity, 1999. **11**(3): p. 299-308.

91. Wilson, A., H.R. MacDonald, and F. Radtke, *Notch 1-deficient common lymphoid precursors adopt a B cell fate in the thymus.* J Exp Med, 2001. **194**(7): p. 1003-12.

92. Han, H., et al., *Inducible gene knockout of transcription factor recombination signal binding protein-J reveals its essential role in T versus B lineage decision.* Int Immunol, 2002. **14**(6): p. 637-45.

93. Tanigaki, K., et al., *Notch-RBP-J signaling is involved in cell fate determination of marginal zone B cells.* Nat Immunol, 2002. **3**(5): p. 443-50.

94. Apelqvist, A., et al., *Notch signalling controls pancreatic cell differentiation.* Nature, 1999. **400**(6747): p. 877-81.

95. Hald, J., et al., *Activated Notch1 prevents differentiation of pancreatic acinar cells and attenuate endocrine development.* Dev Biol, 2003. **260**(2): p. 426-37.

96. Ayala, R., T. Shu, and L.H. Tsai, *Trekking across the brain: the journey of neuronal migration.* Cell, 2007. **128**(1): p. 29-43.

97. Hatten, M.E., *New directions in neuronal migration.* Science, 2002. **297**(5587): p. 1660-3.

98. Franz, C.M., G.E. Jones, and A.J. Ridley, *Cell migration in development and disease.* Dev Cell, 2002. **2**(2): p. 153-8.

99. Vicente-Manzanares, M., D.J. Webb, and A.R. Horwitz, *Cell migration at a glance.* J Cell Sci, 2005. **118**(Pt 21): p. 4917-9.

100. Wehrle-Haller, B. and B.A. Imhof, *Actin, microtubules and focal adhesion dynamics during cell migration.* Int J Biochem Cell Biol, 2003. **35**(1): p. 39-50.

101. Edenfeld, G., et al., *Notch and Numb are required for normal migration of peripheral glia in Drosophila.* Dev Biol, 2007. **301**(1): p. 27-37.

102. Fuss, B., et al., *Cell movements controlled by the Notch signalling cascade during foregut development in Drosophila.* Development, 2004. **131**(7): p. 1587-95.

103. Wang, X., J.C. Adam, and D. Montell, *Spatially localized Kuzbanian required for specific activation of Notch during border cell migration.* Dev Biol, 2007. **301**(2): p. 532-40.

104. Prasad, M. and D.J. Montell, *Cellular and molecular mechanisms of border cell migration analyzed using time-lapse live-cell imaging.* Dev Cell, 2007. **12**(6): p. 997-1005.

105. De Bellard, M.E., et al., *Disruption of segmental neural crest migration and ephrin expression in delta-1 null mice.* Dev Biol, 2002. **249**(1): p. 121-30.

106. Weller, M., et al., *Jagged1 ablation results in cerebellar granule cell migration defects and depletion of Bergmann glia.* Dev Neurosci, 2006. **28**(1-2): p. 70-80.

107. Siekmann, A.F. and N.D. Lawson, *Notch signalling limits angiogenic cell behaviour in developing zebrafish arteries.* Nature, 2007. **445**(7129): p. 781-4.

108. Loomes, K.M., et al., *Characterization of Notch receptor expression in the developing mammalian heart and liver.* Am J Med Genet, 2002. **112**(2): p. 181-9.

109. Iso, T., Y. Hamamori, and L. Kedes, *Notch signaling in vascular development.* Arterioscler Thromb Vasc Biol, 2003. **23**(4): p. 543-53.

110. Oka, C., et al., *Disruption of the mouse RBP-J kappa gene results in early embryonic death.* Development, 1995. **121**(10): p. 3291-301.

111. Swiatek, P.J., et al., *Notch1 is essential for postimplantation development in mice.* Genes & Development, 1994. **8**(6): p. 707-19.

112. McCright, B., et al., *Defects in development of the kidney, heart and eye vasculature in mice homozygous for a hypomorphic Notch2 mutation.* Development, 2001. **128**(4): p. 491-502.

113. Garg, V., et al., *Mutations in NOTCH1 cause aortic valve disease.* Nature, 2005. **437**(7056): p. 270-4.

114. Oda, T., et al., *Mutations in the human Jagged1 gene are responsible for Alagille syndrome. [see comments].* Nature Genetics, 1997. **16**(3): p. 235-42.

115. Timmerman, L.A., et al., *Notch promotes epithelial-mesenchymal transition during cardiac development and oncogenic transformation.* Genes Dev, 2004. **18**(1): p. 99-115.

116. Noseda, M., et al., *Notch activation results in phenotypic and functional changes consistent with endothelial-to-mesenchymal transformation.* Circ Res, 2004. **94**(7): p. 910-7.

117. Donovan, J., et al., *Tetralogy of fallot and other congenital heart defects in Hey2 mutant mice.* Curr Biol, 2002. **12**(18): p. 1605-10.

118. Gessler, M., et al., *Mouse gridlock: no aortic coarctation or deficiency, but fatal cardiac defects in Hey2 -/- mice.* Curr Biol, 2002. **12**(18): p. 1601-4.

119. Kokubo, H., et al., *Targeted disruption of hesr2 results in atrioventricular valve anomalies that lead to heart dysfunction.* Circ Res, 2004. **95**(5): p. 540-7.

120. Sakata, Y., et al., *Ventricular septal defect and cardiomyopathy in mice lacking the transcription factor CHF1/Hey2.* Proc Natl Acad Sci U S A, 2002. **99**(25): p. 16197-202.

121. Kokubo, H., et al., *Mouse hesr1 and hesr2 genes are redundantly required to mediate Notch signaling in the developing cardiovascular system.* Dev Biol, 2005. **278**(2): p. 301-9.

122. Grego-Bessa, J., et al., *Notch signaling is essential for ventricular chamber development.* Dev Cell, 2007. **12**(3): p. 415-29.

123. Rones, M.S., et al., *Serrate and Notch specify cell fates in the heart field by suppressing cardiomyogenesis.* Development, 2000. **127**(17): p. 3865-76.

124. Han, Z. and R. Bodmer, *Myogenic cells fates are antagonized by Notch only in asymmetric lineages of the Drosophila heart, with or without cell division.* Development, 2003. **130**(13): p. 3039-51.

125. Schroeder, T., et al., *Recombination signal sequence-binding protein Jkappa alters mesodermal cell fate decisions by suppressing cardiomyogenesis.* Proc Natl Acad Sci U S A, 2003. **100**(7): p. 4018-23.

126. Watanabe, Y., et al., *Activation of Notch1 signaling in cardiogenic mesoderm induces abnormal heart morphogenesis in mouse.* Development, 2006. **133**(9): p. 1625-34.

127. Gourdie, R.G., S. Kubalak, and T. Mikawa, *Conducting the embryonic heart: orchestrating development of specialized cardiac tissues.* Trends Cardiovasc Med, 1999. **9**(1-2): p. 18-26.

128. Myers, D.C. and G.I. Fishman, *Molecular and functional maturation of the murine cardiac conduction system.* Trends Cardiovasc Med, 2003. **13**(7): p. 289-95.

129. Eisenberg, L.M. and R.R. Markwald, *Cellular recruitment and the development of the myocardium.* Dev Biol, 2004. **274**(2): p. 225-32.

130. Bastide, B., et al., *Gap junction protein connexin40 is preferentially expressed in vascular endothelium and conductive bundles of rat myocardium and is increased under hypertensive conditions.* Circ Res, 1993. **73**(6): p. 1138-49.

131. Delorme, B., et al., *Expression pattern of connexin gene products at the early developmental stages of the mouse cardiovascular system.* Circ Res, 1997. **81**(3): p. 423-37.

132. Gros, D., et al., *Restricted distribution of connexin40, a gap junctional protein, in mammalian heart.* Circ Res, 1994. **74**(5): p. 839-51.

133. Kanzawa, N., et al., *Competency of embryonic cardiomyocytes to undergo Purkinje fiber differentiation is regulated by endothelin receptor expression.* Development, 2002. **129**(13): p. 3185-94.

134. Kondo, R.P., et al., *Development of the cardiac conduction system as delineated by minK-lacZ.* J Cardiovasc Electrophysiol, 2003. **14**(4): p. 383-91.

135. Kupershmidt, S., et al., *Replacement by homologous recombination of the minK gene with lacZ reveals restriction of minK expression to the mouse cardiac conduction system.* Circ Res, 1999. **84**(2): p. 146-52.

136. Thomas, P.S., et al., *Elevated expression of Nkx-2.5 in developing myocardial conduction cells.* Anat Rec, 2001. **263**(3): p. 307-13.

137. Artavanis-Tsakonas, S., M.D. Rand, and R.J. Lake, *Notch signaling: cell fate control and signal integration in development.* Science, 1999. **284**(5415): p. 770-6.

138. Fischer, A., et al., *The Notch target genes Hey1 and Hey2 are required for embryonic vascular development.* Genes Dev, 2004. **18**(8): p. 901-11.

139. Koo, B.K., et al., *Mind bomb 1 is essential for generating functional Notch ligands to activate Notch.* Development, 2005. **132**(15): p. 3459-70.

140. McCright, B., J. Lozier, and T. Gridley, *A mouse model of Alagille syndrome: Notch2 as a genetic modifier of Jag1 haploinsufficiency.* Development, 2002. **129**(4): p. 1075-82.

141. Aoyama, N., et al., *Development of the conduction system in the rat heart as determined by Leu-7 (HNK-1) immunohistochemistry and computer graphics reconstruction.* Lab Invest, 1995. **72**(3): p. 355-66.

142. Aoyama, N., R. Kikawada, and S. Yamashina, *Immunohistochemical study on the development of the rat heart conduction system using anti-Leu-7 antibody.* Arch Histol Cytol, 1993. **56**(3): p. 303-15.

143. Ikeda, T., et al., *Leu-7 immunoreactivity in human and rat embryonic hearts, with special reference to the development of the conduction tissue.* Anat Embryol (Berl), 1990. **182**(6): p. 553-62.

144. Luider, T.M., et al., *The distribution and characterization of HNK-1 antigens in the developing avian heart.* Anat Embryol (Berl), 1993. **188**(3): p. 307-16.

145. Nakamura, T., et al., *Distribution of acetylcholinesterase activity in the rat embryonic heart with reference to HNK-1 immunoreactivity in the conduction tissue.* Anat Embryol (Berl), 1994. **190**(4): p. 367-73.

146. Sakai, H., et al., *Immunoelectron microscopic localization of HNK-1 in the embryonic rat heart.* Anat Embryol (Berl), 1994. **190**(1): p. 13-20.

147. Kopan, R., J.S. Nye, and H. Weintraub, *The intracellular domain of mouse Notch: a constitutively activated repressor of myogenesis directed at the basic helix-loop-helix region of MyoD.* Development, 1994. **120**(9): p. 2385-96.

148. Takebayashi-Suzuki, K., et al., *Purkinje fibers of the avian heart express a myogenic transcription factor program distinct from cardiac and skeletal muscle.* Dev Biol, 2001. **234**(2): p. 390-401.

149. Becker, D.L., et al., *Expression of major gap junction connexin types in the working myocardium of eight chordates.* Cell Biol Int, 1998. **22**(7-8): p. 527-43.

150. Minkoff, R., et al., *Connexin expression in the developing avian cardiovascular system.* Circ Res, 1993. **73**(1): p. 71-8.

151. Wettstein, D.A., D.L. Turner, and C. Kintner, *The Xenopus homolog of Drosophila Suppressor of Hairless mediates Notch signaling during primary neurogenesis.* Development, 1997. **124**(3): p. 693-702.

152. Reckova, M., et al., *Hemodynamics is a key epigenetic factor in development of the cardiac conduction system.* Circ Res, 2003. **93**(1): p. 77-85.

153. Heitzler, P., et al., *Genes of the Enhancer of split and achaete-scute complexes are required for a regulatory loop between Notch and Delta during lateral signalling in Drosophila.* Development, 1996. **122**(1): p. 161-71.

154. Heitzler, P. and P. Simpson, *The choice of cell fate in the epidermis of Drosophila.* Cell, 1991. **64**(6): p. 1083-92.

155. Tamaddon, H.S., et al., *High-resolution optical mapping of the right bundle branch in connexin40 knockout mice reveals slow conduction in the specialized conduction system.* Circ Res, 2000. **87**(10): p. 929-36.

156. van Rijen, H.V., et al., *Impaired conduction in the bundle branches of mouse hearts lacking the gap junction protein connexin40.* Circulation, 2001. **103**(11): p. 1591-8.

157. Gutstein, D.E., et al., *Conduction slowing and sudden arrhythmic death in mice with cardiac-restricted inactivation of connexin43.* Circ Res, 2001. **88**(3): p. 333-9.

158. Del Amo, F.F., et al., *Expression pattern of Motch, a mouse homolog of Drosophila Notch, suggests an important role in early postimplantation mouse development.* Development, 1992. **115**(3): p. 737-44.

159. Reaume, A.G., et al., *Expression analysis of a Notch homologue in the mouse embryo.* Dev Biol, 1992. **154**(2): p. 377-87.

160. Krebs, L.T., et al., *Notch signaling regulates left-right asymmetry determination by inducing Nodal expression.* Genes Dev, 2003. **17**(10): p. 1207-12.

161. Hamburger, V. and H.L. Hamilton, *A series of normal stages in the development of the chick embryo. 1951. [see comments]*. Developmental Dynamics, 1992. **195**(4): p. 231-72.

162. Jin, Z., M.D. Chau, and Z.Z. Bao, *Sema3D, Sema3F, and Sema5A are expressed in overlapping and distinct patterns in chick embryonic heart.* Dev Dyn, 2006. **235**(1): p. 163-9.

163. Nye, J.S., R. Kopan, and R. Axel, *An activated Notch suppresses neurogenesis and myogenesis but not gliogenesis in mammalian cells.* Development, 1994. **120**(9): p. 2421-30.

164. Chau, M.D., et al., *Notch signaling plays a key role in cardiac cell differentiation.* Mech Dev, 2006. **123**(8): p. 626-40.

165. Geiger, B., et al., *Broad spectrum pan-cadherin antibodies, reactive with the C-terminal 24 amino acid residues of N-cadherin.* J Cell Sci, 1990. **97 (Pt 4)**: p. 607-14.

166. Faissner, A., *Monoclonal antibody detects carbohydrate microheterogeneity on the murine cell adhesion molecule L1.* Neurosci Lett, 1987. **83**(3): p. 327-32.

167. Kruse, J., et al., *Neural cell adhesion molecules and myelin-associated glycoprotein share a common carbohydrate moiety recognized by monoclonal antibodies L2 and HNK-1.* Nature, 1984. **311**(5982): p. 153-5.

168. Hoffman, S. and G.M. Edelman, *A proteoglycan with HNK-1 antigenic determinants is a neuron-associated ligand for cytotactin.* Proc Natl Acad Sci U S A, 1987. **84**(8): p. 2523-7.

169. Pesheva, P., A.F. Horwitz, and M. Schachner, *Integrin, the cell surface receptor for fibronectin and laminin, expresses the L2/HNK-1 and L3 carbohydrate structures shared by adhesion molecules.* Neurosci Lett, 1987. **83**(3): p. 303-6.

170. Nicolas, M., et al., *Notch1 functions as a tumor suppressor in mouse skin.* Nat Genet, 2003. **33**(3): p. 416-21.

171. Blanpain, C., et al., *Canonical notch signaling functions as a commitment switch in the epidermal lineage.* Genes Dev, 2006. **20**(21): p. 3022-35.

172. Delfini, M.C., et al., *Delta 1-activated notch inhibits muscle differentiation without affecting Myf5 and Pax3 expression in chick limb myogenesis.* Development, 2000. **127**(23): p. 5213-24.

173. Ahnfelt-Ronne, J., et al., *Preservation of proliferating pancreatic progenitor cells by Delta-Notch signaling in the embryonic chicken pancreas.* BMC Dev Biol, 2007. **7**(1): p. 63.

174. Murtaugh, L.C., et al., *Notch signaling controls multiple steps of pancreatic differentiation.* Proc Natl Acad Sci U S A, 2003. **100**(25): p. 14920-5.

175. D'Souza-Schorey, C., *Disassembling adherens junctions: breaking up is hard to do.* Trends Cell Biol, 2005. **15**(1): p. 19-26.

176. Lin, M.I., et al., *Trk C receptor signaling regulates cardiac myocyte proliferation during early heart development in vivo.* Dev Biol, 2000. **226**(2): p. 180-91.

177. Viebahn, C., et al., *Low proliferative and high migratory activity in the area of Brachyury expressing mesoderm progenitor cells in the gastrulating rabbit embryo.* Development, 2002. **129**(10): p. 2355-65.

178. Romano, L.A. and R.B. Runyan, *Slug is an essential target of TGFbeta2 signaling in the developing chicken heart.* Dev Biol, 2000. **223**(1): p. 91-102.